

AN ABSTRACT OF THE THESIS OF

Hiroyuki Tsutsumi for the degree of Doctor of Philosophy in Geosciences presented on March 7, 1996. Title: Evaluation of Seismic Hazards From the Median Tectonic Line, Japan and Blind Thrust Faults in the Los Angeles Metropolitan Area, California.

Abstract approved: _____


Robert S. Yeats

This thesis analyzes active geologic structures in densely populated areas in Japan and southern California based on geological, geophysical, and paleoseismological observations.

Chapter 2 discusses segmentation and paleoseismology of the Median Tectonic Line, Japan. We identified 12 geometric segments along the Median Tectonic Line separated by discontinuities such as en echelon steps, bends, changes in strike, and gaps in the surface trace. The recurrence interval and surficial offset for surface-rupturing earthquakes at four individual sites on the Median Tectonic Line in Shikoku Island are 1000-3000 years and 5-8 m, respectively. Part of the fault zone ruptured most recently during or after the 16th century A.D.; this rupture may be correlated to the 1596 Keicho-Kinki earthquake.

Chapter 3 discusses active and late Cenozoic tectonics of the northern Los Angeles fault system, California. We mapped the subsurface geology of the northern Los Angeles basin from the City of Santa Monica eastward to downtown Los Angeles, based on an extensive set of oil-well data. The northern Los Angeles fault system developed through an early to late Miocene extensional regime and a Plio-Pleistocene contractional regime. The uplift of the oxygen isotope substage 5e marine terrace at Pacific Palisades and an estimated dip greater than 45° suggest a dip-slip rate as large as 1.5 mm/yr for the Santa Monica Mountains blind thrust fault, a rate considerably smaller than a previous estimate.

Chapter 4 discusses the geologic setting of the 1971 San Fernando and 1994 Northridge earthquakes, two of the most devastating earthquakes in southern California history. We mapped the subsurface geology of the northern San Fernando Valley that lies at the updip projection of the two earthquake faults. The San Fernando Valley is underlain by a series of north-dipping blind thrust faults. The thick accumulation of the

Plio-Pleistocene Saugus Formation in the Sylmar basin and Merrick syncline is a surface expression of the south-dipping 1994 Northridge thrust that is overlain by the north-dipping 1971 San Fernando fault at a depth of ~5 km.

© Copyright by Hiroyuki Tsutsumi

March 7, 1996

All Rights Reserved

**Evaluation of Seismic Hazards From the Median Tectonic Line, Japan and Blind Thrust
Faults in the Los Angeles Metropolitan Area, California**

by

Hiroyuki Tsutsumi

A THESIS

submitted to

Oregon State University

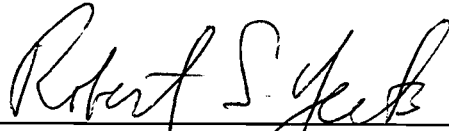
in partial fulfillment of
the requirements for the
degree of

Doctor of Philosophy


Completed March 7, 1996
Commencement June 1996

Doctor of Philosophy thesis of Hiroyuki Tsutsumi presented on March 7, 1996

APPROVED:



Major Professor, representing Geosciences



Chair of Department of Geosciences

Dean of Graduate School

I understand that my thesis will become part of the permanent collection of Oregon State University libraries. My signature below authorizes release of my thesis to any reader upon request.



Hiroyuki Tsutsumi, Author

ACKNOWLEDGMENT

I would like to thank the major professor, Dr. Robert S. Yeats, for his guidance throughout the graduate study at Oregon State University. I am also grateful to the committee members, Drs. Philip L. Jackson, LaVerne D. Kulm, Robert J. Lillie, and Charles L. Rosenfeld for their guidance and encouragement. Dr. Gary J. Huftile provided instructions on basic techniques of subsurface geologic analysis. I greatly benefited from discussions with Cheryl Hummon, Craig L. Schneider, and Thomas L. Wright. I would also like to acknowledge continuous guidance and encouragement by Dr. Atsumasa Okada of Kyoto University and Dr. Takashi Nakata of Hiroshima University, Japan. I have been supported by the United States Information Agency as a Fulbright scholar. Researches in chapters 3 and 4 were funded by grants from the National Earthquake Hazards Reduction Program, National Science Foundation, and Southern California Earthquake Center. Subsurface data for these studies were provided by the petroleum industry.

CONTRIBUTION OF AUTHORS

The three main chapters of this thesis are manuscripts that are in press, submitted, or to be submitted to geoscience journals. Robert S. Yeats was the Principal Investigator of research projects presented in Chapters 3 and 4, and was closely involved with each of the investigations. Specific contributions to these manuscripts by authors are listed below.

Chapter 2: Atsumasa Okada and Hiroyuki Tsutsumi have collaborated in geomorphic mapping and trench excavations of the Median Tectonic Line since 1988, through which most of the data presented in this paper were gathered. Hiroyuki Tsutsumi is the primary author of the paper.

Chapter 3: Hiroyuki Tsutsumi analyzed the geology west of the Newport-Inglewood fault zone and is the primary author of the paper. Robert S. Yeats evaluated a slip rate of the Santa Monica Mountains blind thrust fault based on topographic profiles constructed from a digital elevation model. He also identified many problems addressed in this paper. Cheryl Hummon and Craig L. Schneider analyzed the geology east of the Newport-Inglewood fault zone in their MS theses, and part of their analysis was incorporated in this paper. Gary J. Huftile provided guidance into the subsurface geologic mapping and regional geology throughout this project.

Chapter 4: Hiroyuki Tsutsumi analyzed the geology in the Pacoima oil field and surrounding areas and is the primary author of the paper. Robert S. Yeats analyzed the geology of the Cascade oil field and closely supervised the work by Tsutsumi.

TABLE OF CONTENTS

	<u>Page</u>
Chapter 1: Introduction.....	1
Chapter 2: Segmentation and Holocene Surface Faulting on the Median Tectonic Line, Southwest Japan	3
Abstract.....	4
Introduction.....	4
Regional Setting.....	5
Methodology.....	9
Segmentation Model.....	11
Paleoseismology	17
Tsunden Segment.....	17
Chichio Segment.....	22
Okamura Segment.....	25
Sea of Iyo Segment.....	26
Discussion	27
Correlation of the Most Recent Surface-Rupturing Earthquake on the MTL to a Historical Earthquake	27
Probable Rupture Length of Surface-Rupturing Earthquakes on the MTL	29
Space-Time Distribution of Holocene Faulting.....	30
Recurrence Interval of Large Earthquakes at Individual Sites Along the MTL.....	33
Conclusion.....	34

TABLE OF CONTENTS (Continued)

	<u>Page</u>
Acknowledgments	35
Chapter 3: Active and Late Cenozoic Tectonics of the Northern Los Angeles Fault System, California	37
Abstract.....	38
Introduction.....	39
Regional Setting.....	41
Overview of the Study Area	41
Stratigraphy.....	44
Major Geologic Structures	47
Santa Monica Fault System.....	47
Structures East of the West Beverly Hills Lineament.....	55
Newport-Inglewood Fault Zone.....	59
Discussion	60
Interaction Between the Northern Los Angeles Fault System and Newport-Inglewood Fault Zone.....	60
Slip Rate of Pliocene to Early Pleistocene Structures Based on Analysis of Growth Strata	61
Late Quaternary Slip Rate of the Santa Monica Mountains Blind Thrust Fault.....	62
Late Cenozoic Tectonic Evolution of the Northern Los Angeles Basin.....	66
Early to late Miocene extensional tectonics.....	66

TABLE OF CONTENTS (Continued)

	<u>Page</u>
Early Pliocene to early Pleistocene contractional tectonics	71
Contemporary tectonics	72
Conclusion	73
Acknowledgments	74
Appendix.....	76
Chapter 4: Geologic Setting of the 1971 San Fernando and 1994 Northridge Earthquake Zones in the San Fernando Valley, California	79
Abstract.....	80
Introduction.....	80
Regional Setting.....	82
Stratigraphy.....	86
Structural Geology.....	93
Miocene Normal Faults.....	93
Pliocene (pre-Saugus) Reverse Faults.....	94
Quaternary (post-Saugus) Reverse Faults.....	97
Mission Hills fault	97
Northridge Hills fault.....	98
Verdugo fault	101
1971 San Fernando fault.....	103
Discussion	104

TABLE OF CONTENTS (Continued)

	<u>Page</u>
Geologic Evidence of the 1994 Northridge Fault in the Northern San Fernando Valley.....	104
Fault Slip Rate and Seismic Hazard in the San Fernando Valley.....	108
Structural Evolution of the Northern San Fernando Valley Area.....	109
Conclusion.....	111
Acknowledgments	112
Appendix.....	113
Chapter 5: Conclusions.....	115
Bibliography.....	116

LIST OF FIGURES

<u>Figure</u>	<u>Page</u>
2.1 Index map showing current plate tectonic regime in southwest Japan.....	6
2.2 Active tectonic map of Chubu, Kinki, Chugoku, and Shikoku Districts.....	8
2.3 Map showing segments of the MTL.....	12
2.4 Acoustic profiler record across the Sea of Iyo segment (top) and correlation of three cores with 2a radiocarbon ages (bottom) modified from Ogawa et al. [1992]	18
2.5 Log of the east and west walls in trench 1 across the Tsunden segment at Donari.....	19
2.6 Log of the east wall of trench 2 across the Chichio segment at Kamikirai	23
2.7 Right-laterally offset rice paddy dikes (I to V) aligned on the projected fault trace of the Chichio segment at Kamikirai.....	24
2.8 Map showing active faults in western Kinki and eastern Shikoku	28
2.9 Space-time diagram of surface-rupturing earthquakes on the MTL during the past 8000 years	32
3.1 Map of the western Transverse Ranges, Los Angeles basin, and northern end of the Peninsular Ranges	40
3.2 Index map of the study area showing topography, surface and subsurface geologic structures, oil fields, and location of cross sections A-A' to G-G' (Figures 3.4a-3.4g).....	42
3.3 Stratigraphic chart of the northern Los Angeles basin	45
3.4 Cross sections (a) A-A' to (g) G-G' across major geologic structures of the study area.....	49
3.5 Timing of faulting and structural growth of principal structures in the northern Los Angeles basin	54
3.6 Subsurface structure contour maps (a) on the base of Pico strata (~2.5 Ma) and (b) base of Repetto strata (~5 Ma).....	56

LIST OF FIGURES (Continued)

<u>Figure</u>	<u>Page</u>
3.7 Topographic profiles across the western Transverse Ranges	65
3.8 Calculation of left slip on the Malibu Coast-Raymond fault since the early Miocene	68
3.9 Schematic reconstruction of structural features during three tectonic stages in the northern Los Angeles area	69
4.1 Tectonic map of the western Transverse Ranges, California	81
4.2 Index map of the San Fernando Valley	83
4.3 Stratigraphy of the San Fernando Valley	87
4.4 Cross sections across major geologic structures in the San Fernando Valley	88
4.5 Tectonic map of the Santa Susana Mountains and northern San Fernando Valley	95
4.6 Unmigrated seismic profile along Balboa Boulevard; (a) uninterpreted and (b) interpreted	99
4.7 Cross section down to 20 km depth across the central San Fernando Valley, including 1971 San Fernando and 1994 Northridge earthquake zones	105
4.8 The San Fernando Valley and vicinity during the early to late Miocene after removal of 50°-60° clockwise rotation documented by Kamerling and Luyendyk [1979] and Hornafius et al. [1986]	110

LIST OF TABLES

<u>Table</u>		<u>Page</u>
2.1	Radiocarbon dates for samples from trench 1 (Tsunden segment) and trench 2 (Chichio segment)	21
2.2	Summary of event dates of the Okamura segment	21
2.3	Historical strike-slip earthquakes in Japan with moment magnitude > 6.8.....	31
2.4	Comparison of active strike-slip faults with wide range of slip rates	31

LIST OF PLATES

Plates

1. Location of cross sections in the northern Los Angeles basin
2. Fault plane contour map of the Santa Monica and Ranch faults
3. Structure contour map of the base of Pico strata (~2.5 Ma)
4. Structure contour map of the base of Repetto strata (~5 Ma)
5. Cross section A-A'
6. Cross section B-B'
7. Cross section C-C'
8. Cross section D-D'
9. Cross section E-E'
10. Cross section F-F'
11. Cross section G-G'
12. Location of cross sections in the San Fernando Valley
13. Cross section H-H'
14. Cross section I-I'
15. Cross section J-J'
16. Cross section K-K'
17. Cross section L-L'

EVALUATION OF SEISMIC HAZARDS FROM THE MEDIAN TECTONIC LINE, JAPAN AND BLIND THRUST FAULTS IN THE LOS ANGELES METROPOLITAN AREA, CALIFORNIA

Chapter 1: Introduction

This thesis describes active geologic structures in densely populated areas in Japan and southern California based on geological, geophysical, and paleoseismological observations. It is composed of three main chapters, each of which is a journal manuscript that was submitted or will be submitted for publication. Chapter 2 will be published in the March, 1996 issue of Journal of Geophysical Research. Chapter 3 was submitted for publication to Geological Society of America Bulletin in June, 1995, and the manuscript is currently in revision. Chapter 4 will be submitted for publication in a modified form to a geoscience journal. Many data related to Chapters 3 and 4 which were not included in submitted manuscripts are included in this thesis as plates.

Although each paper discusses different areas based on different techniques, the unifying theme of this thesis is to better evaluate the seismic hazards from faults underlying densely populated areas. As dramatically demonstrated by the 1994 Northridge, California and 1995 Hyogo-ken Nanbu (Kobe), Japan earthquakes, moderate earthquakes in urban areas could cause more damage than a much larger earthquake on a more distant fault. Accurate geological and seismological assessment of the source of earthquakes is essential for the mitigation of damages from future earthquakes, because all subsequent geotechnical and engineering analyses are based on the assessment. The geological assessment typically involves mapping of active faults and estimating their slip rates and recurrence intervals, which is the central topic of this thesis.

Chapter 2 discusses segmentation and paleoseismology of the Median Tectonic Line, Japan, based on geomorphic mapping and paleoseismological investigations. This 300-km-long fault has one of the highest slip rates in onshore Japan and underlies population centers of Shikoku Island. This paper synthesizes information on the Holocene faulting along this fault from previously published and new studies. Most of the data presented in this paper were collected while I was a graduate student at Hiroshima University during 1987 and 1991. The paper was written into the present form at Oregon State University under the guidance of Professor Robert S. Yeats.

Chapters 3 and 4 discuss active and late Cenozoic tectonics of two adjacent basins in the Los Angeles metropolitan area, California. Chapter 3 describes the northern Los Angeles fault system that marks the boundary between the Santa Monica Mountains and Los Angeles basin. Recent geomorphic and geotechnical studies revealed that this fault

system has been active in the late Quaternary. We analyze the subsurface geology of the fault system based primarily on oil-well data. We present new data on the three-dimensional geometry, timing of faulting, and slip rate of the fault system, which would lead to a better assessment of seismic hazard in the northern Los Angeles basin.

Chapter 4 discusses geologic setting of the 1971 San Fernando and 1994 Northridge earthquakes, two of the most devastating earthquakes in southern California history. We mapped the subsurface geology of the San Fernando Valley that lies at the updip projection of the two earthquake faults, based on oil-well and seismic data. Although the 1994 earthquake ruptured a previously unrecognized fault that extends upward only to a depth of ~5 km, there are near-surface geologic expressions of this blind thrust fault which might have led us to identify the fault prior to the 1994 earthquake. We also constrain more closely the location and slip rate of previously suspected but poorly defined blind thrust faults beneath this densely populated suburb of Los Angeles.

**Chapter 2: Segmentation and Holocene Surface Faulting on the Median
Tectonic Line, Southwest Japan**

Hiroyuki Tsutsumi

Department of Geosciences, Oregon State University, Corvallis

Atsumasa Okada

Department of Geophysics, Kyoto University, Kyoto, Japan

This chapter is from:

Hiroyuki Tsutsumi and Atsumasa Okada, Segmentation and Holocene surface faulting on the Median Tectonic Line, southwest Japan, Journal of Geophysical Research, in press, 1996.

Copyright by the American Geophysical Union

Abstract

The Median Tectonic Line (MTL) active fault system is a 300-km-long, arc-parallel, right-lateral strike-slip fault related to oblique subduction of the Philippine Sea plate beneath the Eurasian plate at the Nankai trough, southwest Japan. The fault on Shikoku Island has a slip rate of 5-10 mm/yr, one of the highest in onshore Japan. We identified 12 geometric segments along the MTL separated by discontinuities such as en echelon steps, bends, changes in strike, and gaps in the surface trace. A chronology of latest Holocene surface faulting on the MTL was constructed based on previously published and new work including trenching, geomorphic mapping, and acoustic profiling and piston coring of the submarine extension of the fault zone. The MTL probably does not rupture along its entire length in a single earthquake but instead consists of multiple "earthquake segments" that rupture independently of one another. The recurrence interval and surficial offset for surface-rupturing earthquakes at four individual sites on the MTL in Shikoku Island are 1000-3000 years and 5-8 m, respectively. The relatively long recurrence interval and large surficial offset per earthquake suggest large seismic moment release during surface-rupturing earthquakes on the MTL, as commonly observed for Japanese moderate to large intraplate earthquakes. Because the predicted rupture lengths based on empirical relations between surface displacement and rupture length are considerably larger than those of individual segments, large earthquakes on the MTL probably rupture multiple geometrically defined segments. The fault was previously thought to be unruptured at least in the past 1000 years based on the absence of historical evidence for destructive earthquakes. However, trench excavations show that part of the MTL ruptured most recently during or after the 16th century A.D. with at least 6.9 ± 0.7 m of slip along the main fault trace. This rupture may be correlated to the 1596 Keicho-Kinki earthquake, but further geological and historical investigations are needed to confirm this hypothesis.

Introduction

In the past two decades, researchers analyzing patterns of historical surface-rupturing earthquakes have found strong correlations between structural and geometric features of fault zones and sites of rupture nucleation and termination [Aki, 1979; Sibson, 1985, 1986, 1987; King, 1986; Barka and Kadinsky-Cade, 1988; Crone and Haller, 1991; dePolo et al., 1991; Machette et al., 1991; Tsukuda, 1991; Zhang et al., 1991]. These observations are important in that we may be able to characterize the size of future earthquakes along a fault or within a region if earthquakes follow the characteristic model of Schwartz and Coppersmith [1984]. However, the rupture extent of large earthquakes may not be readily predictable. For example, the M_w 7.3 Landers, California, earthquake of

1992 ruptured five distinct faults separated by en echelon steps as large as 3 km in width [Sieh et al., 1993]. Nevertheless, a detailed model of the rupture process of this earthquake based on inversion of geodetic, geologic, and seismographic data suggests that the two principal en echelon steps are related to retardation of the propagating ruptures [Wald and Heaton, 1994]. As we learn more about the dynamic rupture processes of modern earthquakes, we also need to look at historic and late Quaternary earthquakes for rupture patterns along a fault through multiple earthquake cycles. In this paper, we describe the late Holocene behavior of the Median Tectonic Line (MTL), a large strike-slip fault in southwest Japan.

The MTL is an arc-parallel, right-lateral strike-slip fault (Figure 2.1) related to oblique subduction of the Philippine Sea plate beneath the Eurasian plate along the Nankai trough [Fitch, 1972]. Arc-parallel strike-slip faults are capable of generating moderate to large earthquakes such as the 1892 Tapanuli earthquake on the Great Sumatran fault [Reid, 1913] and the M_w 7.7 Luzon earthquake of 1990 on the Philippine fault. The MTL is the longest continuous active fault in onshore Japan with one of the highest late Quaternary slip rates, 5-10 mm/ $^{\circ}$ C yr on Shikoku [Okada, 1973a, 1980; Research Group for Active Faults of Japan, 1991]. However, there are no historical documents suggesting destructive earthquakes along the fault zone for at least the past 1000 years [Usami, 1987]. In addition, the MTL underlies an urban corridor of Kinki and Shikoku and is adjacent to densely populated areas such as the Kyoto-Osaka-Kobe megacities (population more than 10 million), representing one of the largest earthquake risks in the country (Figure 2.1). Information on the timing and slip in prehistoric earthquakes is important for better assessments of seismic hazard from the fault. This paper presents a segmentation model and a chronology of late Holocene surface-rupturing earthquakes of the MTL based on geological and paleoseismological observations from previously published and new studies.

Regional Setting

The MTL, extending from Chubu westward to Kyushu, is the most pronounced geologic discontinuity in southwest Japan (Figure 2.1). Originating in the late Mesozoic, the MTL separates the low pressure-high temperature Ryoke metamorphic belt to the north and the high pressure-low temperature Sambagawa metamorphic belt to the south for over 1000 km [e.g., Hashimoto and Kanmera, 1991]. In Kinki and Shikoku, the Ryoke belt is overlain by the Upper Cretaceous Izumi Group consisting of interbedded sandstone and shale. The eastern end of the MTL is truncated by the NNW trending Itoigawa-Shizuoka Tectonic Line which was proposed by Nakamura [1983] as a plate boundary between the

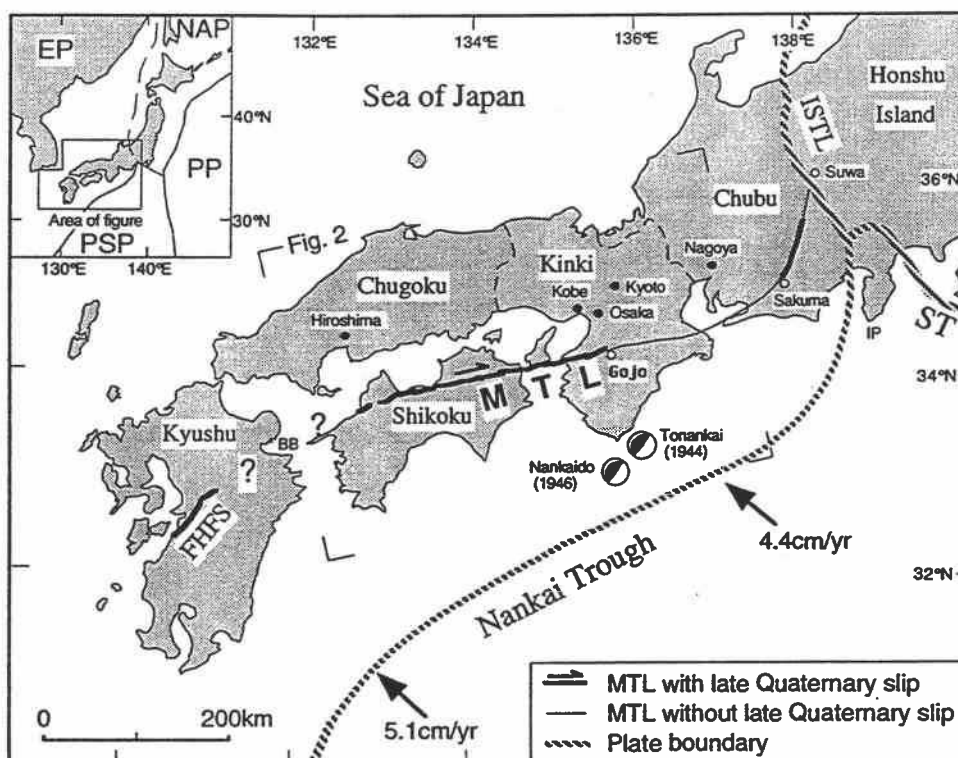


Figure 2.1 Index map showing current plate tectonic regime in southwest Japan. Plate convergence vectors along the Nankai trough are calculated based on work by Seno et al. [1993]. Focal mechanisms of Tonankai and Nankaido earthquakes are after Kanamori [1972]. The Median Tectonic Line (MTL) is a right-lateral strike-slip fault accommodating part of the arc-parallel component of plate motion. Its location and late Quaternary activity are not well defined in Kyushu and offshore between Kyushu and Shikoku. Abbreviations in the inset are EP, Eurasian plate; NAP, North American plate; PP, Pacific plate; PSP, Philippine Sea plate. Abbreviations in the figure are BB, Beppu Bay; FHFS, Futagawa-Hinagu fault system; IP, Izu Peninsula; ISTL, Itoigawa-Shizuoka Tectonic Line; ST, Sagami trough. Chubu, Chugoku, Kinki, Kyushu, and Shikoku represent geographic districts; Kyushu and Shikoku Districts are islands, whereas Chubu, Chugoku, and Kinki Districts (their boundaries are shown) are part of Honshu Island. Location of Figure 2.2 is shown.

Eurasian and North American plates (Figure 2.1). Fitch [1972] first proposed that right-lateral strike-slip along the MTL is related to oblique subduction of the Philippine Sea plate beneath the Eurasian plate along the Nankai trough. He suggested that the oblique convergence vector between the plates is partitioned into an arc-normal component (underthrusting along the subduction zone) and an arc-parallel component (right-lateral slip along the MTL). However, this strain partitioning is incomplete: a large portion of the arc-parallel component as well as the arc-normal component is accommodated by subduction zone earthquakes along the trough such as the 1944 Tonankai and 1946 Nankaido earthquakes (Figure 2.1). The right-lateral shear is distributed over a wide area of the upper plate (Figure 2.2), and only a fraction of the shear is accommodated by slip on the MTL. The convergence rate between the plates is calculated as 4.4 cm/yr off Kinki and 5.1 cm/yr off Kyushu based on a model by Seno et al. [1993].

Evidence of late Quaternary faulting is recognized along a 300-km-long portion of the MTL in western Kinki and Shikoku (Figure 2.1). Some parts of the MTL in Chubu and Kyushu have also been active in the Quaternary, but the slip rate there is significantly lower than in western Kinki and Shikoku [Okada, 1973a; Research Group for Active Faults of Japan, 1991]. The late Quaternary movement along the MTL is predominantly right-lateral strike-slip, with a vertical component of displacement which is generally less than one tenth of the horizontal component [Okada, 1973a, 1980]. The active trace of the MTL in western Kinki and Shikoku consists of parallel to subparallel en echelon faults with lengths of several kilometers to several tens of kilometers. Some of the active faults reactivate the terrane boundary between the Sambagawa and Izumi belts, while others are less than a few kilometers to the north of the boundary. These late Quaternary faults are usually referred to as the Median Tectonic Line active fault system, to distinguish them from the MTL as a terrane boundary [Okada, 1973a, 1980]. In the remainder of this paper, we call this active fault system "the MTL" and the terrane boundary between the two belts "the terrane boundary of the MTL" for convenience. Based on offset stream channels and terrace risers, the average horizontal slip rate of the MTL in the late Quaternary is estimated as 1-3 mm/¹⁰C yr in western Kinki [Okada and Sangawa, 1978] and 5-10 mm/¹⁰C yr in Shikoku [Okada, 1970, 1973b]. These are among the highest slip rates for onshore active faults in Japan [Okada, 1973a, 1980; Research Group for Active Faults of Japan, 1991]. The MTL in Chubu (Figure 2.1) is characterized by linear valleys with right-laterally deflected stream channels. The average late Quaternary slip rate there is probably less than 1 mm/¹⁰C yr [Research Group for Active Faults of Japan, 1991]. Between Sakuma in Chubu and Gojo in Kinki, the terrane boundary of the MTL has not been reactivated in the late Quaternary [Okada, 1973a]. The submarine segment of the MTL between Shikoku and Kyushu has

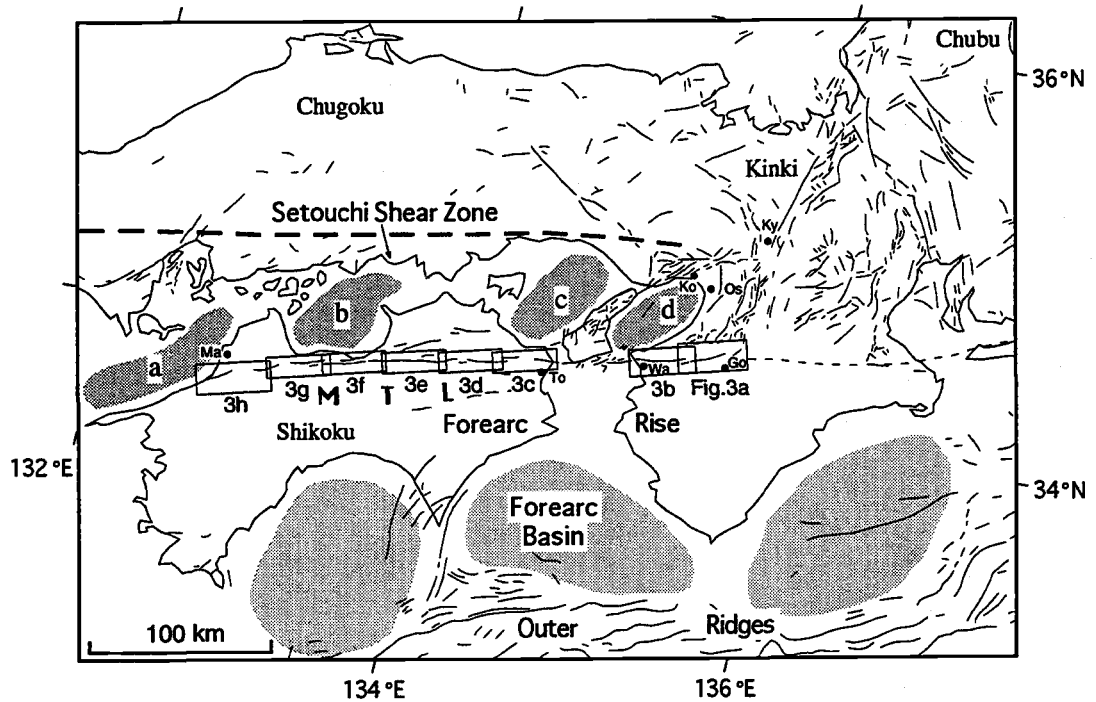


Figure 2.2 Active tectonic map of Chubu, Kinki, Chugoku, and Shikoku Districts. Active faults (solid lines) after Research Group for Active Faults of Japan [1992] and structural zonation after Sugiyama [1994]. Region north of the Median Tectonic Line (MTL) has much higher concentration of active faults than region to south. Dashed line east of Gojo (Go) indicates the terrane boundary of the MTL which has not been reactivated in the late Quaternary. Shaded areas indicate basins. The basins in the Setouchi shear zone are a, Sea of Iyo; b, Sea of Hiuchi; c, Sea of Harima; d, Osaka Bay. The rectangles show locations of Figures 2.3a to 2.3h. Abbreviations of cities are Go, Gojo; Ko, Kobe; Ky, Kyoto; Ma, Matsuyama; Os, Osaka; To, Tokushima; Wa, Wakayama.

not been mapped. In Kyushu, the NE trending Futagawa-Hinagu fault system (Figure 2.1) with a late Quaternary slip rate of 0.8 mm/¹⁴C yr is probably the western extension of the MTL [Research Group for Active Faults of Japan, 1991; Chida, 1992]. Extensive normal faulting and active volcanism characterize a zone north of the MTL in Kyushu. The scope of this study is limited to the MTL in western Kinki and Shikoku where the slip rate is relatively high and where we have conducted extensive paleoseismological investigations involving detailed geologic mapping and exploratory trench excavations.

There is a remarkable contrast in distribution of active faults from one side of the MTL to the other (Figure 2.2). The area north of the MTL, especially Chubu and Kinki, contains one of the largest concentrations of active faults in Japan with numerous historical destructive earthquakes catalogued by Usami [1987]. These faults are interpreted to take up the right-lateral slip on the MTL east of where it becomes inactive near Gojo [Sangawa, 1986]. They are classified into NW trending left-lateral and NE trending right-lateral strike-slip faults and north trending reverse faults. Maximum compressional stress direction based on the conjugate sets of strike-slip faults is E-W to WNW-ESE. The Setouchi shear zone (Figure 2.2) is a broad right-lateral shear zone north of the MTL marked by a series of NE trending anticlines (islands) and synclines (basins) [Tsukuda, 1992; Sugiyama, 1994]. In contrast, there are very few active faults onshore south of the MTL (Figure 2.2). This zone between the MTL and forearc basins to the south is considered to behave as a rigid microplate translating to the west in response to oblique plate convergence [Tsukuda, 1992]. Historical and instrumental seismicity of the MTL is very low, unlike other large, comparable strike-slip faults worldwide [Ishikawa, 1992]. Because of the absence of historical documents of destructive earthquakes along the fault [Usami, 1987], the MTL was previously thought to be unruptured for at least the past 1000 years.

Methodology

The primary information used in fault segmentation studies are physical characteristics (geometric and structural features) and coseismic behavior (historical and paleoseismological data) [Schwartz and Coppersmith, 1986; dePolo and Slemmons, 1990]. Because paleoseismological data are currently available for only a portion of the MTL, we construct a segmentation model based primarily on the geometric and structural features of the fault zone. Thus the term "segment" in this paper is equivalent to "geometric segment" or "structural segment" of dePolo et al. [1991]. A geometric or structural segment does not necessarily fail separately from neighboring segments. An earthquake rupture may be confined to a single segment, or it may extend to multiple segments, as in the case for many large historical earthquakes [Barka and Kadinsky-Cade, 1988; dePolo et al., 1991;

Tsukuda, 1991]. We use the term "earthquake segment" to specify a part of the fault zone that ruptures as a unit during a single earthquake.

Observations of large historical strike-slip earthquakes show that termination of earthquake ruptures is closely related to distinct structural and geometric discontinuities. Sibson [1985, 1986, 1987] suggested, based on observations of historical strike-slip earthquakes in California, that releasing steps act as kinematic barriers capable of arresting coseismic ruptures. Compilation of data on historical surface ruptures worldwide led Knuepfer [1989] to conclude that strike-slip ruptures often end at bends, steps, and branch or crosscutting structures. Four prominent historical strike-slip surface ruptures in Japan started at restraining steps or bends, and most of them ended at releasing ones [Tsukuda, 1991]. In this study, we identify segment boundaries based on prominent en echelon steps, bends, changes in strike, and gaps in the fault trace. Geologic data, such as slip rate and presence of scarps on late Quaternary geomorphic surfaces, are also incorporated. In addition, we consider whether active faulting is accommodated by the reactivation of the terrane boundary of the MTL or by the formation of new faults.

In the past three decades, surface traces of the MTL have been mapped in detail in western Kinki [Okada and Sangawa, 1978; Sangawa, 1978] and in Shikoku [Kaneko, 1966; Okada, 1968, 1970, 1972, 1973b; Okada and Tsutsumi, 1990]. Late Quaternary slip rates were calculated at several localities by dating fluvial sediments and related geomorphic surfaces through conventional ^{14}C dating and tephrochronology. These data, along with further field observations, were compiled into 1:25,000-scale strip maps of the MTL in western Kinki [Mizuno et al., 1994] and Shikoku [Mizuno et al., 1993]. We use these strip maps for identifying segment boundaries in this study. Ogawa et al. [1992] mapped the shallow-marine segment of the MTL in the Sea of Iyo off western Shikoku (Figure 2.2) using a high-resolution (about 10-30 cm) single-channel acoustic profiler that images the uppermost several tens of meters of sediment. The submarine segment of the MTL between Kinki and Shikoku was mapped by Hydrographic Department Maritime Safety Agency [1979] and Geological Survey of Japan [1995]. However, late Quaternary faulting in this portion of the MTL is poorly constrained, and this area is not discussed in the remainder of this paper.

Since 1984, we have logged more than 10 exploratory trenches across three segments of the MTL in Shikoku to date individual surface-rupturing earthquakes. Most trench sites yielded abundant soil organic matter within alluvial fan sequences for conventional ^{14}C dating. We also obtained more than 50 pottery fragments ranging in age from a few hundred to several thousand years old. These pottery fragments were identified by archaeologists T. Makabe and S. Tanabe. The Kikai-Akahoya air fall ash (K-Ah),

which erupted from south of Kyushu about 6300 years B.P. and the Aira-Tanzawa air fall ash (AT), which erupted from the southern end of Kyushu about 21,000-25,000 years B.P. [Machida and Arai, 1992], form useful time-stratigraphic markers in some trenches. Ogawa et al. [1992] dated individual surface-rupturing earthquakes along the MTL in the Sea of Iyo by correlating piston cores across the fault zone. In this paper, we present results of new paleoseismological studies and briefly summarize previously published work.

Segmentation Model

Based on the criteria described in the preceding section, we identified 12 geometric or structural segments along the MTL in western Kinki and Shikoku (Figure 2.3). We describe the criteria used to define the segment boundaries.

The faults on the south side of the 60-km-long and 10-km-wide Izumi Range are divided into two segments based on contrasting geomorphic features separated by a 0.1-km-wide releasing step north of Uchida (Figures 2.3a and 2.3b). The Gojodani segment to the east traverses the southern slope of the Izumi Range, whereas the Negoro segment to the west bounds the Izumi Range against late Quaternary alluvial fans. Progressively older middle to late Quaternary fluvial terraces are preserved at higher elevations east of the step, while these terraces are overlain by latest Pleistocene to Holocene deposits to the west. The Gojodani segment is a few kilometers north of the terrane boundary of the MTL, a north dipping reverse fault in the early to middle Pleistocene [Sangawa, 1978, 1986]. The right-lateral strike-slip displacement on the Gojodani segment is transferred eastward to the Kongo fault across a restraining double bend northeast of Hashimoto (Figure 2.3a). North of Gojo, the Kongo fault curves about 90°, and the north trending portion is a reverse fault with a middle to late Quaternary vertical slip rate of 0.4 mm/yr [Research Group for Active Faults of Japan, 1991]. East of Gojo, no late Quaternary fault is identified along the terrane boundary of the MTL in Kinki. The Negoro segment has a late Quaternary slip rate of 0.9-3.1 mm/yr (horizontal) and 0.1-0.4 mm/yr (vertical) [Okada and Sangawa, 1978]. The horizontal slip rate is an order of magnitude greater than the vertical slip rate, a common feature along most of the MTL. West of the Negoro segment, two inferred faults are mapped by Mizuno et al. [1994], but little is currently known about the late Quaternary faulting along these structures.

In eastern Shikoku, we identified five segments along the MTL that mark the physiographic boundary between the 90-km-long and 15-km-wide Sanuki Range and the alluviated valley floor of the Yoshino River (Figures 2.3c, 2.3d, and 2.3e). The Naruto segment is separated from the Tsunden segment by absence of scarps on Holocene alluvial

Figure 2.3 Map showing segments of the MTL. Arranged from east to west with slight overlap between each figure (matching lines are shown). See Figure 2.2 for location of each figure. Areas of pre-early middle Pleistocene strata are shaded. Solid thick lines show fault traces of the MTL; dashed where inferred and dotted where concealed. Half-sided arrows indicate direction of horizontal movement, and bars with balls are on downthrown side. Thin dashed lines in Figures 2.3a, 2.3b, 2.3g, and 2.3h show part of the terrane boundary of the MTL which has not been reactivated in the late Quaternary. Large open arrows indicate proposed segment boundaries. Location of trench sites are shown by solid rectangles. Scale bars and north arrows in Figures 2.3a and 2.3e are applicable to the other figures. Fault traces from Mizuno et al. [1993, 1994], and those in the Sea of Iyo from Ogawa et al. [1992].

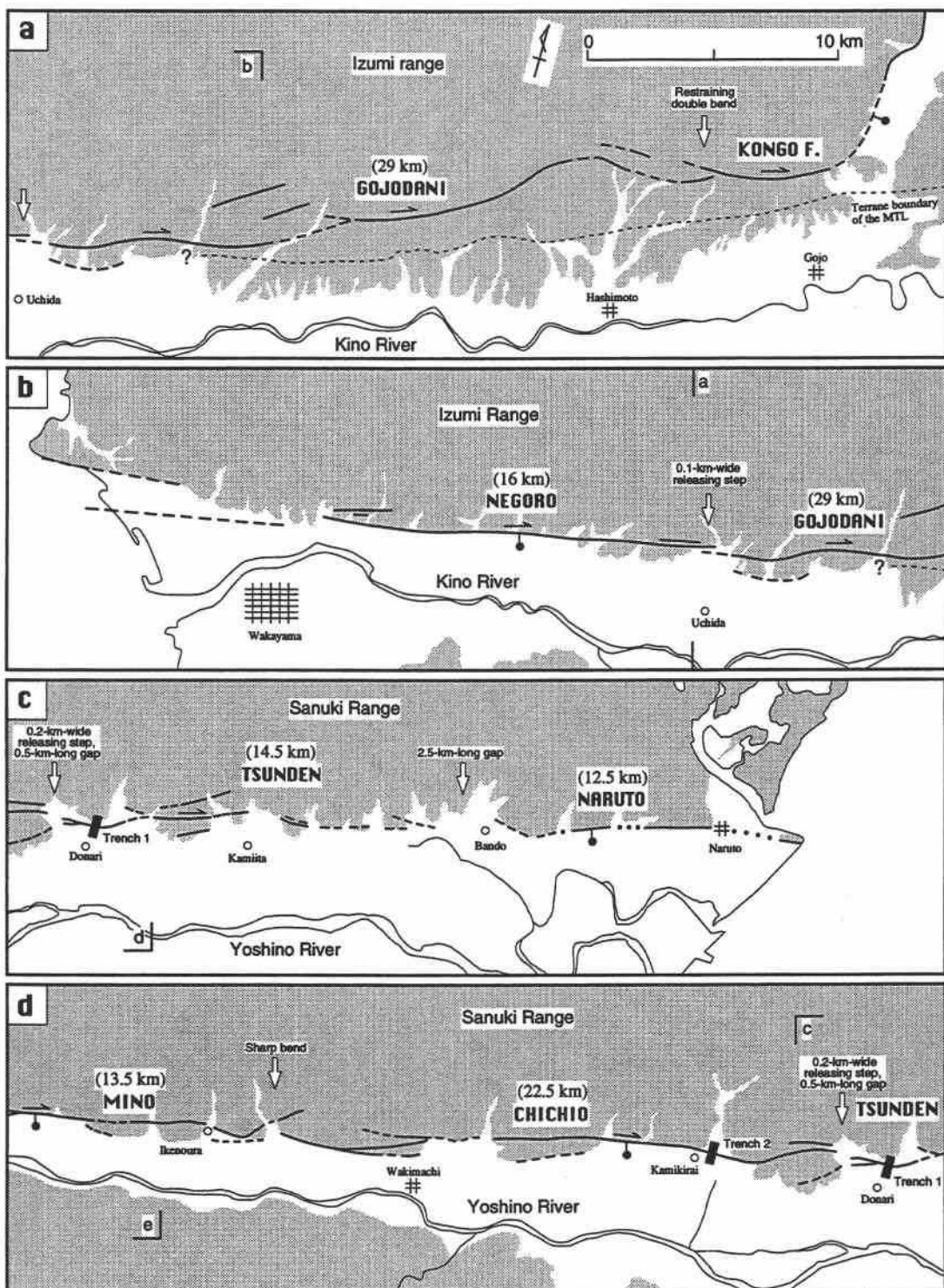


Figure 2.3

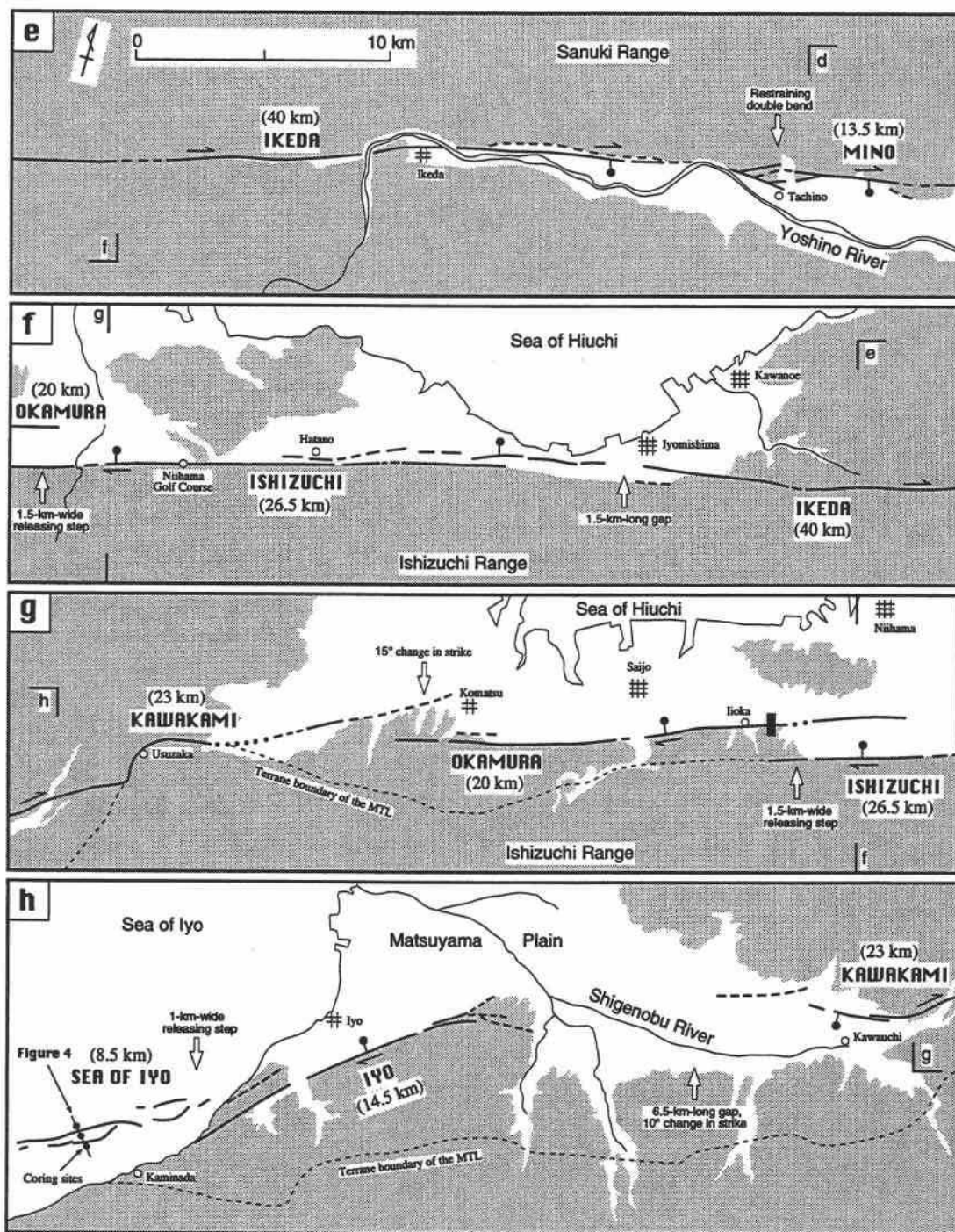


Figure 2.3 (Continued)

surfaces, which results in a 2.5-km-long gap in the surface trace at Bando (Figure 2.3c). The boundaries between the other four segments are identified based primarily on the fault geometry; all segments have higher scarps on progressively older late Quaternary alluvial fan surfaces and similar slip rates. The Tsunden segment is separated from the Chichio segment by a 0.2-km-wide releasing step and 500-m-long gap in the surface trace at Donari (Figure 2.3c). We do not consider a 1.5-km-long gap in the surface trace on an active alluvial fan surface north of Kamiita to be a segment boundary because the fault trace connects smoothly across this gap. Right-lateral stream offsets along the Chichio segment are as large as 1.5 km, among the largest measured along the MTL. A north trending terrace riser with an estimated age of about 10,000 years B.P. at Kamikirai is offset 60 m right-laterally and 5-6 m vertically [Okada, 1970]. This gives average horizontal and vertical slip rates of 6 mm/¹⁴C yr and 0.5-0.6 mm/¹⁴C yr, respectively, for the Chichio segment. North of Wakimachi, the displacement on the main trace of the Chichio segment is transferred westward to a fault 1 km to the south (Figure 2.3d). However, these fault traces appear to be continuous, and we do not consider this as a segment boundary. The Mino segment strikes N75°E, but its eastern end bends sharply about 40° northward which we identify as a segment boundary (Figure 2.3d). Based on offset stream channels at Ikenoura, Okada [1970] obtained a horizontal slip rate of 8-9 mm/¹⁴C yr for the Mino segment. The fault trace forms a restraining double bend at the boundary with the Ikeda segment near Tachino (Figure 2.3e). The 40-km-long Ikeda segment is the longest segment in the MTL, extending from Tachino westward to Iyomishima (Figures 2.3e and 2.3f). Okada [1968] obtained a horizontal slip rate of 7 mm/¹⁴C yr for the Ikeda segment based on an offset terrace riser immediately west of downtown Ikeda. Horizontal slip rates obtained along the MTL at the southern margin of the Izumi Range are 6-9 mm/¹⁴C yr. Taking into consideration the uncertainties in age determination of geomorphic surfaces, Okada [1970] gave a right-lateral slip rate of 5-10 mm/¹⁴C yr for this portion of the MTL. From Ikeda westward to south of Kawano, the fault trace lies along a structurally controlled, narrow, alluviated valley. Geomorphic features of late Quaternary faulting in this section are obscured by numerous landslides. The Ikeda segment is separated from the Ishizuchi segment by a 1.5-km-long gap in the fault trace where the fault traverses latest Pleistocene alluvial fan surfaces south of Iyomishima. The direction of vertical displacement is reversed across this boundary from up on the north in western Kinki and eastern Shikoku to up on the south in central and western Shikoku.

The faults on the north side of the Ishizuchi Range are divided into three segments (Figures 2.3f and 2.3g). The Ishizuchi segment is the westernmost segment where late Quaternary faulting has reactivated the terrane boundary of the MTL. East of Hatano, the

Ishizuchi segment consists of two parallel fault traces 0.3-0.8 km apart with an overlap of 8.5 km length (Figure 2.3f). Prior to the construction of Niihama Golf Course (Figure 2.3f), there was a WNW trending fault trench on an alluvial fan surface. A wood sample obtained from 8 m beneath the fan surface yielded a 1σ ^{14}C age of 1860 ± 90 years B.P. [Okada, 1973b]. A dendrochronologically calibrated, 2σ calendar age range of 60 B.C. to 420 A.D. for this sample, based on the program of Stuiver and Reimer [1993], constrains the oldest possible age for the most recent surface-rupturing earthquake on the Ishizuchi segment. The Ishizuchi segment overlaps the Okamura segment for 5.5 km with a 1.5-km-wide releasing step south of Niihama, making this the most pronounced segment boundary along the MTL (Figure 2.3g). West of this boundary, the terrane boundary between the Izumi and Sambagawa belts was for the most part not reactivated in the late Quaternary. Instead, the right-lateral displacement is taken up by faults a few kilometers north of the terrane boundary (Figures 2.3g and 2.3h). The Okamura segment strikes parallel to and 1.5 km north of the terrane boundary of the MTL from south of Niihama westward to Komatsu (Figure 2.3g). Tsutsumi et al. [1991] obtained a late Quaternary slip rate of 5-8 mm/ ^{14}C yr for the Okamura segment based on trench excavations at Iioka. West of the Okamura segment, the MTL trends more southerly than to the east. The Kawakami segment is separated from the Okamura segment by a 15° change in strike with an overlap of 3 km length near Komatsu (Figure 2.3g). The Kawakami segment strikes mostly within the Izumi Group; however, a sharp restraining double bend near Usuzaka coincides with the reactivated terrane boundary of the MTL (Figure 2.3g). This segment has a south facing scarp 1.5-2.8 m high on a Holocene alluvial fan surface north of Kawauchi (Figure 2.3h).

The Iyo segment marks the southwestern boundary of the Matsuyama Plain (Figure 2.3h). This segment strikes $\text{N}50^\circ\text{E}$, about 30° more southerly than the general strike of the MTL. A 6.5-km-long gap in the surface trace separates this segment from the Kawakami segment, and there is, in addition, a 10° change in strike. Portions of the gap may be due to the late Holocene sedimentation by the Shigenobu River. We believe the slip rate of this segment is less than that in eastern and central Shikoku because the geomorphic features associated with latest Pleistocene to Holocene faulting are more subdued [Okada, 1972]. The Iyo segment is traced to the coast, but no offshore fault was found by Ogawa et al. [1992] on the direct extension of this onshore fault trace. Using a high-resolution acoustic profiler, Ogawa et al. [1992] mapped submarine faults younger than the K-Ah ash bed 1.5 km offshore from the village of Kaminada (Figure 2.3h). These faults trend almost parallel to the Iyo segment with an intervening 1-km-wide releasing step. We call these offshore faults the Sea of Iyo segment. The western extension of these faults is not mapped, and the

segment could extend farther west. This segment consists of two pairs of faults, the westernmost of which forms a 500-m-wide graben (Figures 2.3h and 2.4). This deformational style is quite different from that observed onshore in western Kinki and Shikoku, but it is similar to the faulting style in Beppu Bay to the west (Figure 2.1) [Shimazaki et al., 1986]. The K-Ah ash bed is vertically offset 8.8 m by the Kaminada-south fault and 7.4 m by the Kaminada-north fault (Figure 2.4). These values give vertical slip rates of more than $1 \text{ mm/}^{14}\text{C yr}$ for these faults, which are at least twice as large as those for the MTL onshore. In many of the profiling records, sediments on both sides of the faults are sharply dragged toward the faults with little vertical separation, a feature characteristic of strike-slip faults observed on trench walls and profiling records. This led Ogawa et al. [1992] to suggest that the faults in the Sea of Iyo have a significant strike-slip component of displacement.

Paleoseismology

As of 1994, more than 10 excavations have been logged and described on the Tsunden, Chichio, and Okamura segments. For the Sea of Iyo segment, acoustic profiling and piston coring surveys were conducted by Ogawa et al. [1992]. We briefly describe the results of these paleoseismological studies from east to west. Trenches across the Tsunden and Chichio segments are described here for the first time. The paleoseismological studies across the Okamura and Sea of Iyo segments are briefly reviewed from Tsutsumi et al. [1991], Ogawa et al. [1992], and Yamazaki et al. [1992]. In these descriptions, we designate the most recent surface-rupturing earthquake for each segment as event A and successively older earthquakes as events B, C, and D.

Tsunden Segment

A trench was logged across the Tsunden segment at Donari (Figure 2.3c) in 1991 and is called trench 1 in this paper. The sediments exposed on the walls in trench 1 are offset along a gently north dipping fault zone (Figure 2.5). The dip of faults as low as 30° is uncommon for the MTL; faults more commonly dip steeper than 70° in other trenches [Tsutsumi et al., 1991; Yamazaki et al., 1992]. This gentle dip appears to be a localized feature associated with a restraining double bend immediately east of the trench site (Figure 2.3c). Primary sedimentary and deformational structures are preserved in the walls of trench 1, except for an artificially modified zone and cultivated soil for rice farming immediately below the present ground surface (Figure 2.5). The sediments on the south side of the fault zone consist of loose, poorly sorted gravels with interbedded sand and silt. Two ^{14}C analyses of organic soil samples (C1E-1 and C1E-3) indicate that these are middle

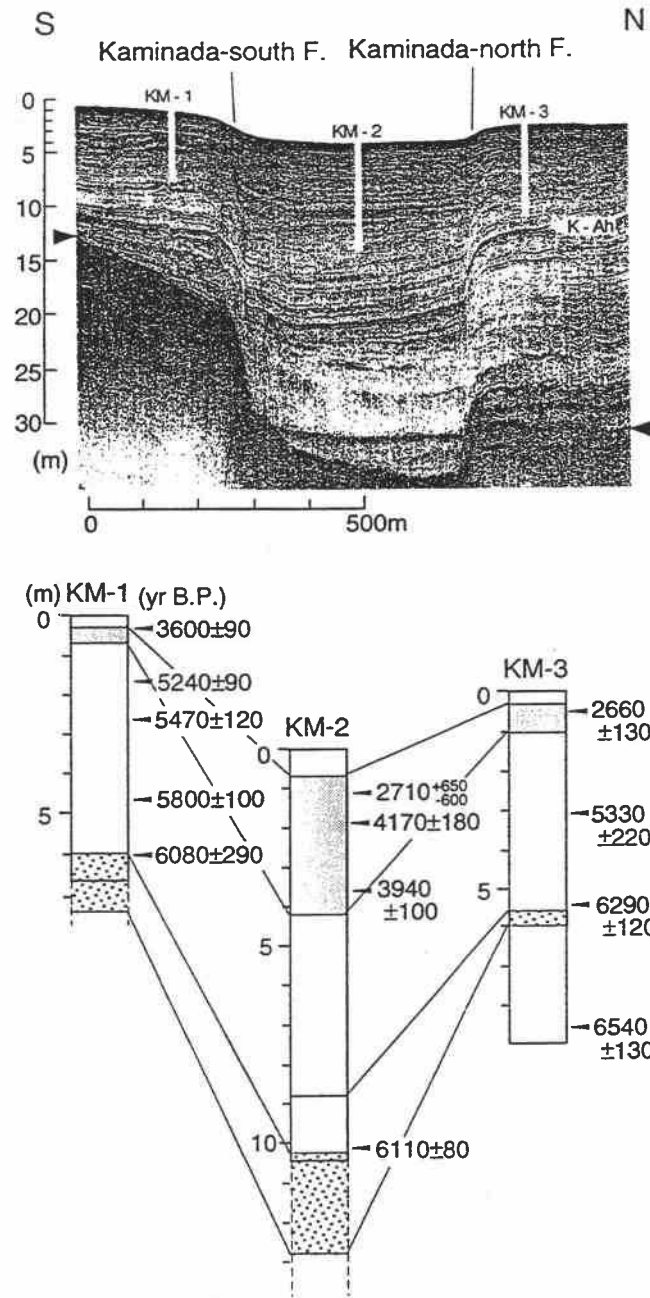


Figure 2.4 Acoustic profiler record across the Sea of Iyo segment (top) and correlation of three cores with 2σ radiocarbon ages (bottom) modified from Ogawa et al. [1992]. See Figure 2.3h for location. KM-1 to KM-3 denote piston core samples. K-Ah and solid triangles in top part identify an ash layer dated at 6300 years B.P. and acoustic basement, respectively. Shaded portions in bottom part indicate sediments with abrupt thickness change across the faults, i.e., layers related to earthquakes. Top of the lower thickened layer in KM-1 and KM-2 does not exactly correlate to that in KM-3. Radiocarbon ages indicate the time of two seismic events as about 6200 years B.P. and 4000 years B.P.

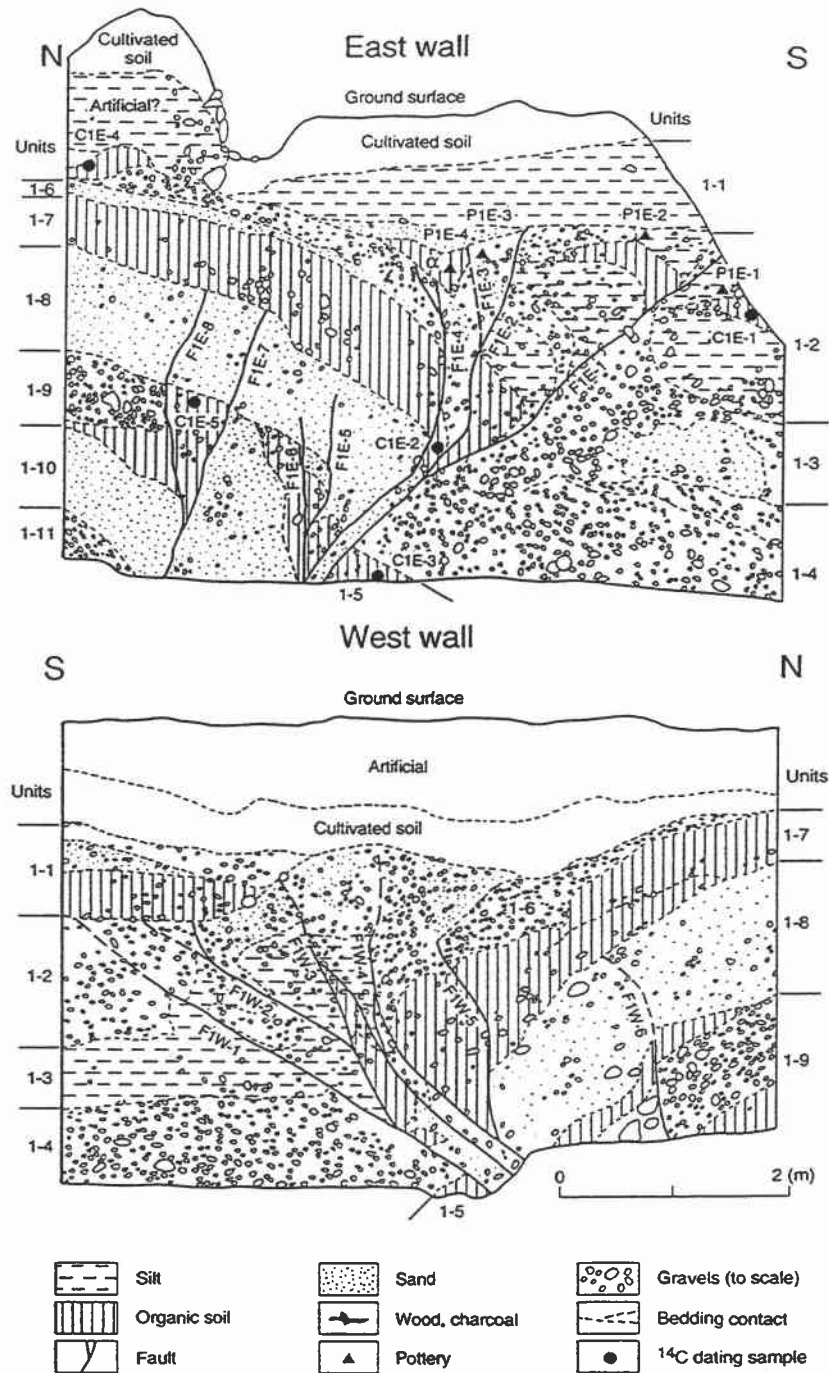


Figure 2.5 Log of the east and west walls in trench 1 across the Tsunden segment at Donari. Faults, units, pottery fragments, and ¹⁴C dating samples are numbered. All pottery was used during or after a Japanese historical period between the 13th and 16th century A.D. Radiocarbon ages (years B.P.) are C1E-1, 1300 ± 80; C1E-2, 7220 ± 260; C1E-3, 6450 ± 200; C1E-4, 710 ± 80; C1E-5, 7630 ± 290. See Table 2.1 for calibration of these ages to calendar dates. Layer α provides stratigraphic evidence for event B; the layer overlies a fault labeled F1E-4 and is cut by a fault labeled F1E-3 which ruptured during event A. Stratigraphic evidence for at least three and possibly four episodes of faulting is identified in this log. See Figure 2.3c for location of the trench.

to late Holocene sediments (Table 2.1). In contrast, the sediments on the north side of the fault zone are finer grained with abundant soil organic matter. The fine sand of unit 1-8 contains reworked volcanic glass of the K-Ah ash (6300 years B.P.), whereas that of unit 1-10 contains reworked glass of the AT ash (21,000-25,000 years B.P.) but no glass of the K-Ah ash. These are consistent with a ^{14}C age of 7630 ± 290 years B.P. (C1E-5) from intervening unit 1-9. These data indicate that the sediments north of the fault zone were deposited in latest Pleistocene to late Holocene time. The sense of apparent displacement across the fault zone is down to the south, suggesting that south facing scarps have ponded the thicker loose gravels to the south.

We identified evidence for three and possibly four surface-rupturing earthquakes on the Tsunden segment in trench 1. The youngest deformation event (event A) breaks all the sediments except for cultivated soil and underlying unit 1-1 along three faults, labeled F1E-1 to F1E-3 on the east wall and along four faults, labeled F1W-1 to F1W-4 on the west wall (Figure 2.5). The faults on the east wall cut layers containing pottery fragments (P1E-1 to P1E-4) which were used during or after a Japanese historical period between the 13th and 16th century A.D. This indicates that the most recent event on the Tsunden segment occurred during or after the oldest possible age for the pottery, the 13th century A.D. Immediately north of F1E-3, a fault labeled F1E-4 terminates below and is overlain by organic soil layer α containing a pottery fragment located at P1E-4. On the west wall, a fault labeled F1W-5 cuts unit 1-6 but does not propagate upsection as high as the faults to the south. This stratigraphic relation suggests an earthquake (event B) separated from event A. Evidence for events C and D are preserved north of the faults that ruptured in the younger events. Faults, labeled F1E-7, F1E-8, and F1W-6, break fine sand of unit 1-8 and are overlain by organic soil of unit 1-7. Though the vertical separation across the fault traces is less than a few centimeters, the upward termination of multiple fault traces at the same stratigraphic horizon is interpreted as evidence for event C. Faults, labeled F1E-5 and F1E-6 on the east wall, break only the lower part of unit 1-8 and may be evidence for event D. However, there is no comparable fault on the west wall. Some fault traces may die out during propagation and may not reach the surface during an earthquake. F1E-5 and F1E-6 terminate within a mapped stratigraphic horizon and could be remnants of event C. In summary, this trench contains evidence for three and possibly four surface-rupturing earthquakes on the Tsunden segment during and after the deposition of unit 1-8 (6300 years B.P.); the most recent event occurred during or after the 13th century A.D.

Table 2.1 Radiocarbon dates for samples from trench 1 (Tsunden segment) and trench 2 (Chichio segment)

Sample ^a	¹⁴ C Age, ^b years B.P.	Calendar Date ^c	Description
C1E-1	1300±80	630-890 A.D.	charcoal
C1E-2	7220±260	5750-6350 B.C.	organic soil
C1E-3	6450±200	5190-5580 B.C.	organic soil
C1E-4	710±80	1220-1400 A.D.	organic soil
C1E-5	7630±290	6140-6750 B.C.	organic soil
C2-1	2250±130	80-440 B.C.	charcoal

^aSamples labeled C1E-1 to C1E-5 were analyzed at Teledyne Isotopes (TI), and sample labeled C2-1 was analyzed at University of Hiroshima (UH). All samples were dated by conventional radiocarbon analysis.

^bCalculations assume a Libby half-life of 5568 years (TI) and 5570 years (UH). Uncertainties are 2 standard deviation counting errors.

^cDendrochronologically calibrated calendar age by Method A from program of *Stuiver and Reimer* [1993], with 2 standard deviation uncertainty. Dates are rounded to nearest 10 years.

Table 2.2 Summary of event dates of the Okamura segment

Event	<i>Tsutsumi et al.</i> [1991] (1984, 1988 Spring)	<i>Yamazaki et al.</i> [1992] (1988 Summer)
A	early 8th century A.D.	4th-7th century A.D.
B	2820-3250 years B.P. (970-1480 B.C.) ^a	circa 2000-3000 years B.P.

^aDendrochronologically calibrated calendar age by Method A from program of *Stuiver and Reimer* [1993], with 2 standard deviation uncertainty. Dates are rounded to nearest 10 years.

Chichio Segment

A 4-m-deep trench (trench 2) across the Chichio segment at Kamikirai was logged in 1991 into floodplain sediments of the Higaidani River (Figure 2.3d). The sediments are latest Holocene fluvial deposits ranging in texture from medium-grained sands to gravels (Figure 2.6). The sense of apparent displacement across the fault zone is down to the south, consistent with Holocene scarps 100 m to the west. The sediments in this trench contain evidence of two episodes of surface faulting along a 2-m-wide fault zone. The fault trace which ruptured in the most recent event (F2-1) offsets all the sediments except for an artificially modified zone immediately below the ground surface (Figure 2.6). Near the top of the fault trace, V-shaped silty deposit β is distinct in texture and color from other fluvial sediments. This deposit is interpreted as cultivated soil for rice farming which filled a coseismic fissure during or immediately after the most recent surface-rupturing earthquake on the Chichio segment. From this deposit, we obtained a pottery fragment (P2-1) which was identified as the mould of a Buddhist artifact used around the 16th century A.D. This age constrains the time of event A on the Chichio segment to be during or after the 16th century A.D. Another fault trace farther south (F2-2) cuts the gravels of unit 2-4 and is overlain by medium-grained sands of unit 2-3. Charcoal fragments (C2-1) embedded in the uppermost part of unit 2-4 were dated at 2250 ± 130 years B.P. This ^{14}C age, calibrated to a 2σ calendar age of 80-440 B.C. (Table 2.1), is consistent with pottery fragments (P2-2 to P2-4) of Yayoi age (approximately between 300 B.C. and 300 A.D.) obtained from the same horizon and thus constrains the oldest possible age for event B.

Interpretation of 1:8000-scale color aerial photographs and 1:1000-scale topographic maps, both prepared for the construction of the Shikoku Highway, led us to identify a series of right-laterally offset rice paddy dikes (I-V in Figure 2.7) east of trench 2 at Kamikirai. These offset dikes are aligned exactly on the eastern projection of a south facing fault scarp 100 m to the west and the faults exposed in trench 2. Because we believe these artificial features to have been straight originally, the present configuration of these dikes may record one or more episodes of surface faulting after rice farming was introduced to Shikoku, presumably more than 1500 years ago. Field measurements of these offsets by a tape are 7.0 m (I), 12.9 m (III), 6.2 m (IV), and 7.6 m (V). The aerial photograph interpretation and field observations suggest that dike II was artificially modified, and thus its deflection point is located 10 m north of the projected fault trace. The asphalt access road to the house between dikes IV and V may have been constructed on an offset rice paddy dike. Three of the offsets are 6.9 ± 0.7 m, and the other is close to twice

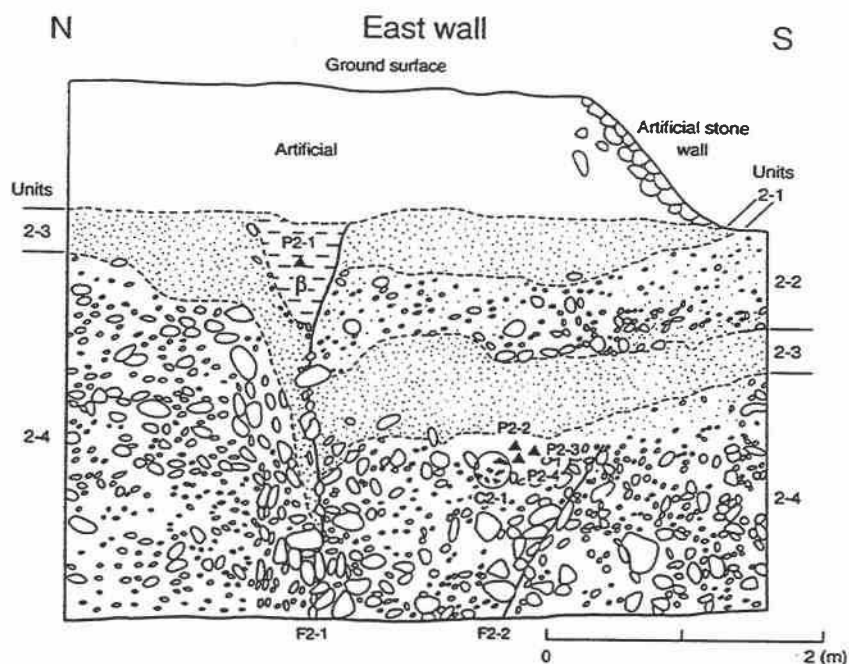


Figure 2.6 Log of the east wall of trench 2 across the Chichio segment at Kamikirai. View is toward the east. Faults, units, pottery fragments, and a ^{14}C dating sample are numbered. Pottery P2-1 was used around the 16th century A.D., and pottery fragments P2-2 to P2-4 are of Yayoi age (between approximately 300 B.C. and 300 A.D.). Charcoal of C2-1 was dated at 2250 ± 130 years B.P. See Table 2.1 for calibration of this age to a calendar date. Sediments are offset by two episodes of faulting. Deposit β near the top of the fault trace is interpreted as cultivated soil for rice farming which filled a coseismic fissure during or immediately after the most recent surface-rupturing earthquake on the Chichio segment. Flat clasts are steepened to near vertical along the fault zone. See Figure 2.3d for location of the trench and Figure 2.5 for symbol legend.

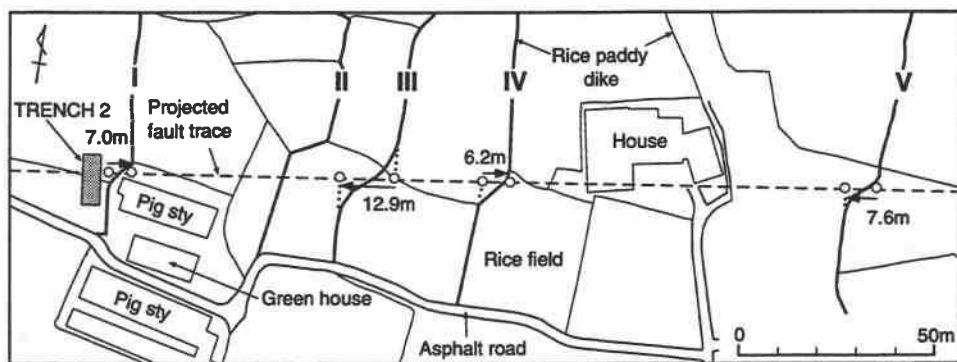


Figure 2.7 Right-laterally offset rice paddy dikes (I to V) aligned on the projected fault trace of the Chichio segment at Kamikirai. Projection is based on a fault scarp located 100 m west of this figure and faults exposed in trench 2. Rice paddy dikes II and III bound an abandoned stream channel of the Higaidani River. Base map from Japan Highway Public Corporation.

that value. We interpret the smaller value to be the slip associated with event A, and the larger value to be the cumulative slip of events A and B, as identified in trench 2.

Okamura Segment

Alluvial fan deposits exposed in a trench across a fault may not record all surface faulting episodes because alluvial fan surfaces are subject to catastrophic erosion and/or nondeposition. One way to counter this problem is to excavate multiple sites and integrate the results. We have excavated three sites on the Okamura segment at Iioka (Figure 2.3g), and the results were reported by Tsutsumi et al. [1991] and Yamazaki et al. [1992]. Tsutsumi et al. [1991] discussed trenches excavated in 1984 and in the spring of 1988, while Yamazaki et al. [1992] analyzed a suite of trenches excavated in the summer of 1988. In what follows, we briefly summarize the results.

In all trench sites, the latest Pleistocene to Holocene sediments are offset by multiple episodes of faulting along vertical to steeply south dipping faults. The dates of the most recent and penultimate events, obtained by Tsutsumi et al. [1991] and Yamazaki et al. [1992], are summarized in Table 2.2. There is a disagreement on the time of event A. All trench sites contain convincing stratigraphic evidence that the most recent rupture was no earlier than the 4th century A.D., but neither of the previous studies presented convincing evidence to constrain the youngest possible date of event A.

Tsutsumi et al. [1991] reported the date of event A as the early 8th century A.D. (Table 2.2). The oldest possible date of event A is constrained by a faulted bed in the 1984 trench, which contains a pottery fragment produced during or after the 8th century A.D. Because there is no historical record of destructive earthquakes along the MTL in central Shikoku, Tsutsumi et al. [1991] concluded that the Okamura segment ruptured prior to the middle to late 8th century A.D., the time that historical documentation of destructive earthquakes of Usami [1987] increased dramatically. However, the assumption used by Tsutsumi et al. [1991] that all historical destructive earthquakes on the MTL since the middle 8th century A.D. were documented by local residents and catalogued by Usami [1987] is invalid. Our trenching shows that the MTL in eastern Shikoku ruptured during or after the 16th century A.D., though there are few historical documents reporting a large earthquake on that part of the MTL in the past 500 years [Usami, 1987]. We also cannot eliminate the possibility that parts of the faulted deposit that contains the pottery produced during or after the 8th century A.D. have been artificially modified since this deposit is immediately below present cultivated soils.

In the summer of 1988 excavation, unfaulted beds containing a pottery fragment produced during or after the 7th century A.D. were interpreted by Yamazaki et al. [1992] to

constrain the time of event A as the 4th-7th century A.D. However, it is the youngest possible date of this pottery, not the oldest possible date, that constrains the youngest possible date of event A. This type of pottery, called Sue-ki, was produced until the end of the 12th century A.D. in Shikoku (S. Tanabe, written communication, 1995), and this age constrains the youngest possible date of event A. In this paper, we use the time range of the 4th-12th century A.D. as the time for event A on the Okamura segment, which is a few hundred to a thousand years older than event A on the Chichio and Tsunden segments.

The date of event B is better constrained by Tsutsumi et al. [1991], which agrees with that determined by Yamazaki et al. [1992]. The date obtained by Tsutsumi et al. [1991] is recalibrated for this paper as 970-1480 B.C. using the program of Stuiver and Reimer [1993]. We use this date of event B in discussions below. By mapping sediments in three dimensions, Tsutsumi et al. [1991] identified a silt layer that tapered and pinched out in the trench site excavated in the spring of 1988. The pinch-out position of the layer has been offset right-laterally across the fault zone. The geometric restoration of the pinch-out positions led Tsutsumi et al. [1991] to estimate 5.7 m right-lateral slip in event A at this portion of the Okamura segment.

Sea of Iyo Segment

In addition to mapping offshore faults in the Sea of Iyo by an acoustic profiler, Ogawa et al. [1992] sampled three cores of 6.7 to 10.4 m length across a graben, using a piston corer. The cores were correlated with one another based on lithology, micropaleontology, and magnetic susceptibility, along with profiling records. To date individual seismic events, Ogawa et al. [1992] obtained thirteen ^{14}C ages, using both conventional and accelerator mass spectrometry (AMS) methods, on calcareous materials from the cores.

Three cores north of, within, and south of a graben in the Sea of Iyo segment (Figures 2.3h and 2.4) contain evidence for at least two surface-rupturing earthquakes [Ogawa et al., 1992]. In two stratigraphic layers, sediments are significantly thicker in KM-2, within the graben, than KM-1 and KM-3, outside of it, while in other layers, thickness of sediments is almost the same (Figure 2.4). Ogawa et al. [1992] inferred that the increased thickness of the two layers is due to surface rupture during earthquakes, producing a depression that was soon filled by younger sediments. Three ^{14}C ages from the lower thickened layer suggest that the older earthquake occurred about 6200 years B.P. [Ogawa et al., 1992]. The timing of the younger earthquake is constrained by five ^{14}C ages between 4170 and 2660 years B.P. from the upper thickened layer. In KM-2, samples from the middle and lower part of the layer yield similar ages of about 4000 years B.P.

This indicates that the 2-m-thick sediments were deposited in a short period of time, probably immediately after the younger faulting event. Therefore Ogawa et al. [1992] estimated the time of the younger event to be about 4000 years B.P. The depositional rate decreased dramatically around 5000 years B.P. from 5 mm/yr to 0.09 mm/yr, probably related to the change from a rising sea level in the early to middle Holocene to a stable sea level in the late Holocene [Ogawa et al., 1992]. Due to this slow depositional rate, stratigraphic evidence of faulting events younger than 4000 years B.P. is not preserved in the cored samples. Vertical offset associated with the older event is 3.5 m on the Kaminada-north fault and 1.6 m on the Kaminada-south fault, while the displacement associated with the younger event is 4.7 m and 7.1 m, respectively. The offset in the younger event is significantly greater than that in the older event and may be a cumulative offset of earthquakes at 4000 years B.P. and later [Ogawa et al., 1992]. In summary, the Sea of Iyo segment ruptured in 6200 years B.P., 4000 years B.P., and possibly sometime later with simultaneous movements of both faults bounding the graben.

Discussion

Correlation of the Most Recent Surface-Rupturing Earthquake on the MTL to a Historical Earthquake

Trench excavations on the Tsunden and Chichio segments on the southern margin of the Sanuki Range show that these segments ruptured during or after the 13th century A.D. and during or after the 16th century A.D., respectively. Because these segments are next to one another, it is possible that they ruptured simultaneously in a single earthquake. These results are rather surprising because the MTL was previously thought to be unruptured in historic time based on the absence of historical records of destructive earthquakes along the fault zone. Are the historical documents regarding the most recent large earthquake on the MTL in eastern Shikoku missing, or was the earthquake on the MTL attributed to other fault zones?

Among the historical earthquakes in the past 500 years recorded by Usami [1987], only the 1596 Keicho-Kinki earthquake was accompanied by a historical document suggestive of slip along the MTL in eastern Shikoku. This earthquake struck a large area of Kinki, including the ancient capital city of Kyoto and the economic center of Osaka (Figure 2.8), resulting in intensive damage to numerous castles, temples, and shrines [Usami, 1987]. The causative faults for this earthquake have been in debate. Tsukuda [1987] and Sangawa [1990] suggested rupture of the ENE trending Arima-Takatsuki Tectonic Line and NE trending Rokko fault system (Figure 2.8) based on distribution of archaeological sites with liquefaction features caused by this earthquake. On the other hand, close examination

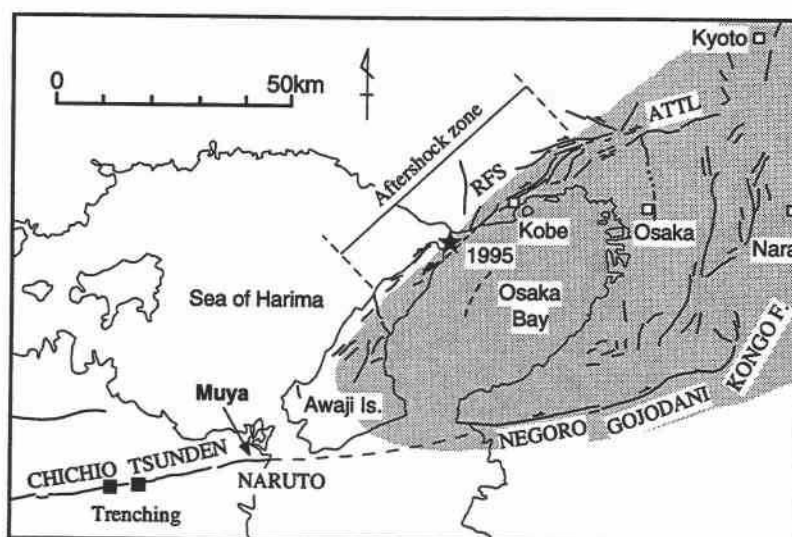


Figure 2.8 Map showing active faults in western Kinki and eastern Shikoku. After Research Group for Active Faults of Japan [1992]. Capital letters denote segments of the MTL. Location of the submarine segment of the MTL between Kinki and Shikoku is not well defined. Abbreviations are ATTL, Arima-Takatsuki Tectonic Line; RFS, Rokko fault system. Shaded area shows the meizoseismal region of the 1596 Keicho-Kinki earthquake after Usami [1987]. A historical document records coseismic uplift of the village of Muya, away from the meizoseismal region. Epicenter and aftershock zone of the M_w 6.9 Hyogo-ken Nanbu (Kobe) earthquake of 1995 are shown after Kanamori [1995].

of historical documents led some historians to suggest that north trending faults from Kyoto to Nara basins were the causative faults for this earthquake (K. Ishibashi, written communication, 1993). Away from the meizoseismal region, a historical document reports that the village of Muya on the north side of the Naruto segment in the eastern end of Shikoku (Figure 2.8) was uplifted during the earthquake and became a salt farm in a few years [Usami, 1987]. This document is suggestive of slip on the Naruto segment in the 1596 earthquake because it is the only active fault in this area which could account for this uplift [Ishibashi, 1989]. Since most large Japanese intraplate earthquakes rupture multiple segments, it is possible that the Tsunden and Chichio segments ruptured along with the Naruto segment during this earthquake. If this was the case, the 1596 Keicho-Kinki earthquake may have been a compound earthquake, rupturing faults in Kinki as well as the MTL in eastern Shikoku. However, some historians have disputed the credibility of the historical document reporting the uplift of the village of Muya during the earthquake (K. Ishibashi, written communication, 1993). The resolution of this problem awaits further identification of geologic evidence for the uplift, trenching on the Naruto segment, and further investigation of historical documents regarding this earthquake. On January 17, 1995, the M_w 6.9 Hyogo-ken Nanbu (Kobe) earthquake ruptured part of the Rokko fault system from northern Awaji Island northeastward to the City of Kobe (Figure 2.8) [Kanamori, 1995]. Trenching across the surface rupture in northern Awaji Island may give an insight into the causative faults for the 1596 earthquake.

Probable Rupture Length of Surface-Rupturing Earthquakes on the MTL

It is well known that fault rupture length, earthquake magnitude, and surface displacement are strongly correlated to one another [e.g., Matsuda, 1977; Bonilla et al., 1984; Wells and Coppersmith, 1994]. Of the three parameters, we were able to measure surface displacement of the most recent earthquakes on the Chichio and Okamura segments. This section discusses probable rupture length associated with these earthquakes based on the updated regression of rupture length on maximum displacement for strike-slip earthquakes by Wells and Coppersmith [1994]. In discussions below, the offsets we measured are assumed to represent the maximum displacements on these two segments.

The most likely rupture length for event A on the Chichio segment with a maximum displacement of 6.9 ± 0.7 m is 100-120 km, while that on the Okamura segment with a maximum displacement of 5.7 m is 100 km, based on the regression of Wells and Coppersmith [1994]. These values should be treated with caution, however. First, the variation in rupture lengths of historical earthquakes for a given displacement is large. For example, rupture lengths within one standard deviation associated with 6.9 m displacement

is 60-210 km. The 1906 San Francisco earthquake ruptured 432 km with a maximum displacement of 6.1 m, whereas the 1891 Nobi earthquake in Japan ruptured only 80 km with a maximum displacement of 8 m (all data are from Table 1 of Wells and Coppersmith [1994]). Second, Japanese intraplate surface-rupturing earthquakes tend to have shorter rupture lengths than the worldwide average for a given displacement. All Japanese historical strike-slip earthquakes with moment magnitude greater than 6.8 had significantly smaller rupture lengths than the most likely rupture length calculated from the regression of Wells and Coppersmith [1994] (Table 2.3). The estimated rupture length for event A on the Chichio and Okamura segments may be regarded as the upper bound of the probable rupture lengths for these earthquakes. Nonetheless, these estimated rupture lengths are significantly longer than the Chichio (22.5 km) and Okamura (20 km) segments. This indicates that ruptures probably extended to multiple segments by propagating through some of the proposed geometric segment boundaries, as is commonly observed for large strike-slip earthquakes worldwide [e.g., Barka and Kadinsky-Cade, 1988; dePolo et al., 1991]. In the preceding section, we suggested the possibility that the Tsunden, Chichio, and Naruto segments (total length of 50 km) ruptured simultaneously during the 1596 Keicho-Kinki earthquake.

Space-Time Distribution of Holocene Faulting

A chronology of surface-rupturing earthquakes on the MTL constructed mainly through trenching and piston coring is depicted in Figure 2.9. Our paleoseismological studies have not covered all segments of the MTL, yet Figure 2.9 shows some interesting patterns of faulting. The MTL may not rupture along its entire length in a single earthquake but instead consists of individual earthquake segments that rupture independently of one another. Overlapping of the time of event A on the Tsunden and Chichio segments suggests the possibility of simultaneous rupture during a large earthquake. In contrast, the last rupture on the Okamura segment took place in an earlier earthquake than event A on the Tsunden and Chichio segments. The trenching results do not allow us to distinguish whether event B on the Chichio segment and event A on the Okamura segment are separate events. Because the time of large earthquakes on the Sea of Iyo segment in the past 4000 years is not known, the relations of earthquakes on this segment to those on the Okamura segment remain ambiguous. If we assume that the Sea of Iyo segment breaks regularly and the most recent event occurred around 2000 years ago, this space-time diagram could be interpreted as eastward sweeping waves of fault activity [Ogawa et al., 1992], though the data points are too sparsely distributed. There could be two waves of activity, the first from 5000 to 2000 years ago and the second from 2000 to the most recent earthquake in eastern

Table 2.3 Historical strike-slip earthquakes in Japan with moment magnitude > 6.8

Earthquake	M_w^a	Most Likely Rupture Length, ^b km	Actual Rupture Length, ^b km	Maximum Displacement, ^a m
1891 Nobi	7.5	120	80	8
1927 Tango	7.1	65	14, 35 (depth)	3
1930 Kita Izu	6.9	75	35	3.8
1943 Tottori	7.0	40	4.7, 33 (depth)	1.5

^aFrom Table 1 of *Wells and Coppersmith* [1994].

^bBased on regression of rupture length on maximum displacement for strike-slip earthquakes worldwide by *Wells and Coppersmith* [1994].

Table 2.4 Comparison of active strike-slip faults with wide range of slip rates

Fault (Site)	Slip Rate, mm/yr ^a	Recurrence Interval, years	Maximum Displacement of Most Recent Event, meters	Seismic Moment of Most Recent Event, ^a $\times 10^{25}$ dyn cm
San Andreas (Wallace Creek) ^b	33.9±2.9	240-450	9.5	670 (1857 Fort Tejon)
Xianshuihe, China (Luhuo) ^c	15±5	150	1.0 (surface), 3.8 (depth)	180 (1973 Luhuo)
Xianshuihe, China (Daofu) ^c	15±5	77 (1904-1981)	1.0 (depth)	10.1 (1981 Daofu)
MTL (Chichio)	5-10	<2450	6.9±0.7	?
MTL (Okamura)	5-8	1300-2700	5.7	?
Nobi, Japan ^{d,e}	2	3000-4000	8	190 (1891 Nobi)
Tanna, Japan ^{f,g}	2	700-1000	2.5-3.5	24 (1930 Kita Izu)
Gomura, Japan ^{h,i}	0.04-0.14	>6000	2.5	46 (1927 Tango)

^a*Wells and Coppersmith* [1994].

^b*Sieh and Jahns* [1984].

^c*Allen et al.* [1991].

^d*Matsuda* [1974].

^e*Okada and Matsuda* [1992].

^f*Research Group for Active faults of Japan* [1991].

^g*Tanna Fault Trenching Research Group* [1983].

^h*Uemura* [1985].

ⁱ*Geological Survey of Japan* [1986].

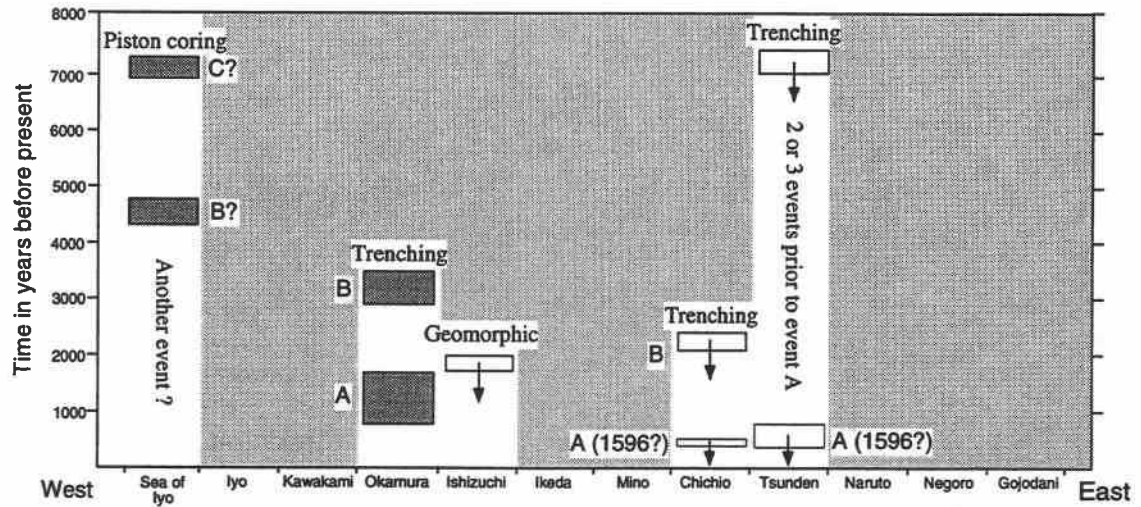


Figure 2.9 Space-time diagram of surface-rupturing earthquakes on the MTL during the past 8000 years. Horizontal axis is not to scale. Dark-shaded rectangles show time range of paleoearthquakes. Open rectangles with arrows show time range which constrain the oldest possible age for earthquakes. Earthquakes on each segments are labeled by A-C. Event A on the Tsunden and Chichio segments may correlate with the 1596 Keicho-Kinki earthquake. Light shading marks area and time range with no data. Radiocarbon ages are calibrated to calendar dates based on work by Stuiver and Reimer [1993].

Shikoku. Machette et al. [1991] reported similar waves of middle to late Holocene fault activity on the Wasatch fault zone.

Recurrence Interval of Large Earthquakes at Individual Sites Along the MTL

Recurrence intervals for successive large earthquakes at individual sites along the MTL are obtained for the Chichio, Okamura, and Sea of Iyo segments (Figure 2.9). The interval between events A and B on the Chichio segment is less than 2450 years (the oldest possible date for event B to the present). If the segment ruptured most recently during the 1596 Keicho-Kinki earthquake, the interval is less than 2050 years. The interval between events A and B on the Okamura segment is 1300-2700 years. The interval between successive events on the Sea of Iyo segment is 2000-3000 years. Average recurrence interval on the Tsunden segment is 1500-2100 years based on three or possibly four earthquakes after the deposition of the K-Ah ash (6300 years B.P.).

In addition to this direct method, the average recurrence interval at individual sites may be calculated based on slip rate and amount of displacement associated with an earthquake by assuming that a characteristic earthquake recurs periodically on each segment. Bard et al. [1990] suggested that ^{14}C ages in the range of 10,000-20,000 may be as much as 3500 years too young based on the comparison of ^{14}C ages with U-Th ages on corals from Barbados. This suggests that the slip rate of the MTL in eastern Shikoku may be 4-9 mm/yr, slightly lower than the 5-10 mm/ ^{14}C yr rate reported by Okada [1970]. Using this preliminary, calibrated slip rate of 4-9 mm/yr and 6.9 ± 0.7 m displacement associated with the most recent event, an average recurrence interval for large earthquakes on the Chichio segment is calculated as 700-1900 years. Similarly, a preliminary, calibrated slip rate of 4-7 mm/yr and 5.7 m displacement associated with the most recent event [Tsutsumi et al., 1991] give an average recurrence interval for large earthquakes on the Okamura segment of 800-1450 years. In summary, we estimate the recurrence interval of large earthquakes at individual sites along most of the MTL on Shikoku to be between 1000 and 3000 years. There is probably no section of the fault zone in western Kinki and Shikoku where large earthquakes recur on the order of a few hundred years or tens of thousands of years.

The MTL is characterized by a relatively long recurrence interval and large surface offset per event. Kanamori and Allen [1986] pointed out that for a given magnitude, earthquakes with long recurrence intervals have shorter rupture lengths than those with short recurrence intervals. In the diagrams of Kanamori and Allen [1986], large intraplate earthquakes in Japan are characterized by short rupture lengths with long recurrence intervals. For example, the 1927 Tango, Japan, and 1976 Motagua, Guatemala,

earthquakes had almost the same M_s but significantly different rupture lengths (35 and 250 km, respectively). The recurrence interval is several thousand years for the Tango earthquake and 180-755 years for the Motagua earthquake [Kanamori and Allen, 1986]. The shorter rupture length for a given magnitude, in turn, suggests a large stress drop associated with greater strength of the fault zone [Kanamori and Allen, 1986]. In the asperity model, a high stress drop may be related to faults with low slip rates because they have more irregular fault traces, permitting greater elastic strain accumulation between successive earthquakes. This indicates that faults with low slip rates are able to generate large earthquakes, though recurrence intervals of those events are relatively long. Table 2.4 compares recurrence interval, displacement per event, and seismic moment associated with historic earthquakes on faults of various slip rates. The seismic moment for the 1891 Nobi, Japan, earthquake is comparable to that for the 1973 Luhuo, China, earthquake even though the slip rate of the Nobi fault system is less than one fifth that of the Xianshuihe fault system. Geomorphic expression of the Gomura fault, Japan, is largely obscured due to its low slip rate [Uemura, 1985; Research Group for Active Faults of Japan, 1991], but it was capable of generating the 1927 Tango earthquake with a moment magnitude of 7.1. The Tanna fault in the Izu Peninsula, Japan (Figure 2.1), appears to be exceptional among Japanese intraplate faults, characterized by a short recurrence interval relative to its slip rate. Wesnousky [1988] pointed out that the complexity of fault traces is a function of cumulative geological offset. The right-lateral offset of stream channels along the MTL is no greater than 2 km [Okada, 1973a]. The relatively long recurrence interval at individual sites along the MTL may be related to irregular fault traces associated with this small cumulative offset.

Conclusion

This paper discusses segmentation and history of surface faulting events on the MTL by integrating published and new geological and paleoseismological data. The MTL in Kinki and Shikoku is geometrically divided into 12 segments, ranging from 10 to 40 km in length, separated by geometric discontinuities such as en echelon steps, bends, changes in strike, and gaps in the surface trace (Figure 2.3). Trench excavations across the Tsunden, Chichio, and Okamura segments revealed that these segments ruptured with recurrence intervals of 1000-3000 years in the late Holocene (Figure 2.9). The interval of successive earthquakes on the Sea of Iyo segment identified by piston coring was 2000-3000 years, slightly longer than that in eastern and central Shikoku. Because the most likely rupture lengths estimated from the amount of displacement for event A on the Chichio and Okamura segments are significantly larger than each segment, these events

probably ruptured more than one geometric segment. Large surface offset and relatively long recurrence interval suggest large seismic moment release during surface-rupturing earthquakes on the MTL, as commonly observed for large Japanese intraplate earthquakes. The Tsunden and Chichio segments ruptured most recently during or after the 13th century A.D. and during or after the 16th century A.D., respectively. These ruptures may be correlated to the 1596 Keicho-Kinki earthquake, but further geological as well as historical studies are needed to confirm this hypothesis.

Implications of this study for seismic hazard assessment for the MTL are summarized as follows. In central Kinki, the displacement on the MTL is transferred to north trending faults (Figure 2.3a), and this may pose a severe seismic risk to the densely populated area north of the MTL. A rupture on the MTL in western Kinki may cascade into the Kongo fault and other north trending reverse faults farther north, resulting in a $M=8$ earthquake rather than $M=7$, which would have a more serious effect on the Kyoto-Osaka-Kobe megacities. The space-time distribution of earthquakes on the MTL (Figure 2.9) gives insights in forecasting long-term behavior of the fault zone. The MTL may not rupture along its entire length in a single earthquake but instead consists of multiple earthquake segments that rupture independently of one another. The MTL in eastern Shikoku is not likely to generate a large earthquake in the next few hundred years based on the most recent rupture within the past 500 years and the average recurrence interval of 1000-3000 years. On the other hand, it would not be surprising if the Okamura and neighboring segments ruptured in the near future. For other parts of the MTL, a better assessment awaits direct dating of latest Holocene and especially the most recent events. Surface-rupturing earthquakes on the MTL appear to be characterized by a high stress drop, as is the case for other Japanese large intraplate earthquakes. High-frequency strong ground motion due to high stress drop should be regarded as plausible. Since the coseismic ruptures are likely to cross multiple geometric barriers, high energy release and strong acceleration at those barriers are also very likely in earthquakes along the MTL.

Acknowledgments

This paper is based on projects in which a number of people collaborated. We especially thank Masataka Ando, Shuichi Hasegawa, Hirofumi Kawakami, and Takashi Nakata for valuable discussions in the field. Tadahiko Makabe and Shozo Tanabe identified pottery obtained from trench excavations. The Japan Highway Public Corporation provided logistic and financial support for trenching. Masataka Ando, Kazuo Huzita, and Tokihiko Matsuda made research grants available for some trench excavations. This paper was substantially improved by constructive and critical reviews by Katsuhiko Ishibashi,

Yoshihiro Kinugasa, Peter Knuepfer, Carol Prentice, and Bob Yeats. Jessie Daligdig, Eikichi Tsukuda, and Akira Sangawa provided useful comments for an early version of the manuscript. English editing was provided by Bob Yeats.

**Chapter 3: Active and Late Cenozoic Tectonics of the Northern Los Angeles
Fault System, California**

Hiroyuki Tsutsumi, Robert S. Yeats, Cheryl Hummon, Craig L. Schneider*, and Gary J.
Huftile

Department of Geosciences, Oregon State University, Corvallis, Oregon 97331

*Present address: Phillips Petroleum Company, 6330 West Loop South, Bellaire,
Texas 77401

This paper was submitted to Geological Society of America Bulletin in June, 1995, and is
currently in revision

Abstract

The northern Los Angeles fault system is a series of surface and subsurface faults at the southern range front of the Santa Monica Mountains. It contains potentially seismogenic structures directly beneath major population centers of the Los Angeles metropolitan area. For a better assessment of seismic hazards, especially in search for blind thrust faults, we mapped active and late Cenozoic faults and folds in the northern Los Angeles basin, using an extensive set of oil-well and surface geologic data. The northern Los Angeles fault system developed through an early to late Miocene extensional regime and a Plio-Pleistocene contractional regime. The Santa Monica, San Vicente, and Las Cienegas faults were initiated as normal faults in the early to late Miocene and were later reactivated as reverse faults, suggesting that the orientation of reverse faults is largely controlled by Miocene extensional tectonics, rather than the Plio-Pleistocene stress field. The Santa Monica and San Vicente faults were a continuous Miocene left-oblique normal fault. Contractional tectonics began in early Pliocene time, with the reactivation of Miocene normal faults and initiation of reverse faults. Many Pliocene structures became inactive by the middle Pleistocene, and deformation in the middle to late Pleistocene is taken up by new active structures. These include the West Beverly Hills Lineament, Wilshire fault, and the active strand of the Santa Monica fault. The West Beverly Hills Lineament is the northernmost segment of the Newport-Inglewood fault zone, which may have propagated northward to the Santa Monica Mountains in the Quaternary. The active Santa Monica-Hollywood fault system is divided into distinct segments by the cross-cutting West Beverly Hills Lineament. The uplift and southward tilting of the oxygen-isotope substage 5e marine terrace north of the City of Santa Monica suggest an uplift rate of as large as 1.0 mm/yr for the Santa Monica Mountains. We estimate the dip of the Santa Monica Mountains blind thrust fault underlying and uplifting the Santa Monica Mountains as greater than 45°, based on the hypocentral location of the 1994 Northridge earthquake and near-surface geologic observations. These data suggest an average dip-slip rate of as large as 1.5 mm/yr for the Santa Monica Mountains blind thrust fault, which is two to four times less than a previously reported slip rate averaged over the past 2.0-3.0 million years based on a balanced cross section. Because the pattern of Quaternary deformation in the northern Los Angeles basin is considerably different from that of Pliocene deformation, a slip rate averaged over the past several million years is probably not representative of that in the late Quaternary. Crustal shortening across the northern Los Angeles fault system accounts for as much as half of a shortening rate of 5 ± 1 mm/yr between the San Gabriel Mountains and Palos Verdes Hills estimated using GPS observations.

Introduction

In the past decade, several moderate-size earthquakes, including the 1987 Whittier Narrows ($M_w=5.9$) and 1994 Northridge ($M_w=6.7$) earthquakes (Figure 3.1), highlighted the seismic hazards posed by blind thrust faults directly underneath the Los Angeles metropolitan area. The Northridge earthquake, for instance, ruptured a south-dipping reverse fault that had not been previously recognized as a major seismic source (Davis and Namson, 1994; Scientists of the U.S. Geological Survey and the Southern California Earthquake Center, 1994; Yeats and Huftile, 1995). Identifying potentially seismogenic blind thrust faults and estimating their slip rates are therefore critical in evaluating the seismic hazards of the Los Angeles metropolitan area. Although Los Angeles has been struck by only several moderate-size earthquakes in historic time, geologic and geodetic data indicate a deficit of seismic energy release (Hauksson and Stein, 1989; Hauksson, 1992; Dolan and others, 1995).

The northern Los Angeles fault system is one of the most important, potentially seismogenic structures in the Los Angeles metropolitan area because it is directly beneath a densely populated area with some of the most costly real estate in the world. Recent geological and geotechnical investigations of surface faults revealed that this fault system has been active in the late Quaternary (Hill, 1979; Crook and Proctor, 1992; Dolan and Sieh, 1992; Dolan and others, 1992, 1993). In addition to obtaining more paleoseismological data for surface faults, it was necessary to look at subsurface information to resolve the three-dimensional geometry, style and timing of deformation, and slip rate for a better assessment of seismic hazards from the northern Los Angeles fault system.

To accomplish this, we mapped the subsurface geology from the City of Santa Monica eastward to downtown Los Angeles based on an extensive set of more than 600 industry oil-well logs, many accompanied by paleontological reports. In this paper, we describe the subsurface extensions of active surface faults as well as Quaternary blind faults and folds in the northern Los Angeles basin. We estimate long-term slip rates for these structures based on surface and subsurface geologic observations. In addition, we define the timing, kinematics, and style of deformation of Miocene to Quaternary structures, and discuss the late Cenozoic tectonic evolution of the northern Los Angeles basin. We also discuss the interaction between the northern Los Angeles fault system and a proposed segment boundary, the Newport-Inglewood fault zone (Hauksson, 1987; Wright, 1991; Dolan and Sieh, 1992).

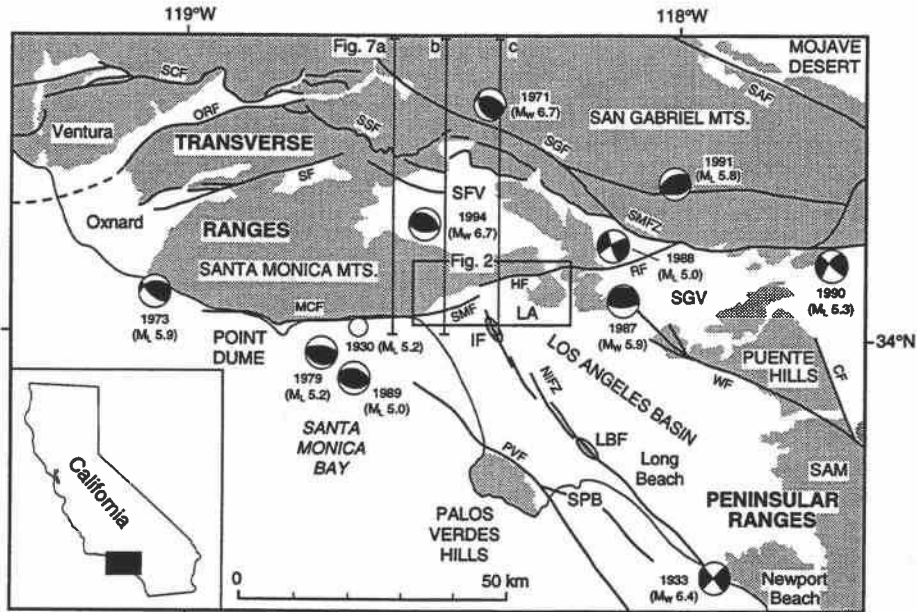


Figure 3.1 Map of the western Transverse Ranges, Los Angeles basin, and northern end of the Peninsular Ranges. Shaded area schematically illustrates hilly and mountainous region. Major late Quaternary faults are from Jennings (1994). Abbreviations for active faults: CF, Chino fault; HF, Hollywood fault; MCF, Malibu Coast fault; NIFZ, Newport-Inglewood fault zone; ORF, Oak Ridge fault; PVF, Palos Verdes fault; RF, Raymond fault; SAF, San Andreas fault; SCF, San Cayetano fault; SF, Simi fault; SGF, San Gabriel fault; SMF, Santa Monica fault; SMFZ, Sierra Madre fault zone; SSF, Santa Susana fault; WF, Whittier fault. The western half of the Oak Ridge fault (dashed) is concealed by Quaternary strata. Focal mechanisms of earthquakes with magnitude 4.9 or greater since 1970 are from Hauksson (1990, 1992). These include the 1971 San Fernando, 1973 Point Mugu, 1979 Malibu, 1987 Whittier Narrows, 1988 Pasadena, 1989 Malibu, 1990 Upland, 1991 Sierra Madre, and 1994 Northridge earthquakes. Focal mechanism of Long Beach earthquake of 1933 and epicenter of Santa Monica earthquake of 1930 are also shown from Hauksson and Gross (1991) and Hauksson and Saldivar (1986), respectively. Other abbreviations: IF, Inglewood oil field; LA, downtown Los Angeles; LBF, Long Beach oil field; SAM, Santa Ana Mountains; SFV, San Fernando Valley; SGV, San Gabriel Valley; SPB, San Pedro Bay. Location of Figure 3.2 and topographic profiles of Figures 3.7a to 3.7c is shown.

Regional Setting

Overview of the Study Area

The Los Angeles basin, one of several deep Cenozoic basins in southern California, locally contains more than 10 km of Neogene to Quaternary strata (Yerkes and others, 1965). The basin is affected by the interaction of east-striking reverse faults of the Transverse Ranges and northwest-striking right-lateral strike-slip faults of the Peninsular Ranges to the south (Figure 3.1). The southern boundary of the Transverse Ranges is also the northern boundary of the Los Angeles basin, marked by the active Malibu Coast-Santa Monica-Hollywood-Raymond fault system. A complex system of southeast- to northeast-striking faults is present in the subsurface south of the range front of the Santa Monica Mountains and this has been a site of extensive petroleum exploration and production.

The study area is bounded on the north by the east-northeast-trending range front of the Santa Monica Mountains and on the south by the Baldwin Hills, the northernmost of a set of en-echelon hills along the predominantly dextral Newport-Inglewood fault zone (Figure 3.2). The area includes oil fields explored and developed throughout this century: the Sawtelle, West Beverly Hills, Cheviot Hills, San Vicente, Sherman, East Beverly Hills, Salt Lake, South Salt Lake, Las Cienegas, and Inglewood fields (Figure 3.2). Inter-field exploratory core holes and wildcat wells provide data for the remainder of the study area.

The area is mostly covered by alluvial-fan deposits derived from the north as well as fluvial deposits of the ancestral Los Angeles River that formerly flowed through the Ballona Gap between the Cheviot Hills and Baldwin Hills (Figure 3.2). In some places, uplifted marine terraces stand above these fluvial deposits (Hoots, 1931; Dolan and Sieh, 1992). Analysis of the tectonic geomorphology, together with trenching and geotechnical investigations, led to the identification of several active surface faults (Figure 3.2). These are the east-northeast-striking Santa Monica and Hollywood faults at the southern margin of the Santa Monica Mountains (Hill, 1979; Wright, 1991; Crook and Proctor, 1992; Dolan and Sieh, 1992), the northwest-striking MacArthur Park fault north of downtown Los Angeles (Dolan and Sieh, 1992), and the north-northwest-striking West Beverly Hills Lineament along the eastern edge of the Cheviot Hills (Wright, 1991; Dolan and Sieh, 1992). The Santa Monica and Hollywood faults are part of the left-lateral strike-slip fault system marking the southern boundary of the Transverse Ranges (Figure 3.1). The West Beverly Hills Lineament is in line with a northern projection of the northwest-striking Newport-Inglewood fault zone (Wright, 1991; Dolan and Sieh, 1992).

The study area also contains late Cenozoic subsurface faults and folds that have little or no topographic expression (Figure 3.2). The topographic scarps along the Santa

Figure 3.2 Index map of the study area showing topography, surface and subsurface geologic structures, oil fields, and location of cross sections A-A' to G-G' (Figures 3.4a-3.4g). See Figure 3.1 for location of this figure. Topographic contour interval 50 m; contour altitudes in italics. Contours above 150 m in the Santa Monica Mountains are not shown. The range front of the Santa Monica Mountains approximately follows the 150 m contour. Surface faults are from Dolan and Sieh (1992). Abbreviations for surface faults: IF, Inglewood fault; SMF (active), active trace of the Santa Monica fault; WBHL, West Beverly Hills Lineament. Abbreviations for oil fields: CH, Cheviot Hills; EBH, East Beverly Hills; IN, Inglewood; LC, Las Cienegas; SA, Sawtelle; SH, Sherman; SL, Salt Lake; SSL, South Salt Lake; SV, San Vicente; WBH, West Beverly Hills. Subsurface structures are shown by shaded lines and letters. Shaded lines are fault plane contours with 500 m interval for subsurface faults: LCF, Las Cienegas fault; NSLF, North Salt Lake fault; SMF (inactive), inactive southern strand of the Santa Monica fault; SVF, San Vicente fault. Dashed lines represent fault tip lines for the blind Santa Monica, San Vicente, and Las Cienegas faults. Shaded lines with arrows north of the central trough denote trace of axial surface of monocline at the base of Repetto strata. X at Pacific Palisades shows the location of the outcrop of the active strand of the Santa Monica fault described by McGill (1989).

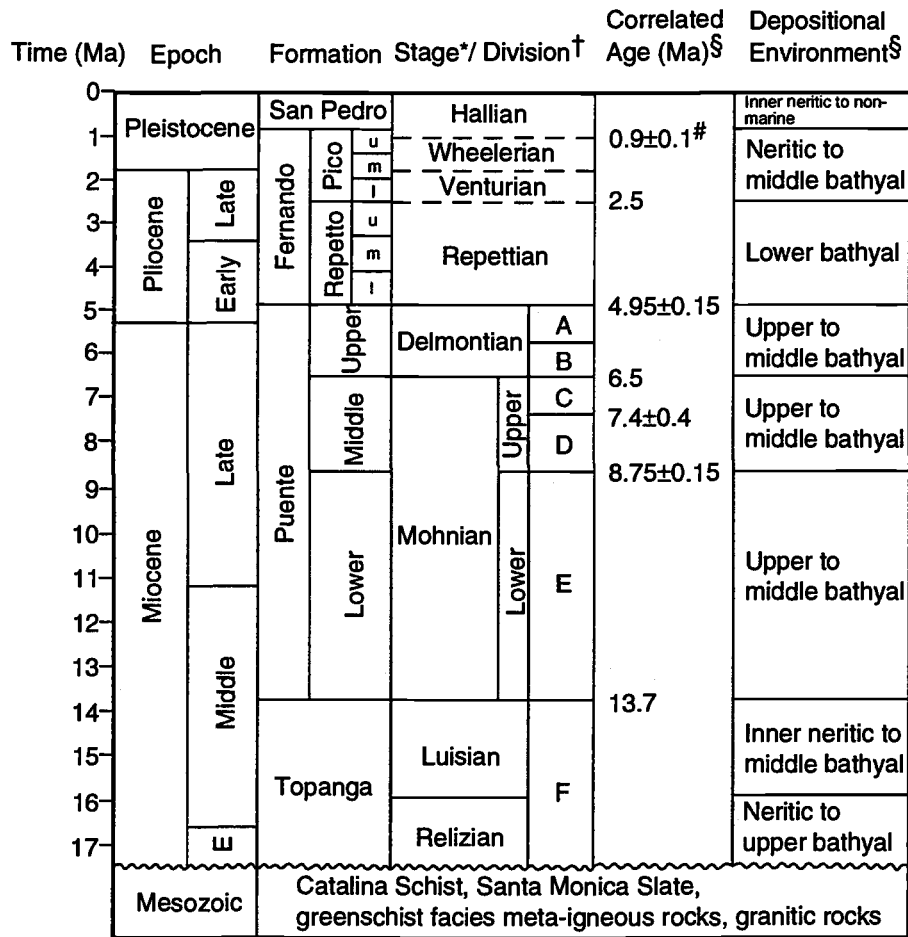
Monica fault are underlain by a series of subsurface faults (Barbat, 1958; Lamar, 1961; Wright, 1991). The East Beverly Hills and Las Cienegas oil fields are underlain by a northwest- to west-northwest-trending south-facing monocline and a secondary blind fault, the Las Cienegas fault. The San Vicente fault is an east-striking blind fault extending through the San Vicente and South Salt Lake oil fields (Schneider and others, 1996). We refer to the zone of these east-striking, surface and subsurface structures as the northern Los Angeles fault system. Historical and instrumental seismicity along the northern Los Angeles fault system is relatively low, with no recorded moderate-size earthquakes (Hauksson, 1990), except for the 1930 Santa Monica earthquake ($M_L=5.2$) which was interpreted to have occurred on the offshore extension of the Santa Monica fault (Figure 3.1; Hauksson and Saldivar, 1986).

The southwestern edge of the study area coincides with the northern edge of the western shelf (Figure 3.2), a structural high extending from the Newport-Inglewood fault zone west to the Palos Verdes Hills and south to San Pedro Bay (Figure 3.1; Wright, 1991). The northern end of the central trough lies between the Baldwin Hills and the East Beverly Hills-Las Cienegas monocline (Figure 3.2). The central trough extends southeast for ~50 km to the Santa Ana shelf and occupies the axial portion of the Los Angeles basin (Yerkes and others, 1965; Wright, 1991). The basement high north of the Las Cienegas fault is called the northern shelf (Figure 3.2; Wright, 1991; Schneider and others, 1996).

Stratigraphy

The distribution, thickness, lithology, and depositional environment of late Cenozoic strata document the structural evolution of the northern Los Angeles basin. We briefly describe the late Cenozoic stratigraphy of the study area (Figure 3.3), following the stratigraphic nomenclature of Blake (1991). The correlation of strata between oil fields in the Los Angeles basin has been based primarily on benthic foraminiferal biostratigraphy. However, as Wright (1991) and Ponti and others (1993) pointed out, the boundaries of benthic foram stages in the Los Angeles basin are time-transgressive, because the distribution of benthic foraminifera is controlled primarily by water depth. To minimize this problem, we use geologically instantaneous time markers, such as bentonite layers, for correlating strata between wells, rather than relying solely on biostratigraphic correlations.

Four types of crystalline basement rocks are found in the study area. Wells north of the West Beverly Hills oil field (Figure 3.2) reach dark gray to black slate correlated to the Santa Monica Slate of Jurassic to Early Cretaceous age (Yerkes and others, 1965; Yerkes and Campbell, 1979). The basement in the Chevron Laurel Core Hole No. 2 well, north of the Sherman oil field (Figure 3.2), is blue to black, marcasite-bearing slate that is also



* Pleistocene and Pliocene from Natland (1952), Miocene from Kleinpell (1938, 1980).

† Wissler (1943, 1958)

§ Blake (1991)

Hummon and others (1994)

Figure 3.3 Stratigraphic chart of the northern Los Angeles basin. Modified from Blake (1991).

correlated to the Santa Monica Slate. The slate is widely exposed in the Santa Monica Mountains north of the study area and is intruded on the east by granitic rocks of the Mesozoic Peninsular Ranges batholith. The western shelf is underlain by the Catalina Schist of Late Jurassic to Early Cretaceous age (Yeats, 1973; Sorensen, 1985), reached by two wells in the study area (Figure 3.2). The basement rocks in the Inglewood oil field are predominantly albite-chlorite-muscovite schist (Yeats, 1973), and those in the Las Cienegas oil field are predominantly gray to green, epidote- and albite-bearing chlorite schist and amphibolite (Yeats, 1973; Sorensen, 1985). These are greenschist facies meta-igneous rocks (Yeats, 1973).

Paleogene rocks are absent in the study area except for strata penetrated by the Morgan Brown U-6 No. 1 well in the San Vicente oil field. The strata are interpreted by Yeats (1973) as redbeds of Paleocene age and are very similar to strata exposed in Solstice Canyon north of Point Dume in the Santa Monica Mountains (Sage, 1973; Seedorf, 1983).

The basement is overlain unconformably by the early to middle Miocene (Relizian to Luisian stages) Topanga Formation (Figure 3.3). This is a heterogeneous sequence of well-indurated, coarse-grained sandstone interbedded with shale and siltstone (Blake, 1991). In wells in the Sawtelle oil field and in the Mobil Brentwood No. 1 well farther west, dark gray to black basalt is interbedded with the Topanga Formation. The basalt is also found in wells in the Inglewood oil field (Wright, 1991) and in the Morgan Brown U-6 No. 1 well (Schneider, 1994). This basalt is probably equivalent to the Conejo Volcanics exposed in the Santa Monica Mountains, radiometrically dated at 15.6 to 13.4 Ma (Weigand and Savage, 1993). The age of the top of the Topanga Formation has been estimated as 13.7 Ma (Blake, 1991). By the time of Topanga deposition, the western shelf was a basement high (Yeats, 1973; Wright, 1991). On the southwestern part of the shelf, the Topanga Formation is absent and the basement is overlain by a conglomerate of less than 80 m thick with clasts of the Catalina Schist known in the petroleum industry as the "Schist-conglomerate" (Wright, 1991).

The Topanga Formation is overlain by the middle Miocene to earliest Pliocene Puente Formation (Figure 3.3). The Puente Formation includes Mohnian-stage and Delmontian-stage strata (Blake, 1991). In the northern Los Angeles basin, lower Mohnian strata consist of less than a few hundred meters of bathyal glauconitic, phosphatic "Nodular Shale." The top of the "Nodular Shale" is correlated to the top of Division E of Wissler (1943, 1958), with an estimated age of 8.75 ± 0.15 Ma (Blake, 1991). The fine-grained, glauconitic lithology suggests slow deposition during the late middle to early late Miocene. The lithology of upper Mohnian strata (Divisions C and D of Wissler, 1943, 1958) varies within the study area. East of the West Beverly Hills Lineament, this interval is

characterized by medium- to coarse-grained feldspathic sandstone interbedded with sandy siltstone. This sequence is the distal end of the Tarzana submarine fan, one of two major late Miocene submarine fans entering the Los Angeles region from the north (Sullwold, 1960; Redin, 1991). In contrast, the same interval in the western part of the study area is finer-grained; massive sandstone beds, locally called "Rancho sand," occur only within overlying Delmontian strata (Divisions A and B of Wissler, 1958). Wright (1991) suggested that the Tarzana submarine fan gradually shifted westward from the East Beverly Hills-Las Cienegas area during late Mohnian time to the Sawtelle-Cheviot Hills area during Delmontian time. In the eastern part of the study area, Delmontian strata consist predominantly of interbedded diatomaceous siltstone and shale. The age of the tops of the Mohnian and Delmontian stages is estimated as 6.5 Ma and 4.95 ± 0.15 Ma, respectively (Blake, 1991).

Overlying the Puente Formation is the earliest Pliocene to early Pleistocene Fernando Formation, divided into the Repetto and Pico members (Figure 3.3). Repetto strata are characterized by fine- to coarse-grained sandstone interbedded with siltstone and shale that represent submarine fan deposition at lower bathyal water depth. The age of the top of Repetto strata is estimated at approximately 2.5 Ma (Blake, 1991). Pico strata consist of siltstone and mudstone interbedded with silty sandstone. The strata are in general finer-grained upward, representing a basin-filling sequence. Drastic southward thickening of Repetto and Pico strata across major structures documents rapid structural growth during the Pliocene and Pleistocene. Pico strata are overlain by much coarser-grained, marine sand and gravel, which are themselves overlain by alluvial and fluvial deposits. The age of the base of marine sand and gravel is estimated at 0.9 ± 0.1 Ma (Hummon and others, 1994).

Major Geologic Structures

Three structural trends are described separately here: the Santa Monica fault system, structures east of the West Beverly Hills Lineament, and the northern end of the Newport-Inglewood fault zone. Subsurface analysis of the Santa Monica fault system and the northern end of the Newport-Inglewood fault zone is presented here for the first time. We briefly summarize subsurface structures east of the West Beverly Hills Lineament that were previously the subject of more topical studies by Hummon and others (1994) and Schneider and others (1996).

Santa Monica Fault System

Faults at the southern range front of the Santa Monica Mountains were shown on the first fault map of California (Lawson and others, 1908), and later described by Hoots

(1931) on the basis of topography and the truncation of the south limb of the Santa Monica Mountains anticline. Subsurface data from subsequent oil exploration led to the identification of the north-dipping left-oblique-slip Santa Monica and Hollywood faults (Barbat, 1958; Lamar, 1961; Yeats, 1968; Campbell and Yerkes, 1976). The Santa Monica fault system, as used in this paper, refers to the zone of faults that extends from Santa Monica Bay eastward to the West Beverly Hills Lineament (Figure 3.2). We describe this fault system from west to east.

In Pacific Palisades, the Occidental Marquez E. H. No. 1 well penetrated a strand of the Santa Monica fault at a depth of 1300 m (Figure 3.4a). This fault brings Delmontian strata over middle Pico strata. The dip of the fault is unknown because only this well has penetrated the fault near the coast. The topographic scarps characterizing the active trace of the Santa Monica fault, locally called the Potrero Canyon fault, is north of and above the strand penetrated by the well (Figure 3.4a). This fault cuts oxygen-isotope substage 5e marine terrace deposits (~125 ka) that overlie Pico strata with angular unconformity; it is exposed in Potrero Canyon north of the City of Santa Monica (Figure 3.2; McGill, 1989). This fault dips northward at about 45° and has thrust Pliocene strata over upper Pleistocene marine terrace deposits. Vertical separation of 47 m on the stage 5e marine terrace platform (McGill, 1989) yields a late Quaternary vertical component of slip rate of approximately 0.4 mm/yr.

East of Pacific Palisades, the active trace of the Santa Monica fault is characterized by broad, south-facing scarps (Hill, 1979; Wright, 1991; Crook and Proctor, 1992). Recent geomorphologic studies by Dolan and Sieh (1992) found that the scarps exhibit a left-stepping, en-echelon pattern and terminate on the east against the West Beverly Hills Lineament (Figure 3.2). These scarps are 3-4 km south of the range front of the Santa Monica Mountains, whereas the Hollywood fault to the east lies at the mountain front (Dolan and Sieh, 1992). The en-echelon pattern of the scarps, coupled with stratigraphic evidence in trenches across the scarps, suggest that the fault has a significant strike-slip component of displacement (Dolan and Sieh, 1992; Dolan and others, 1992). Left-laterally offset streams along the Malibu Coast fault north of Point Dume (Dibblee, 1982; Drumm, 1992) suggest that strike-slip displacement along the Santa Monica fault should also be left-lateral.

North of the active trace, there must have been a Miocene to Pliocene fault at the range front of the Santa Monica Mountains to account for the vertical separation of the Santa Monica Slate that crops out in the mountains but is below well-control in the Sawtelle oil field (Figure 3.4c). In addition, Upper Cretaceous sandstone exposed widely in the Santa Monica Mountains is absent south of the postulated fault, whereas the Topanga

Figure 3.4 Cross sections (a) A-A' to (g) G-G' across major geologic structures of the study area. No vertical exaggeration. See Figure 3.2 for location of cross sections. Well numbers are identified in the Appendix. Wavy lines denote unconformity. Middle to late Quaternary strata are shown by dotted pattern: al, alluvial and fluvial deposits; mg, marine gravels. Upper Repetto strata are lightly shaded and lower Mohnian strata are darkly shaded. Dashed lines in upper Mohnian (Division C) strata in sections (b) and (c) schematically show the shape and axial surface of an overturned fold. Stratigraphic abbreviations: Rep, Repetto; Delm, Delmontian; Mohn, Mohnian. Pins in sections (c) and (d) show pin lines for crustal shortening calculations. In section (b), wells 2 and 3 directed northwest and are projected into the line of section. Location of topographic scarps of the Santa Monica fault and West Beverly Hills Lineament is from Dolan and Sieh (1992).

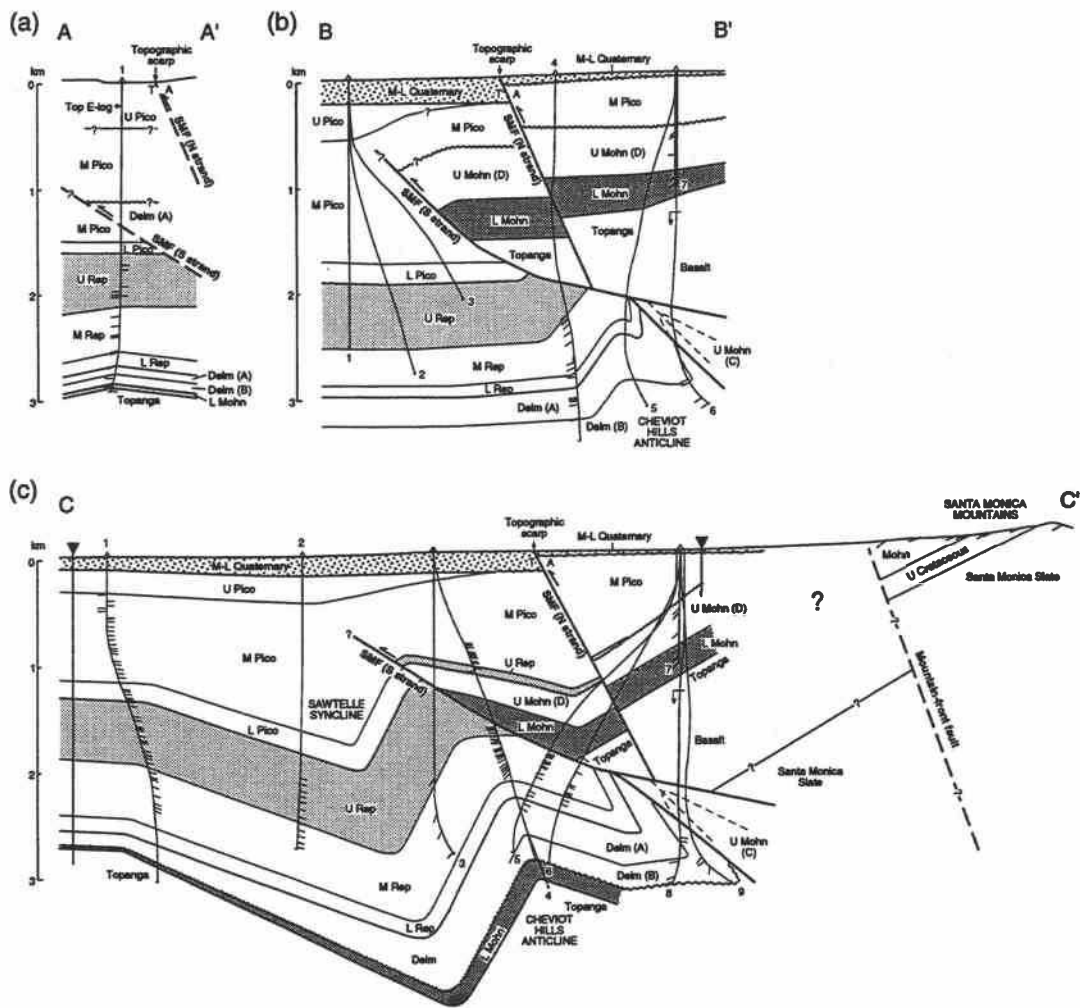


Figure 3.4

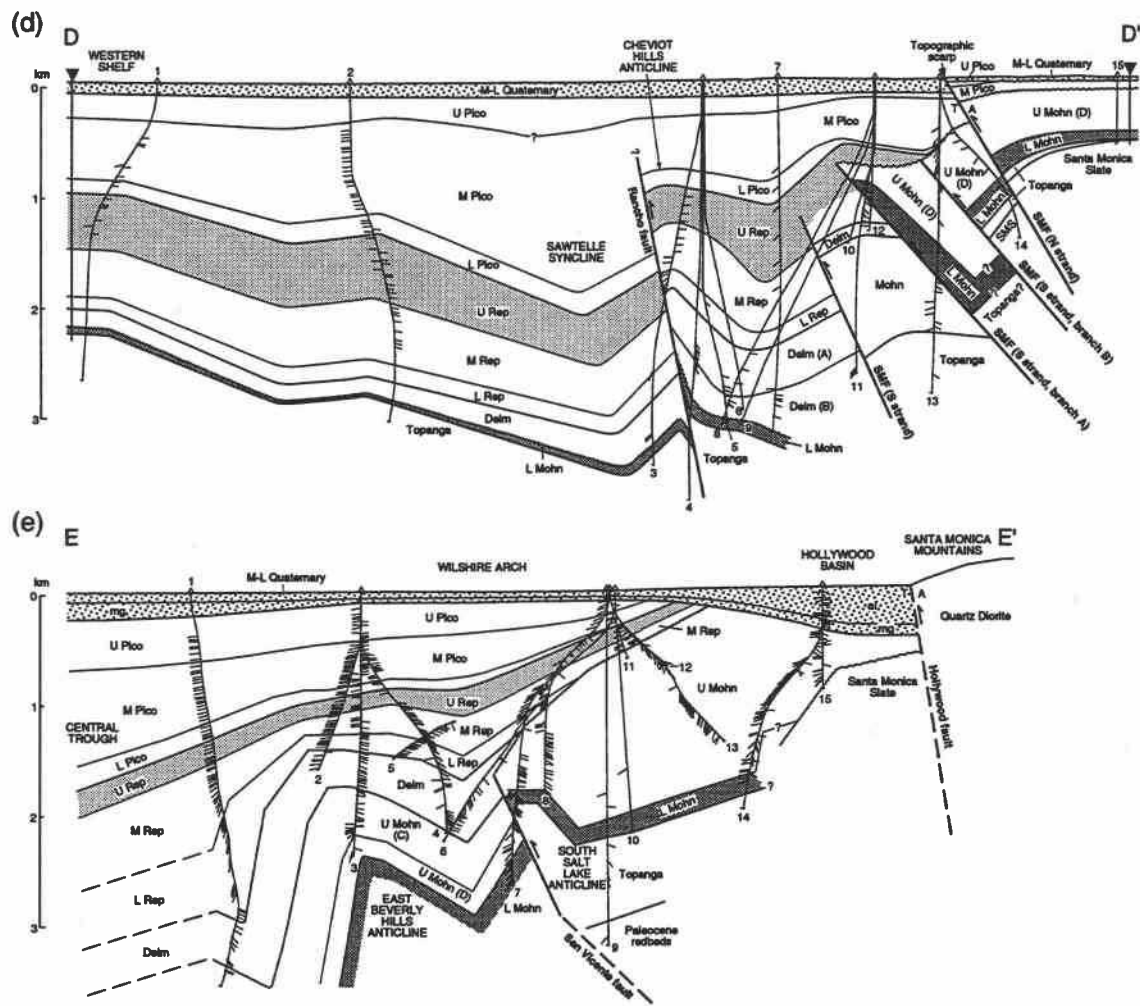


Figure 3.4 (Continued)

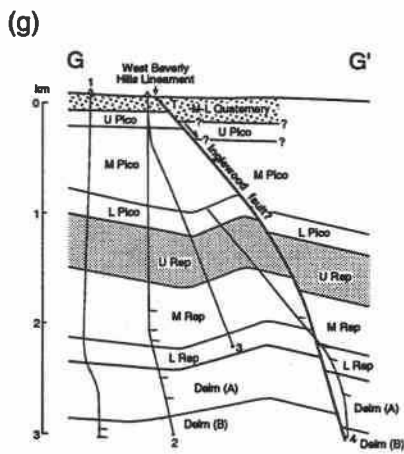
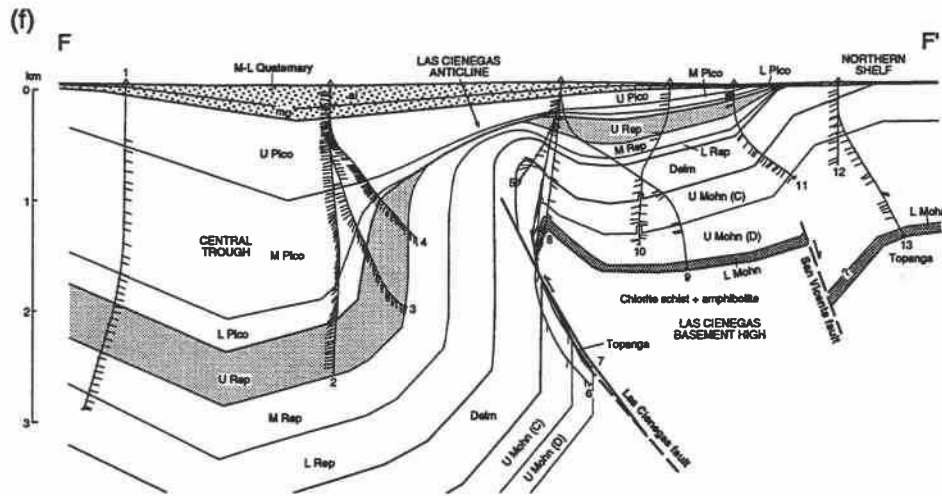


Figure 3.4 (Continued)

Formation greater than 1 km thick in the Sawtelle oil field is absent north of fault. The late Miocene Tarzana submarine fan is also offset 10-15 km left-laterally by the fault at the range front (Lamar, 1961; Redin, 1991).

Subsurface control on the Santa Monica fault system is found in the Sawtelle oil field and farther east. Wells in the Sawtelle oil field penetrated two strands of the Santa Monica fault (Figures 3.4b, 4c). The southern strand is the eastern continuation of the fault penetrated by the Occidental Marquez E. H. No. 1 well near the coast. This fault dips northward at 20°-40° and brings Mohnian strata over Pico strata. This strand is inactive because it is unconformably overlain by undeformed, middle to late Quaternary strata (Figures 3.4b, 4c). Below 2 km depth, there are two fault strands associated with an older period of displacement on the Santa Monica fault. The strata between these strands are fractured organic shale which is exotic to this part of the basin. They are strongly folded with an overturned south limb (C. Hatten, written communication, 1995). The structural relation between these strands suggests that the upper strand is younger. Upper Mohnian strata are present only on the north side of the southern strand of the Santa Monica fault, indicating that this was a normal fault during the middle late Miocene. In contrast, Delmontian strata are present only on the south side of the fault, and Repetto and Pico strata are much thicker on that side. In addition, the thick upper Mohnian strata are structurally higher on the north side of the fault (Figures 3.4b, 4c). This relationship indicates that the early normal fault was reactivated as a reverse fault after the latest Miocene (Figure 3.5).

Topographic scarps (Dolan and Sieh, 1992) are north of and above the inactive southern strand, as they are at Pacific Palisades, near the coast (Figures 3.4a-4c). The active, northern strand causing the scarps was identified in the National Aladdin Durso No. 1 well by the repeat of lower Mohnian strata (Figure 3.4b). This strand is an out-of-sequence fault that merges with the southern strand at a depth of about 2 km. The steep dip of the fault (60°-70°) is supportive of a significant strike-slip component of displacement proposed by Dolan and Sieh (1992). Vertical separation of both the middle to late Miocene Nodular Shale and the base of middle to late Quaternary strata is 200 m on the northern strand, indicating that this fault did not form until the middle Quaternary (Figure 3.5). The footwall of the southern strand contains the Cheviot Hills anticline and Sawtelle syncline (Figures 3.4b, 4c). Delmontian to lower Pico strata show no thickness variation across these structures, indicating that the folding postdates the late Pliocene but predates the deposition of middle Pleistocene strata. Because the southern strand truncates the Cheviot Hills anticline, the reverse faulting on this portion of the Santa Monica fault may not have started until early Pleistocene time.

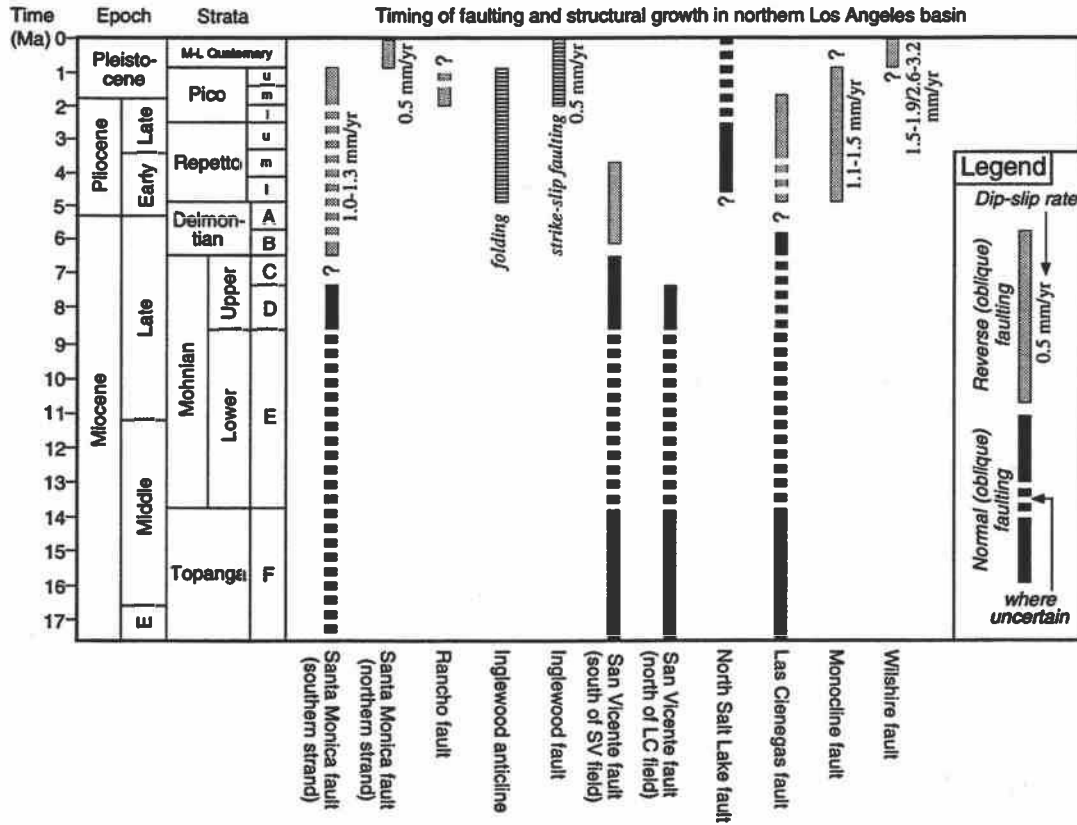


Figure 3.5 Timing of faulting and structural growth of principal structures in the northern Los Angeles basin. Compiled from Wright (1987), McGill (1989), Freeman and others (1992), Hummon (1994), Hummon and others (1994), Schneider and others (1996), and this study. Two inverse models yield slip rate of 1.5-1.9 mm/yr (reverse slip) or 2.6-3.2 mm/yr (right-reverse slip) for the Wilshire fault (Hummon and others, 1994).

East of the Sawtelle oil field, the southern strand of the Santa Monica fault branches into three strands (Figure 3.4d). The direct eastward extension of the southern strand in the Sawtelle oil field terminates the Delmontian Rancho sand (Division B) on the north. As in the Sawtelle oil field, Mohnian strata are thicker on the north side of the fault whereas Delmontian to Pico strata are thicker on the south side. Pico strata here are not offset by the fault, but the southward thickening of the strata indicates that this strand was an active blind fault during the late Pliocene to early Pleistocene. Branch A of the southern strand is in part parallel to bedding of Mohnian strata in the hanging wall (Figure 3.4d). The structure on the hanging wall may be a drag fold associated with normal faulting during the late Miocene. This fault also has thicker Delmontian to Pico strata on the south. North of branch B of the southern strand, the Santa Monica Slate is within well control, and middle Pico strata rest directly on upper Mohnian strata. The topographic scarps are north of and above these blind faults (Figure 3.4d), as they are farther west. However, there is no subsurface control for the active northern strand in the West Beverly Hills area. South of these faults, the Rancho fault dips 80° northward and cuts through the south limb of the Cheviot Hills anticline. This anticline extends northwest to the Sawtelle oil field and east to, but not across, the northern extension of the Inglewood fault (Figures 3.6a, 6b). The anticline in the Sawtelle oil field, however, is not cut by the Rancho fault within well control (Figure 3.4c). The Rancho fault appears to be a localized near-surface manifestation of the blind fault that caused the Cheviot Hills anticline. The thickness variation of strata across the anticline and fault (Figure 3.4d) illustrates major structural growth during the deposition of middle Pico strata (Figure 3.5). Middle to late Quaternary strata lie flat over the Rancho fault and southern strands of the Santa Monica fault (Figure 3.4d), indicating that the deformation here during this time interval is accommodated only by the northern strand of the Santa Monica fault, as is the case farther west.

Structures East of the West Beverly Hills Lineament

The southern edge of the Santa Monica Mountains east of the West Beverly Hills Lineament is sharply defined by the Hollywood fault with a series of linear scarps and faceted spurs (Figure 3.2; Wright, 1991; Dolan and Sieh, 1992). Geotechnical data indicate that the fault zone consists of steeply north-dipping fault strands (Dolan and others, 1993). While the overall geomorphic displacement across the fault zone is down-to-the-south, Dolan and others (1993) reported late Pleistocene buried soils with a down-to-the-north offset. These observations suggest that the Hollywood fault has a significant strike-slip (left-lateral) component of displacement, like the Malibu Coast and Santa Monica faults (Dolan and others, 1993). The Raymond fault to the east is also considered to be a

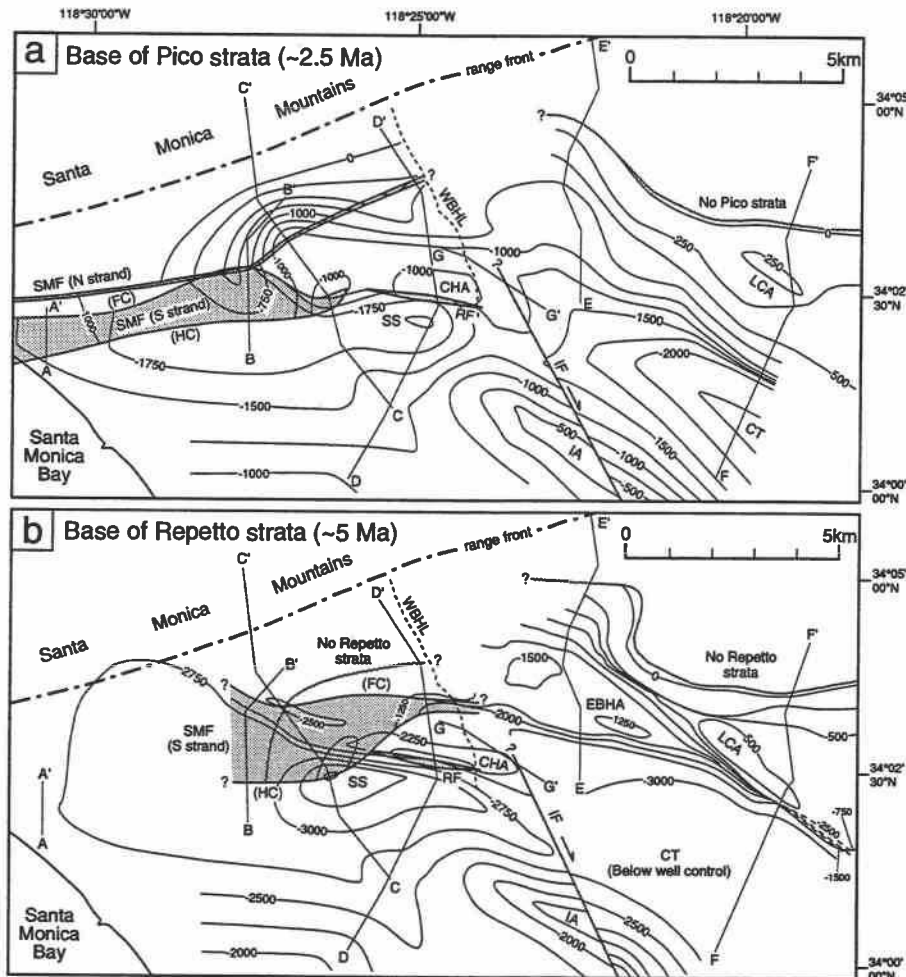


Figure 3.6 Subsurface structure contour maps (a) on the base of Pico strata (~2.5 Ma) and (b) base of Repetto strata (~5 Ma). Contour interval is 250 m. Below 1500 m depth in the East Beverly Hills and Las Cienegas areas in map (b), contour interval is 500 m. Contours are dashed where the base of Repetto strata is overturned. Abbreviations for faults: IF, Inglewood fault; RF, Rancho fault; SMF (N strand), northern strand of the Santa Monica fault; SMF (S strand), southern strand of the Santa Monica fault. FC and HC denote footwall cutoff and hanging wall cutoff of the southern strand of the Santa Monica fault. Half-sided arrows along the Inglewood fault (IF) show direction of strike-slip movement. Fault planes of the Rancho fault, and the southern and northern strands of the Santa Monica fault are shaded. Branches A and B of the southern strand of the Santa Monica fault are not shown for simplicity. Abbreviations for structural features: CHA, Cheviot Hills anticline; CT, central trough; EBHA, East Beverly Hills anticline; IA, Ingleswood anticline; LCA, Las Cienegas anticline; SS, Sawtelle syncline. Locations of cross sections A-A' to G-G', the West Beverly Hills Lineament (WBHL), and range front of the Santa Monica Mountains are shown for reference. Contours on the Ingleswood anticline are simplified from Wright (1987).

predominantly left-lateral strike-slip fault based on earthquake focal-mechanism solutions and offset streams (Bryant, 1978; Crook and others, 1987; Jones and others, 1990). Because of the absence of wells, the subsurface configuration of the Hollywood fault is poorly defined.

The Hollywood basin, with more than 300 m of middle to late Quaternary strata, lies immediately south of and parallel to the Hollywood fault (Figures 3.2, 3.4e; Hummon and others, 1994). East of the Sherman oil field, the Hollywood basin is bounded on the south by the North Salt Lake fault, a north-dipping ($\sim 60^\circ$) normal-separation fault subparallel to the Hollywood fault (Wright, 1991; Hummon, 1994). The North Salt Lake fault appears to converge eastward with the Hollywood fault (Wright, 1991), and may be a branch fault with an opposite sense of vertical displacement. Because the North Salt Lake fault is clearly expressed on a structural contour map of the base of fresh-water-bearing strata (Hill and others, 1979), it may extend upward very close to the surface. In the Texaco Hollywood Core Hole No. 1 well, the lowest Repetto strata dip $\sim 30^\circ$ south toward the North Salt Lake fault, whereas the dip at the Repetto-Pico contact is nearly horizontal, suggesting that Repetto strata may be growth strata related to Pliocene normal faulting on the fault (Hummon, 1994, plate 7). The normal faulting continued into Pleistocene time because Pico strata appear to be juxtaposed against Mohnian strata across the fault (Hummon, 1994).

The dominant structure east of the West Beverly Hills Lineament is a south-facing monocline (Figures 3.2, 3.4e, 3.4f). Systematic southward thickening of Repetto and Pico strata indicates that this monocline was active during the Pliocene and early Pleistocene (Figure 3.5). Schneider and others (1996) proposed that the monocline was caused by a blind reverse fault in the basement (Monocline fault) beneath well control. The thinning of uppermost Delmontian (earliest Pliocene) sandstone onto the crest of the East Beverly Hills anticline illustrates that the initiation of structural growth of the anticline is synchronous with the formation of the monocline (Schneider and others, 1996).

Similar to the southern strands of the Santa Monica fault, the San Vicente fault has significantly thicker and structurally higher upper Mohnian strata on the hanging wall (Figures 3.4e, 4f), suggesting that this was a normal fault during the late Miocene, subsequently reactivated as a reverse fault. The San Vicente fault and the southern strands of the Santa Monica fault align well across the West Beverly Hills Lineament and they may have formed a continuous normal fault in the late Miocene. The subsequent reverse slip on the San Vicente fault is much less than that on the Santa Monica fault; most of the crustal shortening east of the West Beverly Hills Lineament has been taken up by the monoclinical uplift farther south. The San Vicente fault south of the San Vicente oil field shows clear

evidence of reverse faulting during Delmontian to middle Repetto time (Figures 3.4e, 3.5). In contrast, the fault north of the Las Cienegas oil field which bounds the Las Cienegas basement high on the north has little evidence of reverse faulting (Figure 3.4f). Yet the strata above show monoclinical deformation up on the north. Wright (1991) interpreted the deformation as buckling of strata against the basement high, called block-edge forced folding. This portion of the San Vicente fault shows clear evidence that the initiation of normal faulting on the San Vicente fault dates back to the early to middle Miocene (Figure 3.5); the Topanga Formation is 0 to 200 m thick on the Las Cienegas basement high, whereas it is as much as 600 m thick north of the fault (Schneider and others, 1996). The Topanga Formation about 700 m thick in the Morgan Brown U-6 No. 1 well suggests that normal faulting on the San Vicente in the East Beverly Hills area also started during early to middle Miocene time (Figure 3.4e).

The base of middle Pleistocene marine gravels is arched into a broad, west-plunging anticline (Wilshire arch) between the central trough and Hollywood basin (Figures 3.2, 3.4e; Hummon and others, 1994). The deformational pattern of the Wilshire arch is different from that of the monoclinical uplift, suggesting a change of tectonic style in middle Quaternary time (Figure 3.5). Hummon and others (1994) proposed that the arch is underlain by the potentially seismogenic Wilshire fault located beneath well control. A fault-bend fold model indicates a reverse slip rate of 1.5-1.9 mm/yr, whereas a three-dimensional elastic-dislocation model indicates a right-reverse slip rate of 2.6-3.2 mm/yr. The latter model explains the Hollywood basin as the subsiding back limb of the fold above the blind right-reverse slip Wilshire fault (Hummon and others, 1994).

Eastward to the Las Cienegas area, the monocline becomes more prominent with increasing depth of the central trough (Figures 3.4f, 3.6a). The monocline and the secondary Las Cienegas anticline trend more northerly than equivalent structures in the East Beverly Hills area, almost parallel to the surficial MacArthur Park fault (Figures 3.2, 3.6b). The Las Cienegas anticline was caused by reverse slip on the north-dipping Las Cienegas fault that marks the southern boundary of the Las Cienegas basement high. This fault offsets Delmontian and Mohnian strata but not Repetto strata (Figure 3.4f). Nevertheless, the thinning of Repetto to middle Pico strata onto the anticlinal crest illustrates that the fault was an active blind reverse fault in the Pliocene and early Pleistocene (Figure 3.5; Schneider and others, 1996). In the cross section in Figure 3.4f, Topanga volcanic rocks are entrained in the Las Cienegas fault whereas the Topanga Formation is absent on the Las Cienegas basement high. This observation, coupled with the fact that the Los Angeles area was under an extensional stress regime during the time of Topanga deposition (Wright,

1991; Crouch and Suppe, 1993), suggests that the Las Cienegas fault was a south-dipping normal fault during the early to middle Miocene (Schneider and others, 1996).

East of the Las Cienegas area, the northern shelf slopes gradually southeast to the Whittier Narrows area. The southern edge of the shelf, expressed as a monoclinical flexure in upper Pliocene and Quaternary strata, is aligned along a possible easterly extension of the Las Cienegas fault (Wright, 1991).

Newport-Inglewood Fault Zone

The northwest-striking Newport-Inglewood fault zone bounds the Los Angeles central trough on the west. The fault zone is characterized at the surface by a series of faults and anticlinal hills extending from the Baldwin Hills southeast to Newport Beach where it continues offshore (Figure 3.1; Harding, 1973; Yeats, 1973; Barrows, 1974). The seismicity (Hauksson, 1987, 1990) and the orientation parallel to the relative slip vector between the Pacific and North American plates suggest that the Newport-Inglewood fault zone is predominantly a right-lateral shear zone. Freeman and others (1992) identified piercing point offsets for multiple stratigraphic layers using electric logs and showed that the right-lateral slip rate of the fault zone has been rather uniform along its length at approximately 0.5 mm/yr since the early Pliocene. Total right-lateral slip since the middle Miocene is estimated as no more than 3 km (Hill, 1971; Yeats, 1973). At least five earthquakes of magnitude 4.9 or greater have been associated with the fault zone since 1920, the largest of which was the M_w 6.4 Long Beach earthquake of 1933 (Figure 3.1; Hauksson, 1987; Hauksson and Gross, 1991). Our subsurface analysis covers the northern end of the Newport-Inglewood fault zone: the Inglewood fault in the Baldwin Hills and the West Beverly Hills Lineament farther north (Figure 3.2).

The Baldwin Hills are underlain by the northwest-trending Inglewood anticline (Figures 3.6a, 6b). The anticlinal crest is offset 1200 m right-laterally along the Inglewood fault, one of the en-echelon faults that comprise the Newport-Inglewood fault zone (Wright, 1987). Striae in well cores within the fault zone in the Baldwin Hills indicate that the latest movement was predominantly strike-slip (Driver, 1943). Cross sections and isopach maps illustrate progressive thinning of Pliocene stratigraphic intervals over the crest of the Inglewood anticline (Wright, 1987). A simple anticline had formed by the end of Pliocene time and it began to be modified by strike-slip faulting on the Inglewood fault in the latest Pliocene (Figure 3.5; Wright, 1987, 1991). Since then, the average right-lateral slip rate in the Baldwin Hills has been approximately 0.5 mm/yr (Freeman and others, 1992).

Wright (1991) and Dolan and Sieh (1992) identified prominent north-northwest-trending, east-facing, 10-20 m high topographic scarps (West Beverly Hills Lineament) along the eastern edge of the Cheviot Hills northward to the mountain front (Figure 3.2). It marks the boundary between dissected alluvial fans and uplifted marine terraces to the west and gently sloping undissected alluvial fans to the east. The lineament is oriented parallel to the northern projection of the Inglewood fault and has been considered a northern extension of the Newport-Inglewood fault zone (Wright, 1991; Dolan and Sieh, 1992). This lineament, however, is approximately 1 km west of the northern projection of the Inglewood fault (Figure 3.2; Dolan and Sieh, 1992), and no well immediately beneath it is cut by a fault. Instead, the easternmost well in the Cheviot Hills oil field is cut by a fault with a 150-m down-to-the-east normal separation of a bentonite bed in lower Repetto strata (Figure 3.4g). This fault is on its expected position if it were a northern extension of the Inglewood fault. These observations suggest that the West Beverly Hills Lineament is underlain by a steeply east-dipping normal-separation fault, a northern extension of the Inglewood fault in the Baldwin Hills (Figures 3.4g, 3.6a, 3.6b). This new interpretation suggests a possibility that the Hollywood basin and the North Salt Lake fault are pull-apart structures related to left slip on the Hollywood fault and right slip on the West Beverly Hills Lineament (Figure 3.2), as opposed to an interpretation proposed by Hummon and others (1994). We are unable to locate the subsurface extension of the lineament farther north because of the structural complexity north of the southern strand of the Santa Monica fault.

Discussion

Interaction Between the Northern Los Angeles Fault System and Newport-Inglewood Fault Zone

How the east-trending Transverse Ranges and northwest-trending Peninsular Ranges structures interact in the northern Los Angeles basin has important implications in seismic hazards evaluation and tectonic evolution of the study area. It has been proposed that the Newport-Inglewood fault zone may serve as a segment boundary for the northern Los Angeles fault system (Hauksson, 1987; Wright, 1991; Dolan and Sieh, 1992). The extensive subsurface data sets from the Cheviot Hills and Baldwin Hills areas allow us to address this question.

A subsurface structure contour map on the base of Pico strata (~2.5 Ma) indicates that the 1200-m right-lateral offset along the Inglewood fault in the Baldwin Hills diminishes rapidly to the north (Figure 3.6a). This map was originally constructed with a contour interval of 60 m (200 feet) but no systematic right-lateral offsets of contours were

detected along the West Beverly Hills Lineament north of the Cheviot Hills anticline. This suggests that the right slip on the Inglewood fault is absorbed by the growth of contractional structures in the Cheviot Hills area as proposed by Wright (1991). The growth of the Cheviot Hills anticline occurred after the deposition of lower Pico strata (latest Pliocene), which is synchronous with the initiation of right slip on the Inglewood fault documented by Wright (1987), suggesting a close kinematic relation between these structures (Figure 3.5). In addition, the Cheviot Hills anticline and Rancho fault appear to be localized structures independent from the Santa Monica fault system; they strike more northerly (Figure 3.6b) and terminate against the southern strand of the Santa Monica fault in the Sawtelle oil field (Figures 3.4b, 4c). To the east, they appear to terminate against the northern projection of the Inglewood fault (Figure 3.6a). The amount of crustal shortening accommodated by the growth of the Cheviot Hills anticline and Sawtelle syncline based on the analysis of growth strata (Schneider and others, 1996) is 450 m, about one-third of the right-lateral offset along the Inglewood fault in the Baldwin Hills. Because of the internal deformation of the block west of the West Beverly Hills Lineament by folding and thrusting, the amount of right-lateral offset should be smaller northward.

It is also possible that the West Beverly Hills Lineament is a young, probable Quaternary structure and thus has a small cumulative displacement. Wright (1991) and Freeman and others (1992) demonstrated that strike-slip faulting on the Newport-Inglewood fault zone was initiated in the south and propagated to the north. Larger right-lateral offset of progressively older late Miocene to Pliocene strata in the Long Beach oil field (Figure 3.1) indicates that strike-slip faulting there was initiated in the late Miocene (Freeman and others, 1992), whereas strike-slip faulting in the Inglewood oil field was initiated in the latest Pliocene (Wright, 1987). It is therefore possible that the West Beverly Hills Lineament, the probable northernmost segment of the Newport-Inglewood fault zone (Wright, 1991; Dolan and Sieh, 1992), formed in the Quaternary and is actively propagating northward to the Santa Monica Mountains. Despite its small cumulative offset, the West Beverly Hills Lineament marks a Quaternary segment boundary for the northern Los Angeles fault system. The active Santa Monica-Hollywood fault system is divided into two discrete segments by the lineament (Dolan and Sieh, 1992), and the Wilshire arch and Hollywood basin do not appear to continue across the lineament (Figure 3.2; Hummon and others, 1994).

Slip Rate of Pliocene to Early Pleistocene Structures Based on Analysis of Growth Strata

Suppe and others (1992) demonstrated that the rates of folding and faulting over millions of years can be calculated based on the analysis of growth strata. Growth strata are

syntectonic strata that are thicker over strongly subsiding areas, thinner over weakly subsiding areas, and absent over uplifting areas. Schneider and others (1996) further developed techniques to determine crustal shortening and dip-slip rates of the blind Monocline fault beneath the East Beverly Hills-Las Cienegas monocline. The amount of horizontal shortening is equal to the bed length of pre-growth strata minus that of the top of growth strata. The dip of the fault causing the structural growth is calculated based on the amount of shortening and relative subsidence (Schneider and others, 1996). They obtained a crustal shortening rate of 0.5-0.7 mm/yr across the Monocline fault during Repetto and Pico time. The dip of the Monocline fault was calculated as approximately 60°N. These calculations yield a dip-slip rate for the Monocline fault of 1.1-1.5 mm/yr (Schneider and others, 1996).

We apply similar calculations for the Cheviot Hills and Sawtelle areas (Figures 3.4c, 4d). In contrast to the East Beverly Hills and Las Cienegas areas, Repetto and Pico strata west of the West Beverly Hills Lineament are cut by faults, and crustal shortening is accommodated by both folding and faulting. The total shortening in the Cheviot Hills area is 1850 m, the difference between the bed length at the base of Repetto strata (11050 m) and that at the top of Pico strata (9200 m) between the two pins in the cross section in Figure 3.4d. The Repetto and Pico time interval lasted between 3.8 and 4.3 m.y. (Figure 3.3), and an average shortening rate here is estimated at 0.4-0.5 mm/yr. This value represents a minimum value because our calculation does not take into consideration the erosion of pre-growth strata, which is poorly constrained. A similar calculation for the Sawtelle oil field (Figure 3.4c) yields a total shortening of 4050 m (11600-7550 m) and an average shortening rate of 0.9-1.0 mm/yr. The larger shortening rate for the Sawtelle area compared to the other areas is primarily due to low-angle faulting along the southern strand of the Santa Monica fault. The northward dip of about 20°-40° yields a dip-slip rate of 1.0-1.3 mm/yr for the southern strand of the Santa Monica fault in the Sawtelle area, which is comparable with that for the Monocline fault east of the West Beverly Hills Lineament.

Late Quaternary Slip Rate of the Santa Monica Mountains Blind Thrust Fault

It has been proposed that oblique slip on many large fault systems in southern California is partitioned into strike-slip along surface faults and dip-slip along blind thrust ramps (Hauksson, 1990; Shaw, 1993; Dolan and others, 1995). According to this view, the surficial Malibu Coast-Santa Monica-Hollywood fault system accommodates left-lateral strike-slip, while the underlying Santa Monica Mountains blind thrust fault accommodates the contractional component of displacement (Dolan and others, 1995). The late Quaternary slip rates of these surface and blind thrust faults are critical for seismic hazards evaluation

in the study area but they are not well constrained, compared with other major fault zones in the western Transverse Ranges (Dolan and others, 1995). Here we estimate the late Quaternary dip-slip rate of the Santa Monica Mountains blind thrust fault based on tectonically deformed marine terraces at Pacific Palisades.

The shoreline angle of the stage 5e terrace at Pacific Palisades ranges from 47 to 110 m above present mean sea level, and this gives an uplift rate of 0.3-0.9 mm/yr, assuming that stage 5e sea level was 6 m higher than present sea level (McGill, 1989). This wide elevation range for the shoreline angle is partly due to north-trending folds mapped by McGill (1989). Part of the uplift is related to the up-on-the-north movement along the active strand of the Santa Monica fault, which exhibits a dip-slip rate of approximately 0.5 mm/yr if the dip of 45° observed at Potrero Canyon continues to depth. The marine platform slopes seaward at about 1.5°-6°, steeper than the typical gradient of about 1°-2° for abrasion platforms (Bradley, 1958). This southward tilt cannot be explained by the reverse faulting on the active strand of the Santa Monica fault dipping to the north, and it is interpreted as broad warping accompanying displacement on the Santa Monica Mountains blind thrust fault beneath the Santa Monica Mountains.

In order to calculate the dip-slip rate of the north-dipping Santa Monica Mountains blind thrust fault from the uplift rate of the marine terrace, it is necessary to constrain the dip of the fault. We estimate the dip of the blind thrust fault as greater than 45°, based on the following observations. The hypocenter of the 1994 Northridge earthquake was at the downdip edge (~18 km depth) of the south-dipping fault plane beneath the southern San Fernando Valley (Hauksson and others, 1995; Mori and others, 1995). Considering the overall dominance of north-dipping faults in the western Transverse Ranges (Dolan and others, 1995; Yeats and Huftile, 1995), it is unlikely that the Santa Monica Mountains blind thrust fault extends shallower than the hypocenter and is truncated by the south-dipping Northridge thrust. We therefore suggest that the Santa Monica Mountains blind thrust fault extends beneath the hypocenter, which constrains the dip of the fault greater than 45°, assuming the fault plane contains no bend. The minimum dip of 45° is for the case in which the two oppositely dipping faults interact at the hypocentral depth. The 1971 San Fernando and 1994 Northridge earthquakes, two of the largest historical earthquakes in the western Transverse Ranges, ruptured fault planes dipping ~45° (Mori and others, 1995).

Alternatively, the blind thrust fault beneath the Santa Monica Mountains may bend as modeled by Davis and Namson (1994). They constructed a north-trending balanced cross section from northern Los Angeles basin through the Sawtelle area northward to the Santa Clara Valley, including the causative fault of the 1994 Northridge earthquake. In this model, the Santa Monica Mountains blind thrust fault dipping at ~65° ramps upward from

their Elysian Park thrust dipping at $\sim 20^\circ$ at a depth of ~ 14 km. Farther north, the Elysian Park thrust interacts with their Pico thrust (Northridge thrust) at the 1994 hypocentral depth. An argument against this model is that there is no evidence in the surface and subsurface geology for the axial surface corresponding to the change in fault dip by 45° . The Mohnian to Delmontian (Blake, 1991) Modelo Formation in the northern flank of the Santa Monica Mountains dips north at 15° - 30° , and this gentle dip continues into the subsurface beneath the San Fernando Valley, all the way to the Mission Hills. The dip of greater than 45° and the highest elevation of the shoreline angle of 110 m (McGill, 1989) suggest that an overall dip-slip rate of the Santa Monica Mountains blind thrust fault in the late Quaternary is as large as 1.5 mm/yr. This slip rate is a half to one-fourth of 3.9-5.9 mm/yr slip rate in the past 2-3 million years for the Elysian Park thrust obtained by Davis and Namson (1994).

We suggest that the difference between the two rates are partly due to comparing a slip rate in the late Quaternary with that in the past few million years. Several lines of evidence suggest that the Quaternary tectonic deformation in the northern Los Angeles area is different from earlier deformation, including the deformation used by Davis and Namson (1994) in their slip rate estimate. The drainage divide in the Santa Monica Mountains is on the north side of the range (Figure 3.7), mainly within the north-dipping Modelo Formation. This results in long southward flowing streams that drain to the ocean and very short north flowing streams that drain to the Los Angeles River along the southern edge of the San Fernando Valley, as previously noted by Hoots (1931). The divide is well north of the crest of the Santa Monica Mountains anticline in the Modelo Formation (Figure 3.7) that was modeled by Davis and Namson (1994) as a fault-propagation fold associated with their Elysian Park thrust. This observation suggests that the Santa Monica Mountains anticline is not active, and the axis of the Quaternary uplift occurs farther north. Therefore a dip-slip rate for the Santa Monica Mountains blind thrust fault averaged over the past few million years is probably not representative of that in the Quaternary.

The evidence for the uplift of the Santa Monica Mountains is, however, entirely topographic, because the Plio-Pleistocene strata, where observed, are either flat-lying or dip toward the range. Major folding and reverse faulting along the Santa Monica fault system predate upper Pico strata, and middle to late Quaternary strata are flat-lying with a minor up-on-the-north displacement along the active strand (Figures 3.4b-4d). In the Hollywood basin, middle Pleistocene marine gravel dips to the north, toward the range (Figure 3.4e). The southern range front of the Santa Monica Mountains between Pacific Palisades and the West Beverly Hills Lineament is not defined by an active fault (Crook and Proctor, 1992; Dolan and Sieh, 1992). The Hollywood fault is an active range-front

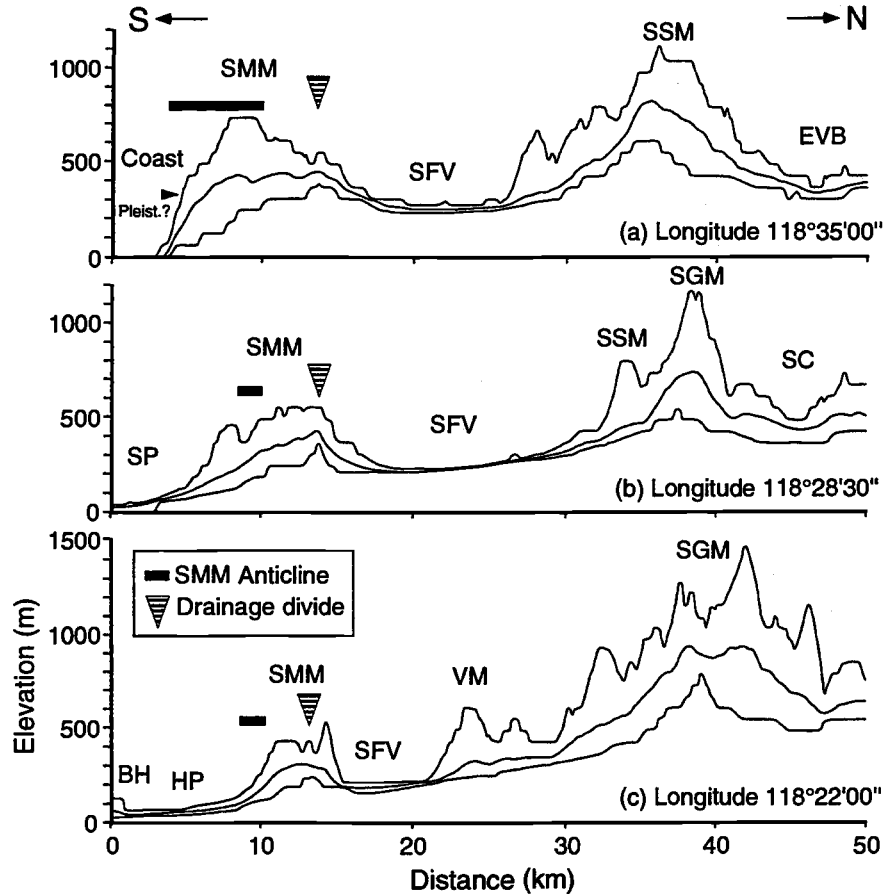


Figure 3.7 Topographic profiles across the western Transverse Ranges. Maximum, minimum, and mean altitude curves are shown, derived from projecting elevations within a 10-km-wide swath. See Figure 3.1 for location of center lines of the profiles. The data are from U.S. Geological Survey Digital Elevation Model with pixel resolution 77.8×91.2 m. See Masek and others (1994) for details of the technique. All profiles are vertically exaggerated by a factor of 15. Maximum altitudes represent the closest approximation to the original tectonically uplifted surface, whereas the difference between maximum and minimum altitudes is a measure of dissection by drainage. The Santa Monica Mountains anticline in Mohnian strata and drainage divide are shown. The horizontal separation of the anticlinal axis and drainage divide suggests that the active uplift of the Santa Monica Mountains is controlled by a different blind fault than the fault related to the Santa Monica Mountains anticline. Abbreviations of topographic features: BH, Baldwin Hills; EVB, East Ventura basin; HP, Hollywood plain; SC, Soledad Canyon; SFV, San Fernando Valley; SGM, San Gabriel Mountains; SMM, Santa Monica Mountains; SP, Sawtelle plain; SSM, Santa Susana Mountains; VM, Verdugo Mountains. The arrow south of the Santa Monica Mountains in the upper figure shows the elevation of the highest marine platform of probable Pleistocene age from McGill (1989). Higher elevation of progressively older marine platforms near Pacific Palisades indicates that the Santa Monica Mountains have been uplifted since at least the middle Pleistocene.

fault east of the lineament but the motion on this fault may be predominantly strike-slip (Dolan and Sieh, 1992; Dolan and others, 1993). These data strongly suggest that the uplift of the Santa Monica Mountains in the Quaternary is primarily accommodated by the Santa Monica Mountains blind thrust fault, in support of the slip-partitioning model by Dolan and others (1995).

Late Cenozoic Tectonic Evolution of the Northern Los Angeles Basin

Comprehensive reviews of the late Cenozoic tectonics of the Los Angeles area were provided by previous studies (e.g., Yerkes and others, 1965; Wright, 1991). Our study focuses on a small but critical area based on a more detailed data set. In this section, we discuss the late Cenozoic tectonic evolution of the northern Los Angeles basin by adding new data and interpretations to previous studies.

Early to late Miocene extensional tectonics

Miocene extension in southern California followed the collision of this portion of the North American plate with the East Pacific Rise in the late Oligocene (Atwater, 1970; Crowell, 1987; Sedlock and Hamilton, 1991). Normal faulting and volcanism during the earliest Miocene (20-24 Ma) were widespread from western California to southwestern Arizona (Tennyson, 1989). After the termination of subduction offshore southern California, a right-lateral transform regime formed by 17-18 Ma (Lonsdale, 1991; Tennyson, 1989). Since then, the western Transverse Ranges rotated clockwise as much as 100° with a westward increase in the net amount of rotation (Kamerling and Luyendyk, 1979; Hornafius and others, 1986). The clockwise rotation of elongated blocks in the western Transverse Ranges was accompanied by left-lateral movement on block-bounding faults including the Malibu Coast-Santa Monica-Hollywood-Raymond fault (hereafter referred to as the Malibu Coast-Raymond fault), and a transtensional stress regime along the block boundaries (Luyendyk, 1991). The Santa Monica Mountains and surrounding areas underwent crustal extension during the middle to late Miocene, accompanied by widespread volcanism (Conejo volcanics) between 16 and 13 Ma and by normal faulting (Campbell and Yerkes, 1976; Crowell, 1987; Wright, 1991; Crouch and Suppe, 1993).

Palinspastic restoration of Paleogene and older features suggested that the Santa Monica Mountains were apparently displaced 60-90 km westward with respect to the Santa Ana Mountains since the early Miocene (Yeats, 1968, 1976; Colburn, 1973; Sage, 1973; Campbell and Yerkes, 1976). These estimates were made before the proposal of the Miocene clockwise rotation of the western Transverse Ranges (Kamerling and Luyendyk, 1979; Hornafius and others, 1986), but Colburn's (1973) estimate of 60 km displacement

was reevaluated against the Miocene rotation model and accepted by Link and others (1984). The integration of surface and subsurface geologic data suggests that only part of the 60-90 km offset is taken up on the Malibu Coast-Raymond fault (Figure 3.8). The eastern edge of the Santa Monica Slate, intruded by granitic rocks of the Mesozoic Peninsular Ranges batholith, is exposed in the Santa Monica Mountains north of the Hollywood fault. In the northern Los Angeles basin, the slate/granite contact is constrained closely by three wells in the Montebello area (Figure 3.8). As previously noted by Dibblee (1982), this contact is offset about 24 km left-laterally across the Malibu Coast-Raymond fault, although Wright (1991) suggested that this is a less reliable piercing point because of different levels of erosion across the fault. Paleocene redbeds are penetrated by the Morgan Brown U-6 No. 1 well (Yeats, 1973) and are exposed in Solstice Canyon northeast of Point Dume but not in adjacent canyons (Sage, 1973; Seedorf, 1983), indicating 26-40 km left-lateral offset (Figure 3.8). These values are significantly smaller than the 60-90 km displacement of the Santa Monica Mountains with respect to the Santa Ana Mountains, indicating that additional displacement must have taken place on a fault south of the Malibu Coast-Raymond fault. We suggest that this fault is the Miocene Santa Monica and San Vicente faults, across which Miocene normal faulting has already been demonstrated. All occurrences of the Santa Monica Slate and Paleocene redbeds are north of these faults, and all occurrences of the Catalina Schist and greenschist facies meta-igneous rocks are south of the faults. We suggest that these rocks were juxtaposed against one another by left slip. The eastern continuation of this fault is not yet mapped, but it could follow the Miocene Whittier fault. Schistose metavolcanics found in Shell Puente No. A-3 and A-6 wells (Figure 3.8) were thought by Schoellhamer and Woodford (1951) and Yeats (1973) to correlate to the Pelona Schist, but Woodford (1960) and Yerkes (1972) suggested that they should be correlated to the Santiago Peak Volcanics of the Santa Ana Mountains, a suggestion that we accept here. If so, these metavolcanics are offset ~25 km left-laterally from the Santiago Peak Volcanics in outcrop to the south. The Quaternary movement of the Whittier fault is predominantly right-lateral strike-slip (Rockwell and others, 1992).

During the deposition of the Topanga Formation, the San Vicente and Las Cienegas faults were normal faults bounding the Las Cienegas basement high on the north and south, respectively (Figure 3.9a). The normal faulting along the Santa Monica fault during this time interval is unclear because we do not know the thickness of the Topanga Formation in the footwall. However, the Santa Monica and San Vicente faults appear to have formed a continuous down-to-the-north normal fault in the late Miocene, and it is possible that the Santa Monica fault was also active during the time of Topanga deposition (Figure 3.9a). The western shelf was already a structural high during the deposition of the Topanga

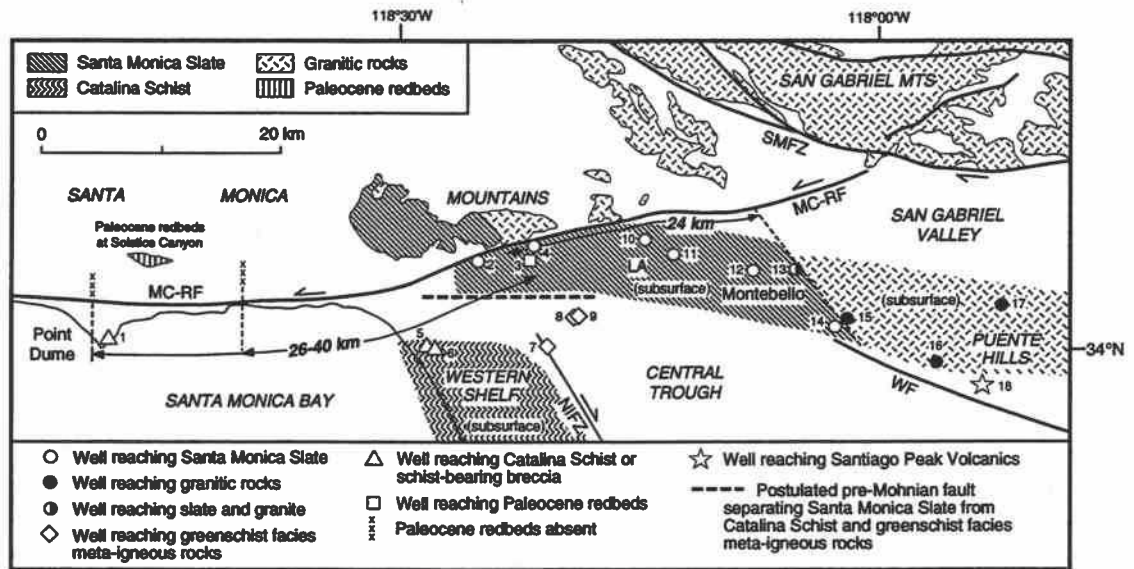


Figure 3.8 Calculation of left slip on the Malibu Coast-Raymond fault since the early Miocene. Abbreviations for faults: MC-RF, Malibu Coast-Raymond fault; NIFZ, Newport-Inglewood fault zone; SMFZ, Sierra Madre fault zone; WF, Whittier fault. Subsurface data south of the Malibu Coast-Raymond fault are from Schoellhamer and Woodford (1951), Yerkes (1972), Yeats (1973), Sorensen (1985), Yeats (unpublished data), and this study. Well numbers are identified in the Appendix.

Figure 3.9 Schematic reconstruction of structural features during three tectonic stages in the northern Los Angeles area. Solid lines with hatches and triangles show normal and reverse faults, respectively. Hatches and triangles are on the hanging-wall side. Half-sided arrows show direction of strike-slip motion. (a) Northern Los Angeles area at ~15 Ma during the deposition of the Topanga Formation. Left slip on the Malibu Coast-Raymond fault is restored but the orientations of the fault and Santa Monica Mountains are shown as they are today. The Santa Monica Mountains have been rotated about 80° clockwise since the early Miocene (Hornafius and others, 1986). Location of the Conejo Volcanics after Wright (1991). Area of figures (b) and (c) is shown by dotted rectangle. (b) Principal structural features during the early Pliocene to early Pleistocene. Abbreviations: CHA, Cheviot Hills anticline; EBHA, East Beverly Hills anticline; LCA, Las Cienegas anticline; LCF, Las Cienegas fault; RF, Rancho fault. (c) Principal structural features during the middle to late Pleistocene. Contour lines in meters are on the base of middle Pleistocene marine gravels from Hummon and others (1994).

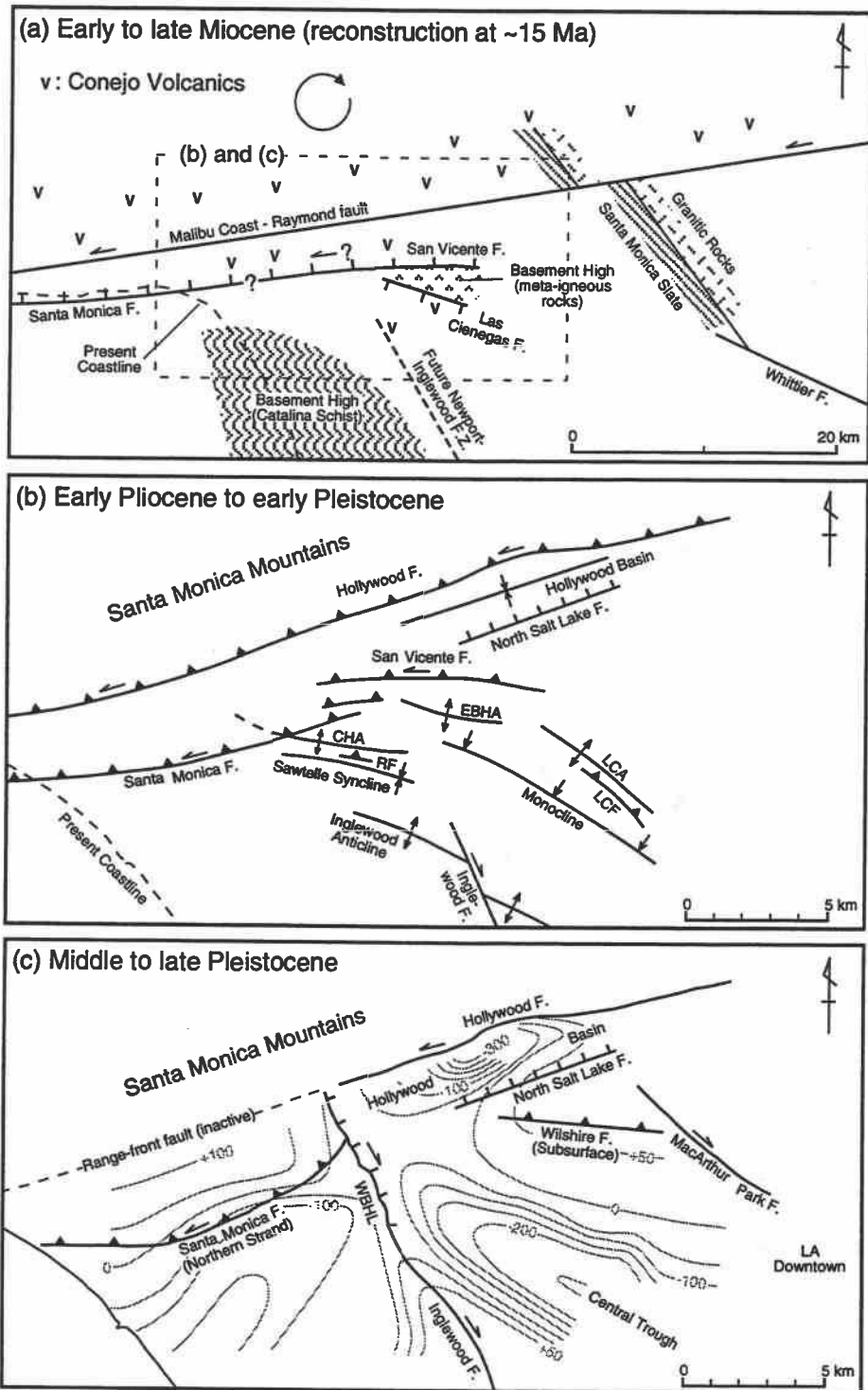


Figure 3.9

Formation (Yeats, 1973; Wright, 1991). After the end of volcanism in the early middle Miocene, the cooling and subsidence of the crust caused a transgression of the shoreline to the east to the present San Andreas fault (Wright, 1991). During 14-9 Ma, the fine-grained deep-water Nodular Shale was deposited fairly uniformly in the northern Los Angeles area with little thickness changes across major faults.

In late Mohnian time (9-6.5 Ma) and probably into Delmontian time (6.5-5 Ma), the Tarzana submarine fan fed the northern Los Angeles area (Sullwold, 1960; Redin, 1991). The fan lapped around the flanks of the northern end of the western shelf where upper Mohnian strata are absent and lower Mohnian Nodular Shale is unconformably overlain by Delmontian strata (Redin, 1991; Wright, 1991). The northern boundary of this structural high is marked by the southern strand of the Santa Monica fault, across which late Miocene normal faulting was already documented (Figure 3.5). The eastern boundary of this structural high lies near the Inglewood fault (Wright, 1991). The non-deposition of upper Mohnian strata over a large area in the northern Los Angeles basin makes it difficult to correlate Tarzana fan strata across the Malibu Coast-Raymond fault and calculate the left-lateral slip on the fault system since the late Miocene. To the east, the Tarzana fan also lapped around the Las Cienegas basement high (Wright, 1991).

Delmontian stage appear to be a transition from extensional to compressional tectonics in the northern Los Angeles basin. The San Vicente fault and probably the Santa Monica fault reactivated as reverse faults in Delmontian time, whereas the Las Cienegas fault was still a south-dipping normal fault (Figure 3.5).

Early Pliocene to early Pleistocene contractional tectonics

The depositional pattern and location of basin margins in the Los Angeles basin became similar to those today in late Miocene time (~7 Ma) by subsidence between the Whittier and Palos Verdes faults and Santa Monica fault system (Wright, 1991). These features were later involved in compressional stress regime in Pliocene, which appear to have resulted from a shift in relative plate motion between the North American and Pacific plates at ~5 Ma (Engebretson and others, 1985). Harbert and Cox (1989) more precisely placed the timing of this shift at 3.9-3.4 Ma. This shift in relative motion marked the beginning of the big bend of the San Andreas fault and accompanying shortening and uplift of the Transverse Ranges (Atwater, 1970; Campbell and Yerkes, 1976; Crowell, 1987; Sedlock and Hamilton, 1991; Wright, 1991).

At the beginning of the Pliocene (~5 Ma), the East Beverly Hills-Las Cienegas monocline was initiated and the Las Cienegas fault was reactivated as a reverse fault (Figures 3.5, 3.9b). The Las Cienegas fault must have been rotated into its present north-

dipping configuration if it had been a south-dipping normal fault in the Miocene (Schneider and others, 1996), though the mechanism of this rotation is unclear. On the opposite flank of the central trough, the growth of the Inglewood anticline also started in the early Pliocene (Figure 3.5; Wright, 1987). The reverse faulting on the Santa Monica and San Vicente fault continued into Pliocene time. However, the reverse offset on the San Vicente fault occurred on a smaller scale than that on the Santa Monica fault (Figures 3.4b-4e), and crustal shortening east of the Newport-Inglewood fault zone was primarily accommodated by the growth of the monocline (Figure 3.9b). The Hollywood fault and its now-inactive western extension along the southern range front of the Santa Monica Mountains would have been a left-oblique slip fault during the late Miocene and Pliocene, in order to account for the 10-15 km of left-lateral offset of the Tarzana submarine fan of Mohnian age (Lamar, 1961; Redin, 1991) as well as the uplift of the range since late Miocene time (Figure 3.9b).

The intense crustal deformation occurred in the late Pliocene and early Pleistocene. The growth of the Inglewood anticline peaked during the deposition of middle Pico strata (Wright, 1987). At the same time, the growth of the Cheviot Hills anticline took place in response to right-lateral slip on the Inglewood fault. In the Sawtelle oil field, the southern strand of the Santa Monica fault truncates the northwestern extension of the Cheviot Hills anticline (Figures 3.4b, 4c), suggesting that the reverse faulting at this portion of the fault may not have begun until the early Pleistocene. Crowell (1976) suggested that the Transverse Ranges have been uplifted in the past 2-3 million years by pronounced crustal shortening. The deformation in the study area may indicate the onset of the uplift of the Santa Monica Mountains, although further investigations are needed to confirm this hypothesis.

Contemporary tectonics

The structural pattern of the Pliocene to early Pleistocene was considerably modified during the middle to late Pleistocene (Figure 3.9c). East of the West Beverly Hills Lineament, the Hollywood fault is predominantly a left-lateral strike-slip fault at the range front of the Santa Monica Mountains (Dolan and Sieh, 1992; Dolan and others, 1993). West of the lineament, however, left slip occurs on the active strand of the Santa Monica fault, leaving the western extension of the Hollywood fault inactive (Wright, 1991; Crook and Proctor, 1992; Dolan and Sieh, 1992). This active strand of the Santa Monica fault is new in the middle to late Pleistocene (Figure 3.5), cutting across the older, southern strands that became inactive prior to the deposition of middle Pleistocene marine gravels (~1 Ma). The West Beverly Hills Lineament and Wilshire arch appear to be also new in this period. A large portion of north-south shortening since the middle Pleistocene east of the

lineament may be accommodated by the blind Wilshire fault. The subsidence of the Hollywood basin and the normal faulting on the North Salt Lake fault started in the Pliocene and continued into the Quaternary. The normal separation on the North Salt Lake fault and West Beverly Hills Lineament is distinct from the contractional movement on other Plio-Pleistocene structures (Figure 3.9c). These may be pull-apart structures related to left slip on the Hollywood fault and right slip on the West Beverly Hills Lineament. The uplift and southward tilt of Pleistocene marine platforms indicate that the Santa Monica Mountains have been uplifted during the Quaternary. This uplift is largely associated with the Santa Monica Mountains blind thrust fault, because active surface faults exhibit only a small up-on-the-north displacement.

A GPS baseline spanning from the San Gabriel Mountains, through the eastern end of the study area, to the Palos Verdes Hills is shortening at a rate of 5 ± 1 mm/yr (Feigl and others, 1993). We suggested a dip-slip rate of as large as 1.5 mm/yr and a dip of greater than 45° for the Santa Monica Mountains blind thrust fault. These yield a north-south shortening rate across this fault as large as 1 mm/yr. Because the crest of the Santa Monica Mountains plunges to the east, we believe that the dip-slip and shortening rates across this blind thrust fault are smaller in that direction. We arbitrarily assign a shortening rate of 0.5 mm/yr for the Santa Monica Mountains blind thrust fault east of the West Beverly Hills Lineament. The slip rate and dip of the Wilshire fault based on two inverse models (Hummon and others, 1994) yield a shortening rate of as large as 2 mm/yr across this structure. These two values together give a north-south shortening rate of as large as 2.5 mm/yr across the northern Los Angeles fault system east of the West Beverly Hills Lineament. This value is half of the shortening rate between the San Gabriel Mountains and Palos Verdes Hills obtained by Feigl and others (1993). The rest of the shortening occurs on other structures, most likely the Sierra Madre fault zone and Palos Verdes fault, characterized by relatively high slip rates (Petersen and Wesnousky, 1994; Dolan and others, 1995; Stephenson and others, 1995).

Conclusion

In this paper, we have described active and late Cenozoic faults and folds in the northern Los Angeles basin based primarily on subsurface geologic data. We defined the timing, kinematics, and rate of deformation of Miocene, Pliocene, and Pleistocene structures and discussed tectonic evolution of the northern Los Angeles area. Many faults formed as normal faults in the early to late Miocene and were later reactivated as reverse faults due to a shift from extensional to contractional stress regime at approximately the beginning of Pliocene time. This implies that the orientation of reverse faults is controlled

by Miocene extensional tectonics rather than the Pliocene-Pleistocene stress field. The relatively steep dips of reverse faults in the study area may also be in part explained by their normal-fault origin.

Contractional tectonics began in early Pliocene time, with the reactivation of Miocene normal faults and initiation of reverse faults. Many Pliocene structures became inactive by the middle Pleistocene, and deformation is taken up by structures new in the middle to late Pleistocene. These structures include the West Beverly Hills Lineament, Wilshire fault, and the active strand of the Santa Monica fault. Although the Santa Monica Mountains are not bounded by major, Quaternary reverse faults, geomorphic evidence suggests that the range has been uplifted in the late Quaternary. We calculated an average dip-slip rate as large as 1.5 mm/yr for the Santa Monica Mountains blind thrust fault underlying and uplifting the Santa Monica Mountains, based on the uplift of the oxygen-isotope substage 5e marine terrace north of the City of Santa Monica. This rate is considerably less than the rate of 3.9-5.9 mm/yr proposed by Davis and Namson (1994) averaged over the past 2-3 million years. Because of a significant change in deformational pattern from the Pliocene to Pleistocene, a slip rate averaged over the past few million years is probably not representative of that in the late Quaternary.

Implications of this study to seismic hazards evaluation in the northern Los Angeles basin are summarized as follows. Most of the subsurface structures in the northern Los Angeles basin are inactive in the late Quaternary, except for the Wilshire fault identified by Hummon and others (1994). The North Salt Lake faults appears to extend close to the surface and may pose surface rupture hazards. The West Beverly Hills Lineament is the northernmost segment of the Newport-Inglewood fault zone and may now be propagating to the Santa Monica Mountains range front. Our lower slip rate for the Santa Monica Mountains blind thrust fault lengthens the calculated recurrence interval for an earthquake on this fault.

Acknowledgments

This research was funded by the National Earthquake Hazards Reduction Program (Grant numbers 14-08-0001-G1967 and 1434-94-G2492) and the Southern California Earthquake Center (Grant number 662704). This assessment of seismic hazards for northern Los Angeles would have been impossible without the cooperation of oil companies that provided well data to us. Charlie Hatten provided geologic information on the Sawtelle oil field, and Jim Dolan provided unpublished results from his geotechnical investigations on the active trace of the Santa Monica and Hollywood faults. We thank Jim Dolan, Charlie Hatten, Tom Rockwell, Kerry Sieh, John Suppe, Jerry Treiman, Jack

West, and Tom Wright for valuable discussions. This manuscript has been greatly improved by reviews from Jim Dolan, Tom Rockwell, and Tom Wright. Contribution No. 230 of the Southern California Earthquake Center.

Appendix

Wells in Figures 3.4 and 3.8

Figure 3.4a (Section A-A')

1. Occidental Marquez E. H. No. 1

Figure 3.4b (Section B-B')

1. Occidental Centinela E. H. No. 1, original hole
2. Occidental Centinela E. H. No. 1, redrill 2
3. Occidental Centinela E. H. No. 1, redrill 1
4. National Aladdin Durso No. 1
5. Occidental Dowlen Federal No. 7, original hole
6. Occidental Dowlen Federal No. 8
7. Occidental Dowlen Federal No. 1, original hole

Figure 3.4c (Section C-C')

1. Cities Service Burns No. 1
2. Standard (Chevron) State of California Core Hole No. 1
3. Signal-Richfield-Conoco U-67 No. 1, original hole
4. Standard (Chevron) Duff Core Hole No. 1, original hole and sidetrack 2
5. Occidental Sawtelle No. 1
6. Occidental Dowlen Federal No. 6
7. Occidental Dowlen Federal No. 1, original hole
8. Occidental Dowlen Federal No. 8
9. Occidental Dowlen Federal No. 12

Figure 3.4d (Section D-D')

1. Texaco Texam No. 1
2. Cities Service Burns No. 1
3. Signal-Richfield Rancho No. 2
4. Signal-Richfield Rancho No. 1
5. Signal-Richfield Rancho No. 7
6. Signal-Richfield Rancho No. 11
7. Gulf (Chevron)-Universal Fox No. 305-F
8. Gulf (Chevron)-Universal Community No. 9-A, original hole
9. Gulf (Chevron)-Universal Community No. 11-A
10. Gulf (Chevron)-Universal Fox No. 4F, original hole
11. Gulf (Chevron)-Universal Fox No. 6F, redrill
12. Gulf (Chevron)-Universal Fox No. 6F, original hole
13. Hudson Los Angeles Country Club No. 1
14. Hudson Los Angeles Country Club No. 3
15. Hudson Los Angeles Country Club Core Hole No. 1

Figure 3.4e (Section E-E')

1. Standard (Chevron) Adamson Core Hole No. 1
2. Standard (Chevron) Saturn Core Hole No. 1, redrill 1
3. Standard (Chevron) Saturn Core Hole No. 1, original hole
4. Standard (Chevron) Saturn Core Hole No. 1, redrill 2
5. Standard (Chevron) San Vicente No. 41
6. Standard (Chevron) San Vicente No. 29
7. Standard (Chevron) San Vicente No. 7
8. Standard (Chevron) San Vicente No. 11
9. Morgan Brown U-6 No. 1
10. Standard (Chevron)-Beverly Fee A No. 2
11. Standard (Chevron) San Vicente No. 79
12. Standard (Chevron) San Vicente No. 71
13. Standard (Chevron) Dorothy Hay Core Hole No. 3
14. Standard (Chevron) Laurel Core Hole No. 2A
15. Standard (Chevron) Laurel Core Hole No. 2

Figure 3.4f (Section F-F')

1. Standard (Chevron) Pacific Telephone Core Hole No. 1
2. Standard (Chevron) Dublin Core Hole No. 1, original hole
3. Standard (Chevron) Dublin Core Hole No. 1, redrill 2
4. Standard (Chevron) Dublin Core Hole No. 1, redrill 1
5. Union (Unocal) Core Hole No. 24
6. Union (Unocal) Fourth Avenue No. 16
7. Union (Unocal) Fourth Avenue No. 17, redrill 1
8. Union (Unocal) Fourth Avenue No. 1
9. Union (Unocal) Fourth Avenue No. 7A
10. Union (Unocal) Core Hole No. 25
11. Union (Unocal) Core Hole No. 22
12. Standard (Chevron) Wilton Core Hole No. 2, original hole
13. Standard (Chevron) Wilton Core Hole No. 2, redrill 1

Figure 3.4g (Section G-G')

1. Gulf (Chevron)-Universal Fox No. 312-F, original hole
2. Signal-Richfield Hillcrest No. 6
3. Signal-Richfield U-49 No. 2
4. Signal-Richfield U-53 No. 2, original hole

Figure 3.8

1. Sovereign Malibu No. 1
2. Hudson Los Angeles Country Club Core Hole No. 1
3. Morgan Brown U-6 No. 1
4. Standard (Chevron) Laurel Core Hole No. 2
5. Pauley Brooks Community No. 1
6. John B. Quinn Venice No. 1
7. Standard (Chevron) Baldwin Cienega No. 105
8. Union Fourth Avenue No. 1, 4, 5, and 7, and Union Murphy No. 1, 2, and 19
9. Union-Signal-Texam U-19 No. 1, original hole
10. Seaboard Park No. 1
11. Seaboard Core Hole No. 5
12. Continental (Conoco)-Merchants Monterey Park Unit No. 1-1
13. Humble South San Gabriel No. 1-1
14. Shell Bartolo No. 1
15. Shell Pellissier No. 1
16. Morton and Sons Rowland Ranch Estate No. 3-1
17. Texaco Garnier No. 1
18. Shell Puente No. A-3 and A-6

**Chapter 4: Geologic Setting of the 1971 San Fernando and 1994 Northridge
Earthquake Zones in the San Fernando Valley, California**

Hiroyuki Tsutsumi and Robert S. Yeats

Department of Geosciences, Oregon State University, Corvallis, Oregon 97331

Abstract

The San Fernando Valley, California, lies at the updip projection of the north-dipping 1971 San Fernando and south-dipping 1994 Northridge earthquake faults. In search for evidence of the previously unrecognized 1994 Northridge blind fault, we mapped subsurface geology of the San Fernando Valley based on industry oil-well and seismic data. Although the aftershock zone of the Northridge fault terminates against the 1971 aftershock zone at a depth of ~5 km, fault-propagation folding related to this fault has ponded a thick sequence of Pleistocene Saugus Formation in the Sylmar basin and Merrick syncline on the hanging wall side of north-dipping reverse faults. The moderate to steep north dip of strata there marks the forelimb of the anticline above the south-dipping Northridge fault. The San Fernando Valley is also underlain by the north-dipping Mission Hills, Verdugo, and Northridge Hills reverse faults. Fault-propagation folds above these faults have tectonic geomorphic expression, suggesting that the faults are active. The merged Northridge Hills and Mission Hills faults are interpreted as the updip extension of the 1971 aftershock zone. These south- and north-dipping reverse faults were initiated sometime during the deposition of the Saugus Formation, which took place from 2.3 to 0.6 Ma. Based on the oldest possible age of the initiation of faulting, we obtain minimum dip-slip rates of 0.3 to 1.1 mm/yr for the north-dipping reverse faults. The San Fernando Valley area has evolved through three distinct tectonic stages since the early Miocene. Normal faulting prevailed throughout the Miocene with a rift extending from the east Ventura basin to the northeastern San Fernando Valley. The Santa Susana and Verdugo faults are reactivated Miocene normal faults. Reverse faulting began with the Pliocene Fernando Formation but all Pliocene faults became inactive by the time of the deposition of the Saugus Formation. The Saugus is cut by younger Quaternary faults, which are currently active.

Introduction

The San Fernando Valley, California, was struck by two of the most devastating earthquakes in southern California history: the 1971 M_w 6.7 San Fernando and 1994 M_w 6.7 Northridge earthquakes (Figure 4.1). These events had similar thrust-type focal mechanisms but their aftershock zones dip in opposite direction [Whitcomb et al., 1973; Scientists of the U.S. Geological Survey and the Southern California Earthquake Center (hereafter referred to as USGS and SCEC), 1994; Hauksson et al., 1995; Mori et al., 1995]. The 1994 event ruptured a previously unrecognized south-dipping reverse fault, allowing for new insights into the active tectonics of the Transverse Ranges of southern

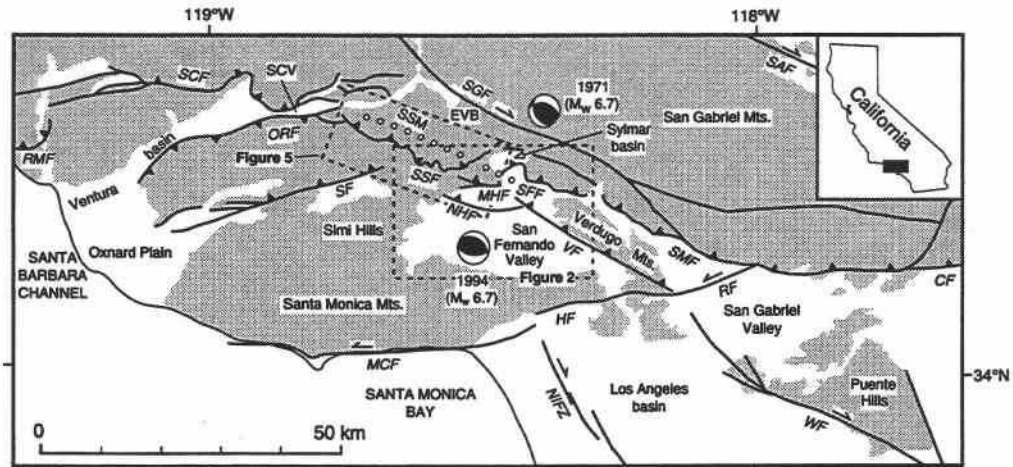


Figure 4.1 Tectonic map of the western Transverse Ranges, California. Hilly and mountainous areas are shaded. Location of Figures 4.2 and 4.5 is shown. Focal mechanism solutions for the 1971 San Fernando and 1994 Northridge earthquakes are shown after Whitcomb et al. [1973] and Hauksson et al. [1995], respectively. Major late Quaternary faults are from Jennings [1994] with revisions based on this study. Abbreviation for faults: CF, Cucamonga fault; HF, Hollywood fault; MCF, Malibu Coast fault; MHF, Mission Hills fault; NHF, Northridge Hills fault; NIFZ, Newport-Inglewood fault zone; ORF, Oak Ridge fault; RF, Raymond fault; RMF, Red Mountain fault; SAF, San Andreas fault; SCF, San Cayetano fault; SF, Simi fault; SFF, San Fernando fault; SGF, San Gabriel fault; SMF, Sierra Madre fault; SSF, Santa Susana fault; VF, Verdugo fault; WF, Whittier fault. Other abbreviations: EVB, East Ventura basin; SCV, Santa Clara Valley; SSM, Santa Susana Mountains. The eastern extension of the south-dipping Oak ridge fault beneath the north-dipping Santa Susana fault (open circles) is from Yeats and Huftile [1995].

California [Davis and Namson, 1994; Hauksson et al., 1995; Mori et al., 1995; Yeats and Huftile, 1995; Huftile and Yeats, 1996].

The northern margin of the San Fernando Valley lies at the updip projection of the two earthquake faults, and geology there may reflect many prehistoric earthquakes similar to the events in 1971 and 1994. Surface geology in and around the San Fernando Valley has been mapped by many investigators following an initial reconnaissance by Kew [1924]. In contrast, subsurface geology beneath a veneer of late Quaternary deposits in the San Fernando Valley is poorly known. Wentworth and Yerkes [1971] described subsurface faults underlying the valley based on geologic data available at that time, but the geometry, timing of faulting, and slip rate of those structures were not well constrained. Detailed subsurface mapping based on industry oil-well data was first carried out in the northwestern margin of the valley by Shields [1977]. We have extended this subsurface mapping eastward based on oil-well data from the recently developed Pacoima oil field and surrounding area, and a series of recently acquired seismic reflection lines from the petroleum industry. We also reinterpreted the work by Shields [1977] on the basis of the seismic data.

In this paper, we discuss the structural geology of the northern San Fernando Valley in light of the 1971 and 1994 earthquakes. An important question addressed here is whether a detailed geologic analysis of the San Fernando Valley would have led us to identify, prior to the earthquake, the south-dipping 1994 earthquake fault as potentially active. Through subsurface analysis, we are now able to constrain more closely the geometry, slip rate, and timing of movement of previously suspected but poorly defined blind thrust faults, leading to a better assessment of seismic hazards in this densely populated suburb of Los Angeles.

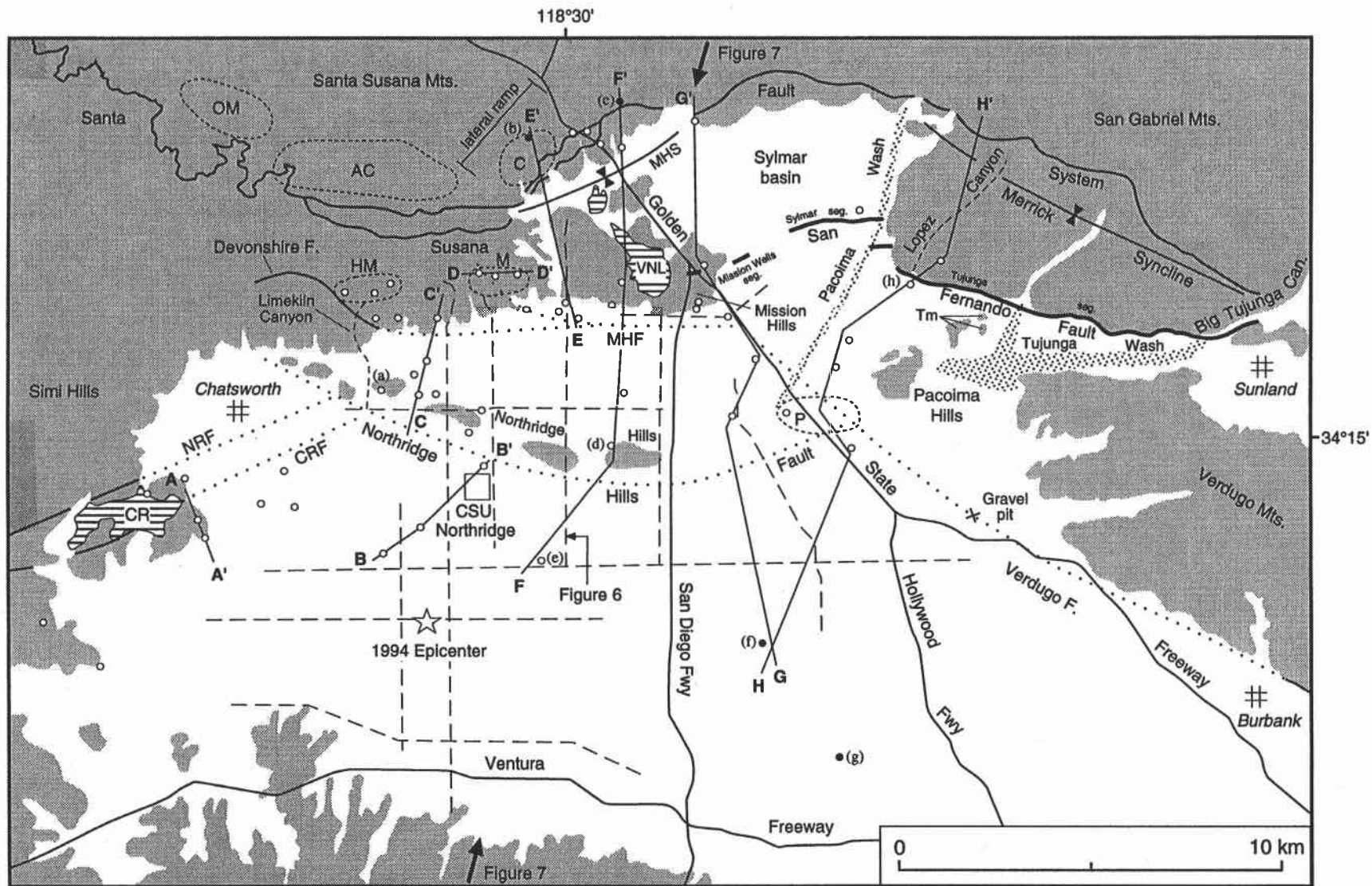
Regional Setting

The San Fernando Valley lies within the western Transverse Ranges of southern California and is bounded on the north by the San Gabriel and Santa Susana Mountains, on the south by the Santa Monica Mountains, on the east by the Verdugo Mountains, and on the west by the Simi Hills (Figure 4.1). The San Gabriel and Verdugo Mountains consist mainly of granitic and gneissic rocks of Mesozoic and older age. Other highlands around the valley are underlain primarily by middle Miocene to Pleistocene sedimentary rocks except for the northwestern margin, which is underlain by the Chatsworth Formation of Late Cretaceous age [Colburn et al., 1981].

Three sets of low hills, i.e. the Mission Hills, Northridge Hills, and Pacoima Hills, are present within the valley (Figure 4.2), and all are related to blind thrust faults

Figure 4.2 Index map of the San Fernando Valley. Area of pre-middle Pleistocene strata is shaded. Individual wells in oil fields are not shown. Cross sections A-A' to H-H' are shown in Figure 4.4. Locations of Figures 4.6 (dashed line) and 4.7 (between arrows) are shown. Abbreviation for faults: CRF, Chatsworth Reservoir fault; MHF, Mission Hills fault; NRF, North Reservoir fault. Abbreviation for oil fields: AC, Aliso Canyon; C, Cascade; HM, Horse Meadows; M, Mission; OM, Oat Mountain; P, Pacoima. Abbreviation for reservoirs: CR, Chatsworth Reservoir; VNL, Van Norman Lake. Other abbreviations: MHS, Mission Hills syncline. Individual wells mentioned in the text: (a), Sunray Porter Estate 81-16; (b), Mobil Macson Mission 1; (c), Ajax McCloskey Hansen 1; (d), Chevron Woo 1; (e), Chevron Frieda J. Clark Core Hole 1; (f), Chevron Leadwell 1; (g), Chevron Hazeltine Core Hole 1; (h), Intex Toon 1.

Figure 4.2



- | | | | | | | | |
|-------------|-------------------------------|---|----------------------------------|---|-----------|-------------|---------------------------|
| — · · · · · | Fault, dotted where concealed | ○ | Oil well | ○ | Oil field | — · · · · · | Seismic line |
| ————— | 1971 San Fernando fault | ● | Oil well reaching basement rocks | ▨ | Reservoir | A — A' | Cross section in Figure 4 |

[Wentworth and Yerkes, 1971; Barnhart and Slosson, 1973; Shields, 1977; Weber, 1980]. The northern margin of the valley is in part marked by the active Santa Susana fault system [Wentworth and Yerkes, 1971; Yeats, 1987a], which is part of a discontinuous north-dipping reverse fault system across the western Transverse Ranges extending from the Red Mountain and San Cayetano faults eastward to the Sierra Madre and Cucamonga faults (Figure 4.1). The Santa Susana fault of Yeats [1987a] extends 28 km from near the Santa Clara Valley to the southeast, across the southern slope of the Santa Susana Mountains, to the northern edge of the Sylmar basin, a deep sub-basin of the San Fernando Valley (Figures 4.1, 4.2). In the Santa Susana Mountains, this fault has thrust a thick conformable middle Miocene to Pliocene sequence on the north over a thin, discontinuous sequence of the same age on the south [Yeats, 1987a]. To the east, the fault turns northeast along the San Fernando lateral ramp to the northern edge of the Sylmar basin (Figure 4.2). The Sierra Madre fault bounds the San Gabriel Mountains on the southwest for more than 40 km (Figure 4.1). Detailed geomorphic mapping and geotechnical trenching revealed evidence for late Pleistocene to Holocene faulting along most of its length [Crook et al., 1987].

The 1971 San Fernando earthquake ruptured the northwestern end of the Sierra Madre fault system with a zone of aftershocks dipping 40° to the northeast. The hypocenter is located near the bottom of aftershocks at about 13 km depth beneath the San Gabriel Mountains [Hanks, 1974; Mori et al., 1995]. The focal-mechanism solution of aftershocks delineated a NNE-trending lateral ramp, down to the west, called the Chatsworth trend [Whitcomb et al., 1973]. This corresponds to the San Fernando lateral ramp on the Santa Susana fault [Yeats et al., 1994]. Primary surface breaks from the eastern end of the Mission Hills eastward to Big Tujunga Canyon for a distance of ~15 km are commonly referred to as the San Fernando fault (Figure 4.2). Slip vectors observed at the surface were predominantly left oblique [Sharp, 1975].

The aftershocks of the 1994 Northridge earthquake delineate a fault extending from a depth of 18 km up to about 5 km, dipping to the southwest at about 40° [Hauksson et al., 1995; Mori et al., 1995]. The hypocenter is located at the bottom of the aftershock zone with an almost pure thrust focal mechanism [Hauksson et al., 1995]. Maximum displacement on the 15-km-long fault plane exceeds 2 m [Hudnut et al., 1996; Wald et al., 1996], but no primary surface ruptures appeared during this event [USGS and SCEC, 1994]. Large parts of the 1971 and 1994 rupture areas overlap along strike, and the western portion of the 1971 fault plane cuts off the eastern portion of the 1994 fault plane at a depth of 5 to 8 km, so that it does not reach the surface [Mori et al., 1995]. Yeats and Huftile [1995] proposed that the 1994 Northridge fault is an eastern extension of the Oak

Ridge fault, a south-dipping reverse fault with a slip rate of 5 mm/yr along the southern edge of the Ventura basin. The Oak Ridge fault was interpreted to continue eastward beneath the active north-dipping Santa Susana fault (Figure 4.1) [Yeats and Huftile, 1995; Huftile and Yeats, 1996].

The locations of industry oil wells and unmigrated seismic reflection lines, the primary data set for this study, are shown in Figure 4.2. The northern San Fernando Valley contains the Horse Meadows, Mission, Cascade, and Pacoima oil fields. The northwestern San Fernando Valley, including the Horse Meadows, Mission, and Cascade oil fields, was described in an unpublished MS thesis by Shields [1977], and the results are incorporated in this paper. We update Shields' [1977] analysis on the Cascade oil field based on deep wells drilled since 1990. The Pacoima oil field was discovered in 1974 and was developed in the 1980s. We update a report on the Pacoima field by Schnurr and Koch [1979] on the basis of additional oil-well data and a seismic reflection line. Inter-field exploratory core holes and wildcat wells provide data for the southern San Fernando Valley and Sylmar basin (Figure 4.2). We used seismic lines to clarify the location and geometry of major subsurface structures. A more detailed analysis of seismic lines, together with other geophysical observations, will be published separately.

Stratigraphy

In this section, we briefly describe the distribution, lithology, and depositional environment of strata in and around the San Fernando Valley, which range in age from late Mesozoic to Quaternary (Figure 4.3). For more complete descriptions, see Oakeshott [1958], Saul [1975], Shields [1977], Seedorf [1983], and Yeats [1987a]. For stratigraphy in the east Ventura basin north of the Santa Susana fault, refer to Yeats et al. [1994].

Two types of crystalline basement rocks are found in and around the San Fernando Valley (Figure 4.3). In the southeastern part of the valley, the Chevron Hazeltine Core Hole 1 and Leadwell 1 wells reached coarse-grained, slightly gneissic, biotite-plagioclase-quartz diorite overlain by the middle to late Miocene Modelo Formation (Figures 4.2, 4.4g). This appears to be equivalent to quartz diorite widely exposed in the eastern Santa Monica Mountains and in the Verdugo Mountains. The granitic basement is Early Cretaceous in age, based on a mean of 25 U/Pb ages of 110 ± 13 m.y. on the batholith in southern California [Larsen et al., 1958]. North-trending seismic lines show that the top of granitic basement slopes gently to the north toward the Mission Hills (Figures 4.4g, h). We do not know the western limit of the granitic basement, however. North of the Santa Susana fault, the Mobil Macson Mission 1 and Ajax McCloskey Hansen 1 wells reached gray to green, hornblende-plagioclase-quartz gneiss with intercalated marble (Figures 4.2,

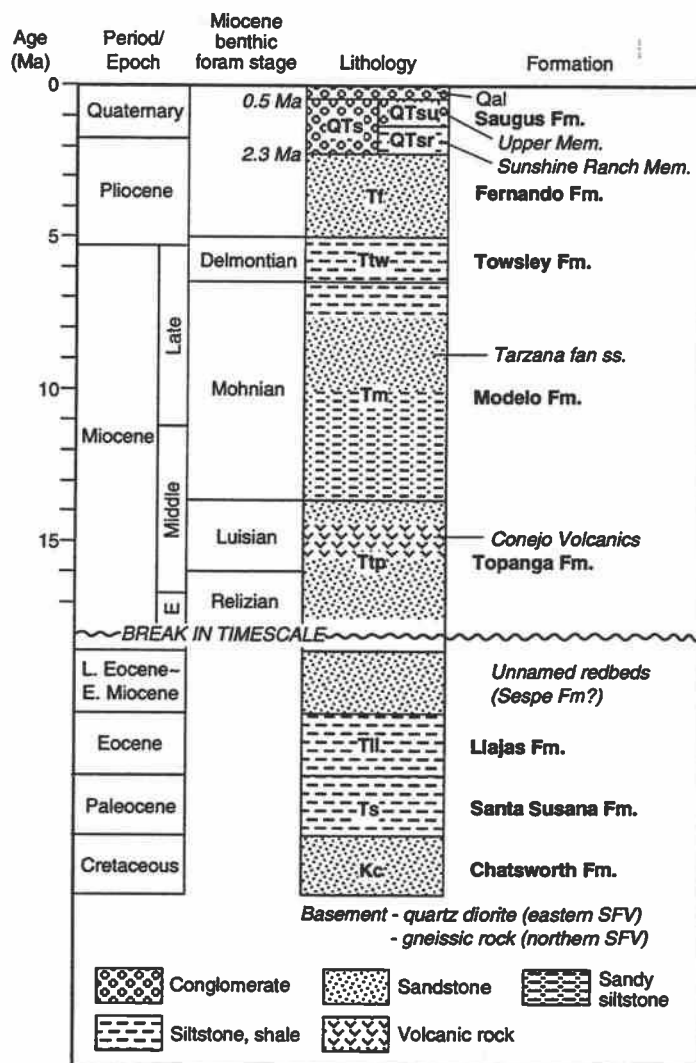


Figure 4.3 Stratigraphy of the San Fernando Valley. Based on Shields [1977], Dibblee [1991a, 1992], and this study. Age of the Saugus Formation is from Levi and Yeats [1993].

Figure 4.4 Cross sections across major geologic structures in the San Fernando Valley. See Figure 4.2 for location of sections and Figure 4.3 for stratigraphic abbreviations. Well numbers are identified in the Appendix. The Saugus Formation is lightly shaded and the Modelo Formation is darkly shaded. Magnetostratigraphic data in Van Norman Lake area by Levi and Yeats [1993] are projected into section (e). Dashed lines in sections (b), (e), (f) show correlation of marker beds within the Fernando and Modelo Formations. Dashed lines in sections (g) and (h) schematically show the shape of folds north of the Mission Hills and Verdugo faults. Note the difference in scale between sections (a) to (e) and sections (f) to (h). Sections (a) to (d) are from Shields [1977] with slight modifications.

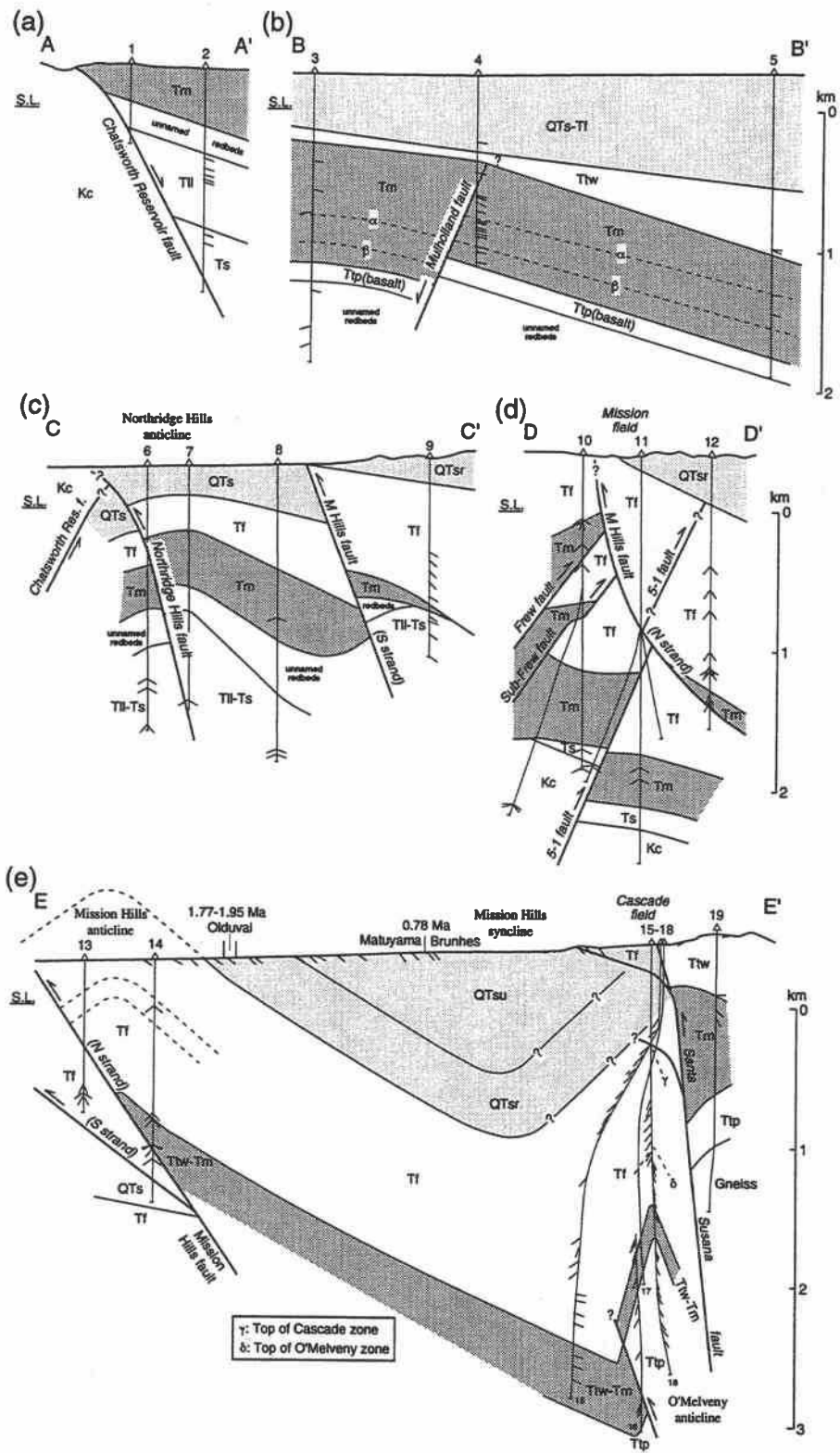


Figure 4.4

4.4e). This is the only basement known from the east Ventura basin south of a ridge of basement adjacent to the San Gabriel fault; it was correlated to the Placerita Series of the San Gabriel Mountains [Yeats, 1987a; Yeats et al., 1994].

Cretaceous and Paleogene sedimentary rocks are present only in the Simi Hills and adjacent western San Fernando Valley [Seedorf, 1983]. The Chatsworth Formation of Late Cretaceous age [Colburn et al., 1981] is widely exposed in the Simi Hills and reached by wells in the western San Fernando Valley, including the Horse Meadows and Mission oil fields [Shields, 1977]. This is predominantly gray to brown, micaceous, arkosic marine sandstone with igneous and metamorphic cobbles [Shields, 1977]. The Chatsworth Formation is at least 1400 m thick in the Simi Hills [Sage, 1971], with the base not exposed or reached by wells [Shields, 1977; Seedorf, 1983; Yeats, 1987a].

Surface exposures of Paleocene-Eocene marine clastic rocks in the San Fernando Valley are limited to near the Horse Meadows oil field, but the strata are widely distributed in the subsurface throughout the western part of the valley [Shields, 1977; Seedorf, 1983]. They are divided into the Santa Susana Formation of Paleocene age and the Llajas Formation of Eocene age (Figure 4.3). Both are gray to brown micaceous siltstone with layers of sandstone [Shields, 1977; Dibblee, 1992]. Commonly, they cannot be differentiated in the subsurface without microfossils. The nonmarine Simi Conglomerate, which underlies the Santa Susana Formation in the western Simi Hills and locally in the central Santa Monica Mountains, is absent in the study area, just as it is absent in the eastern Simi Hills and eastern Santa Monica Mountains [Seedorf, 1983; Yeats, 1987b]. The marine Eocene rocks are overlain by nonmarine variegated strata in the western San Fernando Valley may be correlated to the Sespe Formation of Eocene to early Miocene age (Figure 4.3).

The early to middle Miocene (Relizian to Luisian benthic foram stages) Topanga Formation consists of dark brown to black basaltic flows, conglomerate, and marine sandstone (Figure 4.3). The Topanga Formation is exposed in the Pacoima Hills where it overlies quartz diorite. Basalts were reached by wells in the Pacoima oil field (Figures 4.4g, h) and wells near the California State University at Northridge campus (Figures 4.2, 4.4b). These basalts appear to be correlated to the Conejo Volcanics of the Santa Monica Mountains, which were radiometrically dated at between 13.4 ± 0.9 and 15.6 ± 0.6 m.y. [Weigand and Savage, 1993]. Deep wells in the Cascade oil field reached deep-water marine sandstone of the Topanga Formation (Figure 4.4e), whereas no rocks older than the middle Miocene were reached in the Sylmar basin to the east (Figure 4.4f, g).

The middle to late Miocene (Mohnian stage) Modelo Formation and younger strata are distributed throughout the study area. The Modelo Formation consists mainly of light to

dark brown siltstone and shale and fine- to coarse-grained sandstone (Figure 4.3). Benthic foraminifera from this interval indicate an upper to middle bathyal depositional environment. This formation is about 3000 m thick north of the Verdugo fault, but it is only 1000 m thick in the Pacoima oil field, thinning to the south over a basement high (Figure 4.4h). The thickness of Modelo in the Sylmar basin is unknown. Massive sandstone beds in the Modelo Formation are the main oil-producing zone in the Pacoima field. These sandstone beds are part of the Tarzana submarine fan derived from the north in the late Miocene [Sullwold, 1960]. A high percentage of sandstone in the Modelo in the Chevron Woo 1 and Frieda J. Clark Core Hole 1 wells may indicate the approximate location of the channel of the Tarzana submarine fan (Figures 4.2, 4.4f).

The latest Miocene to earliest Pliocene (Delmontian stage) Towsley Formation is composed of gray to dark brown siltstone and shale with lenses of sandstone beds. This formation is distinguished on the surface by characteristic chocolate brown, fine-grained layers of shale and siltstone [Shields, 1977]. Like the Modelo, the Towsley thins southward from 500 m thick in the Pacoima oil field to 120 m thick in the Chevron Leadwell 1 well (Figures 4.4g, h). In the Horse Meadows and Pacoima oil fields where extensive dipmeter data are available, the Modelo-Towsley contact is an angular unconformity. The age of the Mohnian/Delmontian boundary is estimated as about 5 Ma in the Los Angeles basin [Blake, 1991].

The Pliocene Fernando Formation consists mainly of fine- to coarse-grained fossiliferous sandstone intercalated with siltstone. This represents proximal turbidite faces with blocky electric-log response. The Fernando Formation is the approximate age equivalent of the Repetto Formation in the Los Angeles basin defined by benthic microfauna [Shields, 1977; Blake, 1991]. In contrast to underlying strata, this formation has a relatively constant thickness of 300-500 m throughout most of the study area. It is, however, more than 1500 m thick in the western end of the Sylmar basin and in the Cascade oil field (Figure 4.4e), which is close to its thickness of the Fernando in the Aliso Canyon oil field [Shields, 1977; Yeats et al., 1994]. The Fernando Formation in the Cascade oil field contains two oil-producing zones separated by deep-water siltstone (Figure 4.4e).

The Plio-Pleistocene Saugus Formation consists of light gray pebble-cobble conglomerate and sandstone interbedded with claystone. On outcrops west of Van Norman Lake, the lower Saugus Formation consists predominantly of brackish, light red and green claystone, called the Sunshine Ranch Member, separated from the non-marine Upper Member with abundant conglomerate (Figure 4.3) [Oakeshott, 1958; Saul, 1975]. The Sunshine Ranch Member lenses out eastward near the intersection of the Golden State and

San Diego Freeways. In the subsurface south of the Mission Hills and Verdugo faults, it is possible to differentiate the Sunshine Ranch Member from the Upper Member based on lithology (Figures 4.4g, h). The Saugus Formation is as thick as 1200 m south of the Mission Hills fault but it is much thicker north of the fault in the Sylmar basin (Figures 4.4f-h). The Sunray Stetson Sombrero 1 well penetrated 3600 m of Saugus Formation, but it probably did not reach the bottom of the Upper Member (Figure 4.4g) [Shields, 1977]. The thickness of the Saugus Formation is also greatly affected by the growth of the anticline beneath the Northridge Hills (Figures 4.4f, g). Magnetic-reversal stratigraphy in Van Norman Lake area by Levi and Yeats [1993] indicates that the Saugus Formation was deposited between 2.3 and 0.5 m.y. ago (Figure 4.3).

Most of the San Fernando Valley is covered by alluvial deposits of middle to late Quaternary age. Because electric-logs and mud-logs start at a depth of a few hundred meters, we were unable to map the base of these deposits.

Structural Geology

The San Fernando Valley area is underlain by a series of late Cenozoic faults. These are divided into three groups on the basis of age: Miocene normal faults, Pliocene (pre-Saugus) reverse faults, and Quaternary (post-Saugus) reverse faults [Shields, 1977]. We discuss these faults by integrating seismic data and new well data from the Cascade and Pacoima oil fields with previous work, especially that of Shields [1977] and Yeats [1987a]. The 1994 Northridge earthquake fault is located beneath well control and is discussed separately

Miocene Normal Faults

Three Miocene normal faults were mapped in the northwestern margin of the San Fernando Valley [Shields, 1977]. The Chatsworth and North Reservoir faults marks a boundary between the San Fernando Valley and Simi Hills (Figure 4.2), and are well expressed by a steep gravity gradient [Corbató, 1963]. The Chatsworth Reservoir fault juxtaposes southeast-dipping Paleocene to Miocene strata in the hanging wall against the northwest-dipping Late Cretaceous Chatsworth Formation in the footwall (Figure 4.4a). The fault dips southeast at about 60° and crops out around the Chatsworth Reservoir [Shields, 1977]. The separation of the top of the Chatsworth Formation is about 4 km based on a projection of the Chatsworth-Santa Susana contact exposed in the Simi Valley toward the fault. The Chatsworth Reservoir fault projects northeast to the Limekiln Canyon area beneath late Quaternary alluvial deposits (Figure 4.2), but none of the wells north of the Northridge Hills fault is cut by the Chatsworth Reservoir fault. The difficulty in tracing

the Chatsworth Reservoir fault to the northeast is due to its truncation by the younger Northridge Hills fault (Figure 4.4c) [Shields, 1977]. The North Reservoir fault is in the Chatsworth Formation about 1000 m northwest of the Chatsworth Reservoir fault with a similar orientation (Figure 4.2) [Shields, 1977]. However, its location beneath alluvial deposits and its stratigraphic separation are poorly known because of the lack of subsurface data along the fault. These faults were active, northwest side up, during the time of deposition of the middle to late Miocene Tarzana fan; directional features on the Tarzana fan and the orientation of its western edge are parallel to the faults.

The Mulholland fault cuts the original and redrilled holes of the Atlantic Richfield Northridge Core Hole 1 well with a down-to-the-south sense of movement (Figure 4.4b) [Shields, 1977]. The strike of this fault is poorly constrained because no other wells penetrated this fault. The Modelo Formation is thicker on the downthrown side of the fault, whereas basaltic rocks of the Topanga Formation show the same thickness on both sides of the fault. The separation of marker beds in the Modelo Formation is about 200 m (Figure 4.4b). This fault cuts the Modelo Formation but appears to be overlain unconformably by Fernando Formation and probably by the Towsley Formation (Figure 4.4b) [Shields, 1977]. This suggests that the Mulholland fault was active during the time of deposition of the Modelo Formation [Shields, 1977]. The middle to late Miocene normal faulting along this fault is consistent with that observed in the east Ventura basin to the north [Yeats et al., 1994] and the northern Los Angeles basin to the south [Tsutsumi et al., 1996].

Pliocene (pre-Saugus) Reverse Faults

Reverse faults of Pliocene age are the south-dipping Frew fault system and the north-dipping Torrey-Roosa fault system which truncates the Frew system (Figure 4.5) [Yeats, 1987a]. The Frew fault system consists of several strands of south-dipping pre-Saugus reverse faults and is not exposed at the surface [Yeats, 1987a]. It was discovered in the subsurface in the Aliso Canyon oil field, where it brings Cretaceous and Paleogene rocks on the southwest against the Fernando Formation on the northeast [Yeats, 1987a, section H-H']. The main Frew fault dips 60° SW and has a reverse separation of about 2000 m. The Frew fault continues northwest without change of strike or dip to Gillibrand Canyon and farther west to the Santa Susana oil field with a more westerly trend (Figure 4.5) [Yeats, 1987a]. Between the Aliso Canyon and Santa Susana oil fields, the Frew fault system is truncated by the north-dipping Torrey-Roosa fault system and by the unconformity at the base of the Saugus Formation [Yeats, 1987a]. Southeast of the Aliso Canyon oil field, three strands of the Frew fault system are penetrated by wells in the Mission oil field (Figure 4.4d) [Shields, 1977]. These strands have a combined reverse

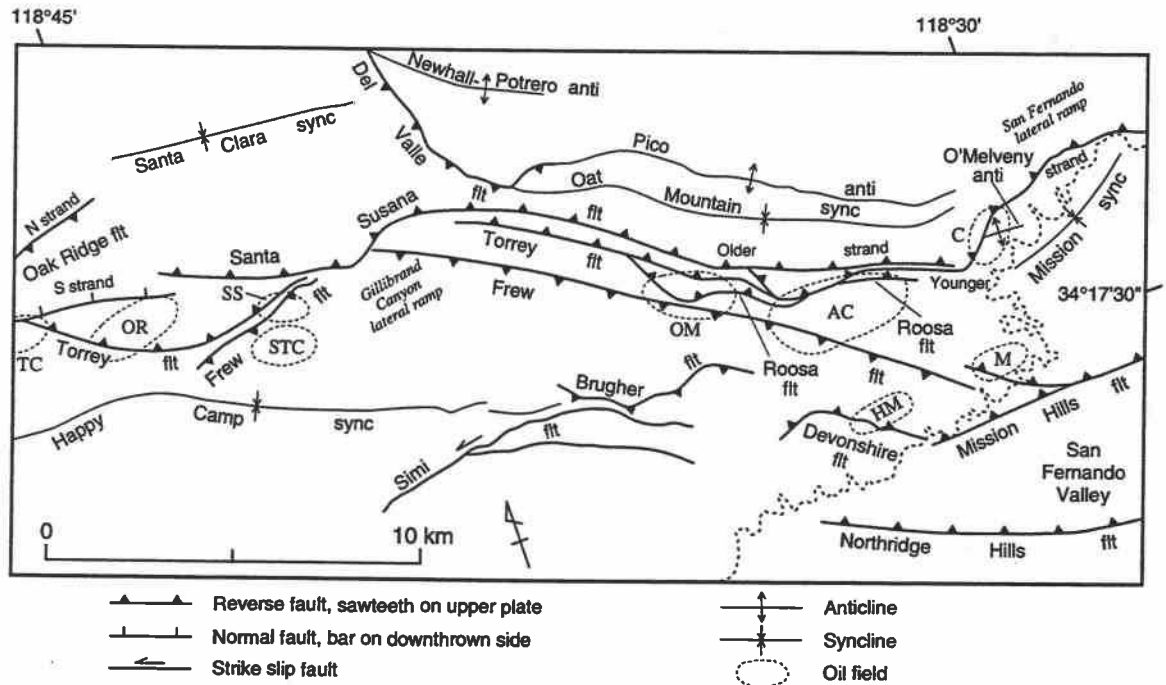


Figure 4.5 Tectonic map of the Santa Susana Mountains and northern San Fernando Valley. See Figure 4.1 for location. The northwestern margin of the San Fernando Valley is shown by dashed line. Because of a cross-cutting relation between the Frew, Oak Ridge, Roosa, Santa Susana, and Torrey faults near the surface, these faults are shown at 1 km depth from Yeats [1987a]. Abbreviation for oil fields: AC, Aliso Canyon; C, Cascade; HM, Horse Meadows; M, Mission; OM, Oat Mountain; OR, Oak Ridge; SS, Santa Susana; STC, South Tapo Canyon; TC, Torrey Canyon.

separation of the Modelo-Fernando contact of about 1700 m. These faults are cut by the northeast-dipping Mission Hills fault. The Frew fault system has not been recognized southeast of the Mission oil field [Shields, 1977]. The total mapped length of the Frew fault between the Santa Susana and Mission oil fields is 24 km [Yeats, 1987a]. The Fernando Formation is much thicker on the downthrown side of the fault system (Figure 4.4d, section H-H' of Yeats, 1987a), suggesting that it formed during the deposition of the Fernando Formation.

The north-dipping Torrey fault extends from the Torrey Canyon oil field southeast to the western end of the Aliso Canyon oil field (Figure 4.5), truncated updip by the Santa Susana fault or the base of the Saugus Formation [Yeats, 1987a, Figure 9.7]. At the western edge of the Aliso Canyon oil field, the Torrey fault dips 75° N and has about 300 m of separation [Yeats, 1987a]. The Roosa fault strikes E to ESE and dips 75° N in the Aliso Canyon oil field, truncating strands of the Frew fault system [Yeats, 1987a, sections H-H' and I-I']. The Roosa fault is truncated updip by the younger strand of the Santa Susana fault in the Aliso Canyon oil field. The Roosa fault terminates at about 4 km northwest of the Aliso Canyon oil field, where it is either truncated by the Torrey fault or it is a splay of that fault (Figure 4.5) [Yeats, 1987a].

East of the Aliso Canyon oil field, the Cascade oil field produces from a steep, nearly symmetrical anticline in the Fernando and Modelo Formations, which we name the O'Melveny anticline (Figure 4.4e). This fold trends ESE, which is discordant to the NE trend of the lateral ramp of the Santa Susana fault, and it appears to be unrelated to that fault (Figure 4.5). The O'Melveny anticline is a south-vergent fold based on a north-dipping fold hinge in the adjacent syncline to the south as established by dipmeter in the UMC Pico Unit 1 well (Figure 4.4e). The steep limbs suggest that the O'Melveny anticline is a rootless, lift-off fold from a décollement at the base of the Miocene shale sequence. It is not a simple, unfaulted anticline, because there is a structural repeat of the Delmontian/Mohnian and Luisian sequence in the UMC O'Melveny Park 2 well. This could be a strand of the fault controlling the south-verging lift-off fold. The Fernando Formation overlies the Modelo Formation conformably, with similar steep dips (Figure 4.4e). The Fernando shows thinning in the anticlinal crest and thickening in the flanks, observed by comparing structure contours of the Cascade and O'Melveny zones. This thinning probably is taken up in the silty sections of Fernando between the two zones.

We propose that the steep O'Melveny anticline, cored by the Modelo Formation, is the eastern continuation of the north-dipping Roosa reverse fault at the Aliso Canyon oil field (Figure 4.5). In section I-I' of Yeats [1987a], with greater details in sections C-C' and D-D' of Lant [1977], the Roosa fault dips steeply to the north, about 15° steeper than the

dip of north-dipping strata, including the Modelo Formation, in the hanging wall. Structure contours on the Roosa fault by Lant [1977] show that the fault trends E to ESE in the Aliso Canyon field and would project eastward to the Cascade field. Arguments for this correlation include the south vergence of the O'Melveny anticline. In addition, both structures predate the emplacement of the younger strand of the Santa Susana fault, because the Roosa fault is cut out by the younger strand [Lant, 1977; Yeats, 1987a] and there is no expression of the O'Melveny anticline in structure contours of the Santa Susana fault by Shields [1977]. There is also no evidence of the O'Melveny anticline in surface dips in the Saugus Formation or in tectonic geomorphology, suggestive that this anticline is inactive and is overlain unconformably by the Saugus Formation.

Quaternary (post-Saugus) Reverse Faults

Mission Hills fault

The Mission Hills fault is an east-trending reverse fault along the southern margin of the Santa Susana Mountains and Mission Hills (Figure 4.2). This fault was first mapped by Oakeshott [1958] on the basis of topography and petroleum industry data. West of Balboa Boulevard, along which the seismic line in Figure 4.6 was shot, this fault branches into two strands (Figures 4.2). The northern strand extends northwest and is cut by several wells in the Mission oil field (Figure 4.4d). The fault dips northeast at about 60°-70° and brings the Modelo Formation over the Fernando Formation [Shields, 1977]. The southern strand extends west to the Limekiln Canyon area, separating the Sunshine Ranch Member to the north from the Upper Member to the south (Figure 4.4c). The NE-dipping Devonshire fault mapped at the surface (Figure 4.2) as well as in the subsurface in the Horse Meadows oil field [Shields, 1977] may be a western extension of the southern strand of the Mission Hills fault.

East of Balboa Boulevard, the Mission Hills fault strikes due east and is penetrated only by the original hole of the Chevron Rinaldi Core Hole 1 well (Figure 4.4g). This well penetrated the steep (~70°) south limb of a fold composed of well-consolidated shale of the Modelo Formation, then reached gently north-dipping sandstone and conglomerate of the Saugus Formation. Because wells as deep as 3000 m, such as the Chevron Carey 1 and Panorama 1 wells, north of the Mission Hills anticline did not penetrate the fault, the dip of the fault must be greater than 60° (Figures 4.4f, g). A south-dipping fault mapped at the surface near the intersection of the San Diego and Golden State Freeways [Shields, 1977; Dibblee, 1991a] appears to be a back thrust of the Mission Hills fault (Figure 4.4g). The north limb of the Mission Hills anticline dips NNW at 60°-70°, almost parallel to or slightly shallower than the dip of the Mission Hills fault (Figures 4.4f, g).

The total mapped length of the Mission Hills fault is about 9 km. This fault is active in the Quaternary because it brings Miocene strata over the Saugus Formation (Figures 4.4e-g). The thickness of the Fernando Formation is about the same on both sides of the fault, suggesting that the Mission Hills fault initiated sometime during the deposition of the Saugus. A set of low hills exposing the Upper Member of the Saugus Formation in an anticline north of the fault is evidence that the Mission Hills fault is potentially active.

On the hanging wall of the Mission Hills fault, the Saugus Formation dips NNE to NNW into the Mission Hills syncline (Figure 4.2). The syncline extends and deepens to the northeast with the thickness of the Saugus Formation increasing from less than 1500 m south of the Cascade field (Figure 4.4e) to more than 3000 m in the Sunray Stetson Sombrero 1 well (Figure 4.4g). East of this well, the synclinal hinge lies at the extreme northern edge of the Sylmar basin or even underneath the Santa Susana fault [Dibblee, 1991a]. This syncline continues east of the Pacoima Wash as the Merrick syncline (Figures 4.2, 4.4h). In contrast to the Sylmar basin, the north and south flanks of the Merrick syncline are well exposed in hilly terrain north of the 1971 San Fernando fault. The Merrick syncline trends southeast and terminates near Big Tujunga Canyon (Figure 4.2) [Dibblee, 1991a, 1991b].

Northridge Hills fault

A series of discontinuous, NW-trending low hills from near the town of Chatsworth eastward to the San Diego Freeway (Figure 4.2), is the topographic expression of part of a south vergent, fault-propagation fold above the blind, north-dipping Northridge Hills fault (Figures 4.4c, f). The hills terminate near the San Diego Freeway, but the subsurface Northridge Hills anticline extends ENE to the Pacoima oil field (Figures 4.4g, h). The absence of hills along the eastern half of the fault may be due to smaller amplitude of the Northridge Hills anticline to the east (Figures 4.4f-h) and erosion/sedimentation in Pacoima and Tujunga Washes (Figure 4.2). The total mapped length of the Northridge Hills fault is 15 km.

In the western half of the hills, the Northridge Hills fault dips northward at about 70° (Figure 4.4c). Here, the fault cuts the Saugus Formation as demonstrated in the Sunray Porter Estate 81-16 well 1 km west of the cross section C-C' (Figure 4.2) [Shields, 1977]. East of the California State University at Northridge campus, the Northridge Hills anticline and underlying fault are documented by a seismic line (Figure 4.6) and well data (Figure 4.4f). In contrast to the fault farther west, the Northridge fault here does not offset reflectors within the Saugus Formation and probably does not offset reflectors in the Fernando Formation (Figure 4.6). The lowermost clearly defined reflector is correlated to

Figure 4.6 Unmigrated seismic profile along Balboa Boulevard; (a) uninterpreted and (b) interpreted. See Figure 4.2 for location. Chevron Frieda J. Clark Core Hole 1 well is projected 600 m from the west, based on a time-depth conversion calculated from sonic log by David Okaya at University of Southern California. See Figure 4.3 for stratigraphic abbreviations. The lowermost clearly defined reflector depicts conglomerate of the Topanga Formation and granitic basement. Because the basement shallows to the east, the top of the Topanga Formation in the Chevron Frieda J. Clark Core Hole 1 well is projected from the west. This reflector is not offset by the Northridge Hills fault, suggesting that the Northridge Hills anticline is a thin-skinned structure. Axial surfaces for the Northridge Hills anticline depicts a growth triangle within the Saugus Formation, evidence that the Northridge Hills fault initiated sometime during the deposition of the Saugus.

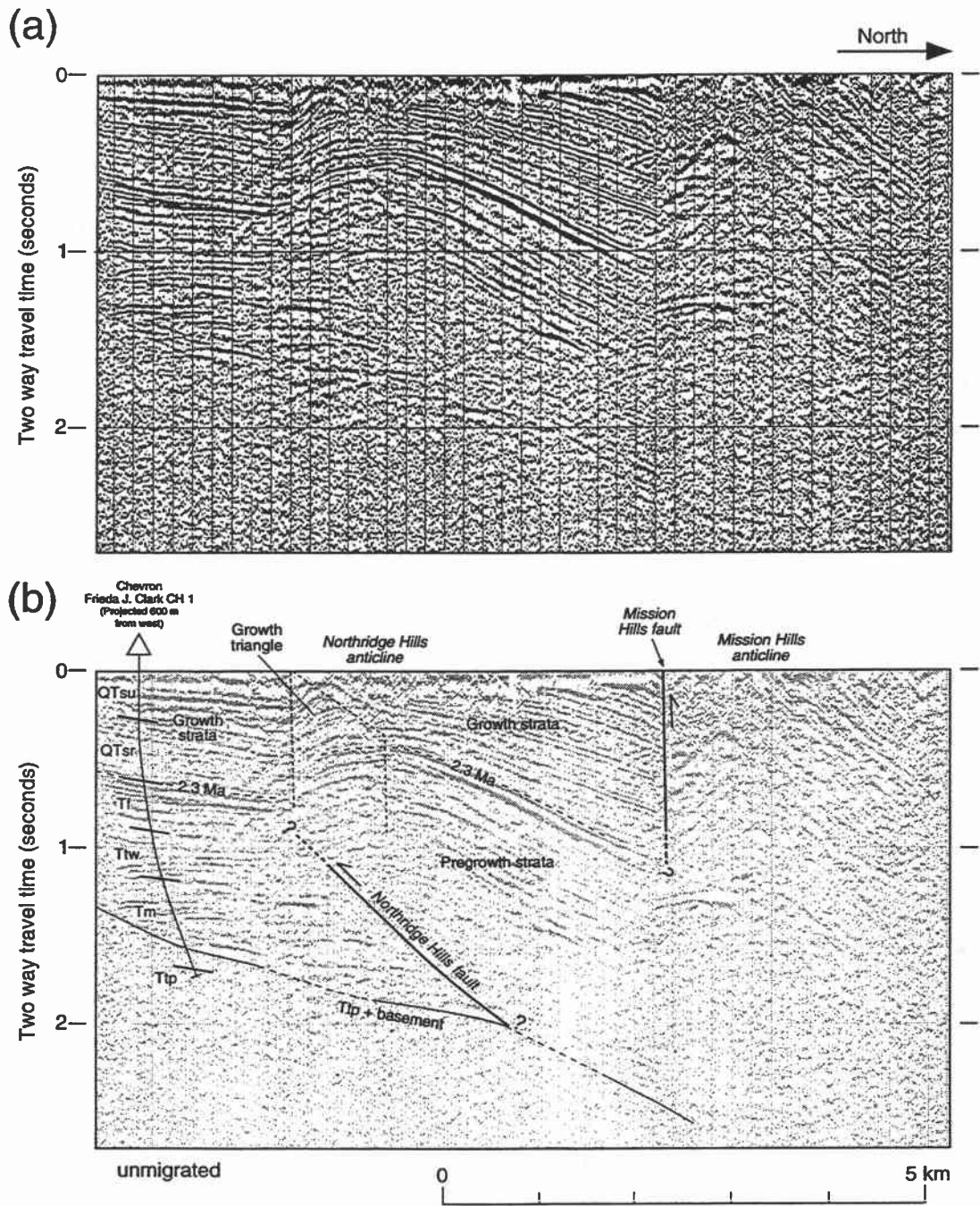


Figure 4.6

thin conglomerate of the Topanga Formation and granitic basement. This reflector dips northward without being offset by the Northridge Hills fault (Figure 4.6), suggesting that the Northridge Hills anticline is a thin-skinned structure. One kilometer east of the seismic line, the Chevron Woo 1 well penetrated the Northridge Hills fault at a depth of 2100 m with stratigraphic repeat of part of the Tarzana fan sandstone of the Modelo Formation (Figure 4.4f).

East of the San Diego Freeway, the Northridge Hills anticline trends ENE to NE except in the eastern part of the Pacoima oil field where it trends due east. The location of this anticline was previously inferred by Weber [1980] based on a steep gradient in the ground-water table. The Northridge Hills fault in the Pacoima oil field is beneath well control, although some wells reached close to the base of the Topanga Formation (Figures 4.4g, h). The Northridge Hills anticline is truncated by the NW-trending Verdugo reverse fault at the eastern end of the Pacoima oil field (Figure 4.4h).

The Northridge Hills fault is considered potentially active because the overlying anticline is expressed by tectonic geomorphology [Wentworth and Yerkes, 1971; Barnhart and Slosson, 1973]. In the subsurface, the Saugus Formation is significantly thicker on the limbs than on the crest of the anticline (Figure 4.4f). The seismic line in Figure 4.6 also depicts an upward narrowing kink band or growth triangle according to the nomenclature of Suppe et al. [1992] within the Saugus Formation. A growth triangle develops within the stratigraphic sequence, called growth strata, deposited during fold growth [Suppe et al., 1992]. The initiation of the structural growth can be recognized at the top of the constant-width kink band, which is slightly above the top of the Fernando Formation for the Northridge Hills anticline (Figure 4.6b). In contrast to the Saugus Formation, the underlying Fernando and Towsley Formations exhibit constant thickness across the fold (Figure 4.4f). These observations suggest that the growth of the Northridge Hills anticline postdates the base of the Saugus Formation, dated at 2.3 Ma by Levi and Yeats [1993].

Verdugo fault

The Verdugo fault extends from the eastern end of the Mission Hills southeast for about 32 km to a termination against the left-slip Raymond fault (Figure 4.1) [Weber, 1980]. The Verdugo fault bounds the southwestern margin of the Verdugo Mountains and is probably responsible for about 1000 m of relief between the mountain crest and valley floor [Wentworth and Yerkes, 1971]. This structural relief is well expressed by a steep gradient of residual gravity [Corbató, 1963]. Tectonic geomorphic features along the Verdugo fault were studied in detail by Weber [1980]. Here we present subsurface data from the Pacoima oil field.

The Verdugo fault near the City of Burbank has a series of southwest-facing scarps on probable Holocene alluvial surfaces (Figure 4.2) [Weber, 1980]. Northwest to the Pacoima Hills, the fault is mostly beneath alluvial deposits, and its location was inferred by Weber [1980] based on the steep gradient of ground-water table and fault exposures in a gravel pit (Figure 4.2). The granitic basement overlain by the north-dipping Topanga and Modelo Formations crop out in the Pacoima Hills that appear to be the northern extension of the Verdugo Hills separated by Tujunga Wash. In the northeastern end of the Pacoima oil field, three wells are cut by a northwestern extension of the Verdugo fault which Schnurr and Koch [1979] called the Haddon fault. This NW-trending fault dips at about 55° , truncating the north limb of the Northridge Hills anticline (Figure 4.4h). We do not know, however, whether this fault plane has been folded by the underlying Northridge Hills anticline. North of the fault is a tightly folded anticline with vertical to overturned south limb. The folded Modelo Formation is directly overlain with angular unconformity by about 50 m of alluvial deposits. North of the Verdugo fault, no well reached basalt of the Topanga Formation (Figure 4.4h).

Paleontologic data are not available for the Intex Toon 1 well northeast of the Pacoima oil field and immediately south of the 1971 surface ruptures (Figure 4.2), but the strata there appear to be the Modelo Formation based on lithology. The Modelo also crops out 500 m south of the surface breaks, north of the Pacoima Hills (Figure 4.2). These observations suggest that the Modelo Formation in the hanging wall of the Verdugo fault is about 3000 m thick, much thicker than in the footwall (Figure 4.4h). The Verdugo fault may be a reactivated Miocene normal fault, similar to others in the Ventura and Los Angeles basins [e.g., Wright, 1991; Yeats et al., 1994; Tsutsumi et al., 1996].

Northwest of the Pacoima oil field, there are no subsurface data to map the extension of the Verdugo fault. Based on ground-water table data, Wozab [1952] and Weber [1980] suggested that the Verdugo fault may curve westward and join the Mission Hills fault, a suggestion we accept. Both faults are north-dipping reverse faults with prominent fault-propagation folds plunging to the west. They also mark the southern boundary of strata that dip moderately to steeply north into the Sylmar basin and Merrick syncline.

The Verdugo fault is considered potentially active because it has scarps on probable Holocene geomorphic surfaces [Weber, 1980]. Because there are no strata younger than the Modelo Formation in the hanging wall of the fault, our subsurface analysis provides little control on Quaternary movement along the Verdugo fault.

1971 San Fernando fault

The 1971 San Fernando earthquake produced primary surface ruptures about 15 km long along the western end of the Sierra Madre fault zone. These were mapped in detail and were generally divided into the Mission Wells, Sylmar, and Tujunga segments (Figure 4.2) [Kamb et al., 1971; U.S. Geological Survey Staff, 1971; Barrows, 1975; Sharp, 1975; Weber, 1975]. The slip vectors along the ruptures had a thrust component of up-on-the-north as well as a left-lateral component of movement [e.g. Sharp, 1975]. We have constructed two cross sections across the ruptures (Figures 4.4g, h) and confirmed earlier observations that the 1971 San Fernando fault, for the most part, ruptured north-dipping bedding planes [Kamb et al., 1971; U.S. Geological Survey Staff, 1971; Barrows, 1975; Sharp, 1975; Weber, 1975].

The surface ruptures of the Mission Wells segment occurred along the contact between the Saugus Formation to the north and Miocene strata on the south [Weber, 1975; Shields, 1977]. The dip of the ruptures was 50°-80°N [Weber, 1975; Sharp, 1975], similar to the dip of the Saugus and older strata penetrated by the Chevron Carey 1 well (Figure 4.4g). To the east, the surface ruptures of the Sylmar segment appeared within gently sloping alluvial plains but these align exactly on the western extension of the contact between the Saugus Formation and Fernando/Towsley strata in the Lopez Canyon area. The dip of the surface breaks was 50°-90°N, essentially parallel to the bedding of the Saugus Formation immediately to the north [Sharp, 1975]. These observations suggest that the Mission Wells and Sylmar segments ruptured along the base of the Saugus Formation (Figure 4.4g).

The Tujunga segment steps to the right about 1300 m from the Sylmar segment and marks the southern front of low hills (Figure 4.2). It is parallel to the strike of the moderately north-dipping Modelo and younger strata to the north [Kamb et al., 1971; U.S. Geological Survey Staff, 1971; Barrows, 1975; Sharp, 1975]. The dip of the surface breaks measured by Sharp [1975] ranged from 15°N to 70°N, which tends to be slightly less than the dip of the Modelo Formation at each locations. Nonetheless, the dip of the ruptures is progressively shallower eastward to Big Tujunga Canyon [Sharp, 1975] in the same direction as the shallowing of dip of the Modelo Formation [Dibblee, 1991a, 1991b]. The age of the strata on the footwall of the Tujunga segment cannot be determined conclusively by paleontologic data, but the strata appear to be the Modelo Formation as described above. Based on these observations, we speculate that the Tujunga segment ruptured along or slightly across a bedding plane within the Modelo Formation (Figure 4.4h). However, we could not identify a discrete fault plane in the Doheny Reeves 1 well.

In summary, the 1971 San Fernando fault appears to have propagated upward following moderately to steeply north-dipping bedding planes: along the base of the Saugus Formation on the Mission Wells and Sylmar segments and along a bedding plane within the Modelo Formation on the Tujunga segment.

Discussion

Geologic Evidence of the 1994 Northridge Fault in the Northern San Fernando Valley

The 1994 Northridge earthquake did not rupture the surface, and the causative fault is below control of industry oil-well and seismic data. Nonetheless, there are near-surface geologic expressions of the active, south-dipping blind fault, which might have led us to identify the fault prior to the 1994 earthquake.

Yeats and Huftile [1995] and Huftile and Yeats [1996] identified geologic features in the Santa Susana Mountains and east Ventura basin which are best explained by faulting on the south-dipping Northridge fault. The active north-dipping Santa Susana fault strikes across the southern slope, not the mountain front, of the Santa Susana Mountains, indicating footwall uplift on the Santa Susana fault [Yeats and Huftile, 1995], similar to that which occurred during the 1994 earthquake [Hudnut et al., 1996]. The Plio-Pleistocene Saugus Formation is ~300 m thick in the footwall block, whereas it is as thick as 2 km in the hanging wall block [Yeats et al., 1994]. This unusual relationship of a Pleistocene basin in the hanging wall block of the active Santa Susana reverse fault, together with footwall uplift, was interpreted to have been caused by reverse faulting on the south-dipping blind Northridge fault [Yeats and Huftile, 1995]. The moderate to steep north dip of the Saugus Formation in the east Ventura basin was interpreted to represent the forelimb of the blind Northridge fault [Davis and Namson, 1994; Yeats and Huftile, 1995; Huftile and Yeats, 1996].

Analogous geologic features are observed in the northern San Fernando Valley. The Sylmar basin, the eastern extension of the east Ventura basin, contains >3 km of the moderately to steeply north-dipping Saugus Formation whereas it is 1.5 km thick south of the Mission Hills fault (Figures 4.4f-h). The Sylmar basin and its eastern extension, the Merrick syncline, are located on the hanging wall of the north-dipping Mission Hills and Verdugo reverse faults (Figures 4.2, 4.7), just as the east Ventura basin is on the hanging wall of the Santa Susana fault (Figure 4.1). We propose that the north-dipping strata north of the Mission Hills and Verdugo faults represent the forelimb of the Northridge blind fault, which has ponded thicker Saugus Formation to the north (Figure 4.7).

In contrast, the thickness of older strata is not affected by the blind Northridge fault. The thickness of the Fernando Formation is about the same on both sides of the

Figure 4.7 Cross section down to 20 km depth across the central San Fernando Valley, including 1971 San Fernando and 1994 Northridge earthquake zones. See Figure 4.2 for location of the section and Figure 4.3 for stratigraphic abbreviations. Wells are identified in the Appendix. Aftershocks for the 1971 and 1994 earthquakes within a 15-km-wide strip including the line of this section are from Mori et al. [1995]. Note that the 1994 aftershocks are overlain by the 1971 aftershocks which lie downdip of the Mission Hills and Northridge Hills faults.

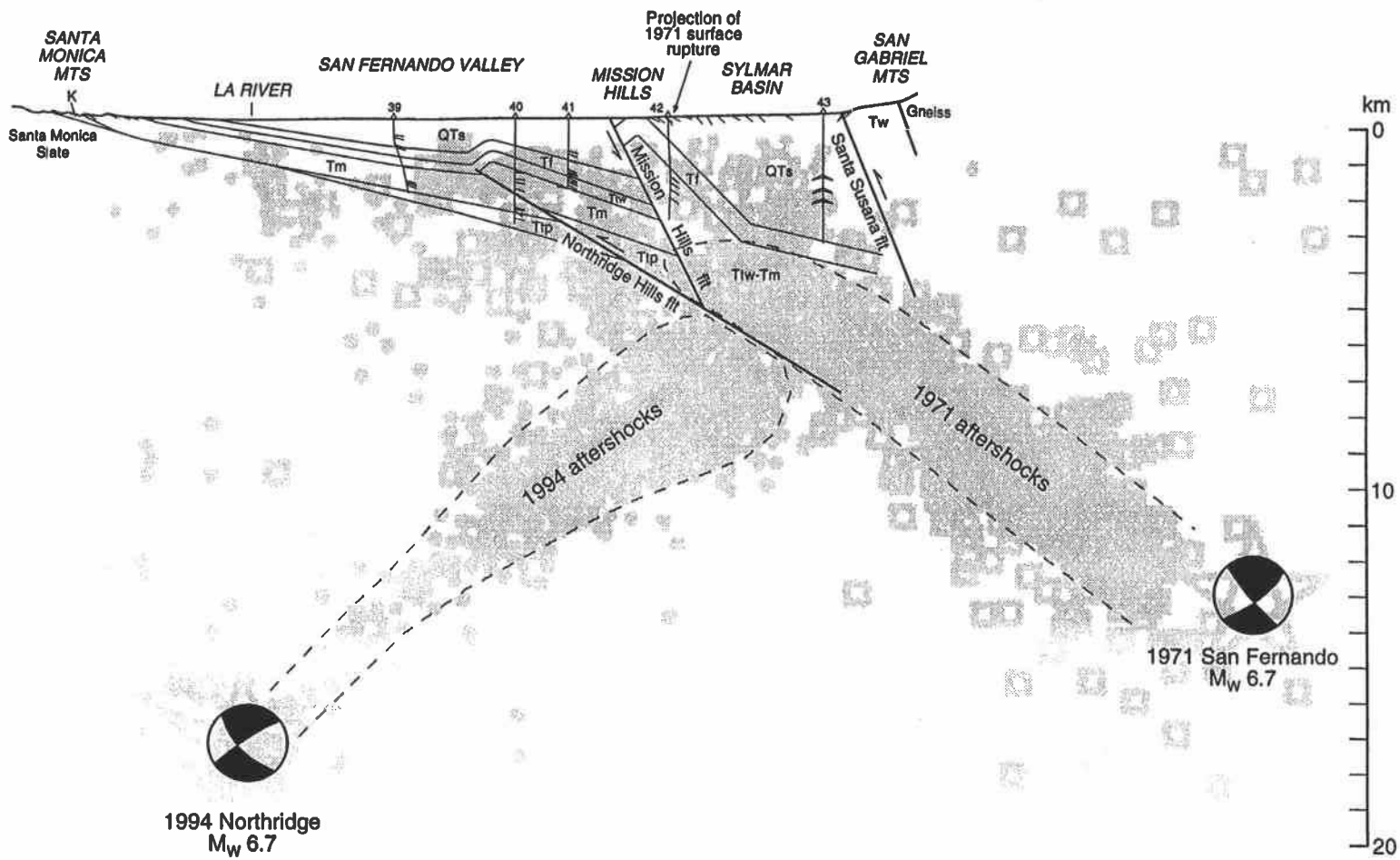


Figure 4.7

Mission Hills fault (Figure 4.4f). A thickness of 850 m of Fernando/Towsley strata exposed in Lopez Canyon is about the same as that south of the Verdugo fault (Figure 4.4h). These observations support the interpretation of Huftile and Yeats [1996] that the initiation of the Northridge fault was sometime during the deposition of the Saugus Formation, between 2.3 and 0.6 Ma based on magnetic stratigraphy by Levi and Yeats [1993].

Davis and Namson [1994] obtained an average dip slip rate of 1.4-1.7 mm/yr on the Northridge fault based on a balanced cross section from the northern Los Angeles basin northward to the Santa Clara Valley. A similar dip-slip rate of 1.7 mm/yr was calculated by Huftile and Yeats [1996] based on the amount of uplift on the base of the Saugus Formation across the forelimb of the Northridge fault in the Santa Susana Mountains and east Ventura basin. These rates are one-third that on the Oak Ridge fault in the Ventura basin, the western continuation of the Northridge fault, indicating an eastward decrease in slip rate on the south-dipping reverse fault system [Yeats and Huftile, 1995; Huftile and Yeats, 1996]. The technique used by Huftile and Yeats [1996] is not applicable in the San Fernando Valley because neither the top nor the bottom of the forelimb can be located by available data.

Several dislocation models of the 1994 earthquake have been presented based on geodetic and strong ground motion data [USGS and SCEC, 1994; Hudnut et al., 1996; Wald et al., 1996]. The eastern edge of the rupture plane in these models are placed near Van Norman Lake or farther west. The Pleistocene basin with thick Saugus deposition which we interpret as the surface expression of the Northridge fault continues farther east as the Merrick syncline and terminates near the City of Sunland (Figure 4.2). This may indicate that a 15-km-long stretch at the eastern edge of the Northridge fault may have been left unruptured during the 1994 event. The northeast trend of the Mission Hills synclinal axis south of the Cascade oil field (Figure 4.2), as defined by surface dips of the Saugus Formation, is discordant to the strike of the Northridge fault defined by 1994 aftershocks. This may be an expression of a lateral ramp on the Northridge fault along the Chatsworth trend of Whitcomb et al. [1973], because the synclinal axis turns to the east in the main Sylmar basin and to the southeast in the Merrick syncline [Dibblee, 1991a; 1992b].

Mori et al. [1995] noted that the 1994 aftershocks are truncated updip by the 1971 aftershocks (Figure 4.7). The base of the 1971 aftershock zone projects upward and southward to the Northridge Hills and Mission Hills faults. These faults may be a branch of the 1971 fault plane and, according to the thrust-front migration model of Ikeda [1983], may be the youngest of all the north-dipping faults. The Mission Wells and Sylmar segments of the 1971 surface breaks occurred north of the Mission Hills fault (Figure 4.7).

Because they had little topographic expressions prior to the earthquake and mostly followed north-dipping bedding planes [Kamb, 1971; U.S. Geological Survey Staff, 1971; Weber, 1975], the 1971 earthquake may not be a characteristic event on the north-dipping fault plane.

Fault Slip Rate and Seismic Hazard in the San Fernando Valley

In addition to the faults that ruptured in 1971 and 1994, the Mission Hills, Northridge Hills, and Verdugo faults are potentially active based on geomorphic and subsurface geologic data. Because the reverse faulting on these faults postdates the base of the Saugus, the age of which is known, it is possible to calculate slip rate for these structures.

The offset on the base of the Saugus along the central portion of the Mission Hills fault is 2200 m in section E-E' and 1650 m in section F-F' (Figures 4.4e, f). In section D-D' near the western end of the fault, the offset is much smaller (Figure 4.4d). Due to sparse subsurface control, certain error bars should accompany these measurements. Taking these uncertainties into consideration, we estimate the maximum offset on the base of the Saugus by the Mission Hills fault is 1500-2500 m. Dividing this by an age for the horizon, 2.3 Ma [Levi and Yeats, 1993], which is the oldest possible age for the initiation of reverse faulting, we obtain a minimum dip-slip rate of 0.65-1.1 mm/yr for the Mission Hills fault. The Northridge Hills fault offsets the massive sandstone bed of the Modelo Formation about 800 m (Figure 4.4f). This yields an minimum dip-slip rate of 0.35 mm/yr for the Northridge Hills fault. The actual rate may be much greater because, in a fault-propagation fold model, slip on the fault decreases toward the fault tip and is consumed in folding above the tip [Suppe and Medwedeff, 1990]. The offset of the base of the Saugus by the Verdugo fault in the Pacoima oil field is constrained only as >1000 m because the Saugus on the hanging wall has been eroded (Figure 4.4h). This yields a minimum dip-slip rate of >0.45 mm/yr for the Verdugo fault.

Although these faults do not have well-defined continuous scarps and are considered to be blind [Wentworth and Yerkes, 1971; Barnhart and Slosson, 1973], they may pose risks of coseismic ground deformation. All these faults have fault-propagation folds with moderately to steeply dipping limbs, which grow with slip along the underlying faults. There are examples of coseismic flexural-slip faulting and related ground deformation during historical earthquakes whereas there are no known examples of those formed by aseismic creep [Yeats, 1986]. The moderate to steep dip of strata along the Mission Hills and Northridge Hills also make the area susceptible to slope failure associate

with strong shaking, as occurred in the Mission Hills area during the 1994 earthquake [Hecker et al., 1995].

Possible earthquake scenarios in the San Fernando valley depends strongly on how these faults interact at depth. Subsurface data suggest that the Northridge Hills and Mission Hills faults merge at a depth of about 5 km (Figure 4.7) and may rupture in a single earthquake. Further north, these may interact with the Santa Susana fault system. The Mission Hills and Verdugo faults may form a continuous fault [Weber, 1980] and could break simultaneously. The resolution for these speculations awaits paleoseismological data on the timing of prehistoric earthquakes on individual faults.

Structural Evolution of the Northern San Fernando Valley Area

Yeats et al. [1994] showed that the predominant structural style of the east Ventura basin in the middle and late Miocene was normal faulting related to the WNW-trending east Ventura rift. During this time interval, the western Transverse Ranges rotated rather uniformly 50°-60° clockwise [Kamerling and Luyendyk, 1979; Hornafius et al., 1986]. Prior to this rotation, the east Ventura rift was oriented WSW-SW (Figure 4.8) [Yeats et al., 1994]. On the eastern extension of this Miocene rift, the Verdugo fault was a north-dipping normal fault during the deposition of the Modelo Formation. The Modelo in the Pacoima oil field contains basaltic rocks (Figure 4.4h), evidence that the rifting there was accompanied by volcanism. No evidence of normal faulting or volcanism is found at the Cascade oil field or along the Mission Hills fault, probably because post-Modelo strata are too thick to allow detailed study of older rocks.

Miocene normal faulting was also documented along the southern boundary of the Simi Hills (Figure 4.8) [Campbell and Yerkes, 1976; Shields, 1977; Yeats, 1987b]. The Simi Hills is underlain by a N- to NW-dipping conformable sequence of Late Cretaceous to Oligocene marine and nonmarine strata, and post-Miocene rocks are deposited only around the margin of the Simi Hills [Yeats, 1987b, Figure 12-1]. At the southeastern margin of the Simi Hills, the older strata disappear beneath the upper Topanga and Modelo Formations, which show southerly dips. These relations indicate that the uplift and northward tilt of the Simi Hills occurred prior to the deposition of the upper Topanga Formation [Yeats, 1987b]. The Tarzana submarine fan was diverted around the Simi Hills; one lobe of the fan flowed southwest along the east Ventura rift [Yeats et al., 1994] and the other southeast through the San Fernando Valley (Figure 4.8). Campbell and Yerkes [1976] explained the northward tilt of the Simi Hills as a block rotation between the ancestral Oak Ridge and Boney Mountain south-dipping normal faults (Figure 4.8). The Chatsworth Reservoir and North Reservoir faults appear to have been part of this south-dipping normal fault system

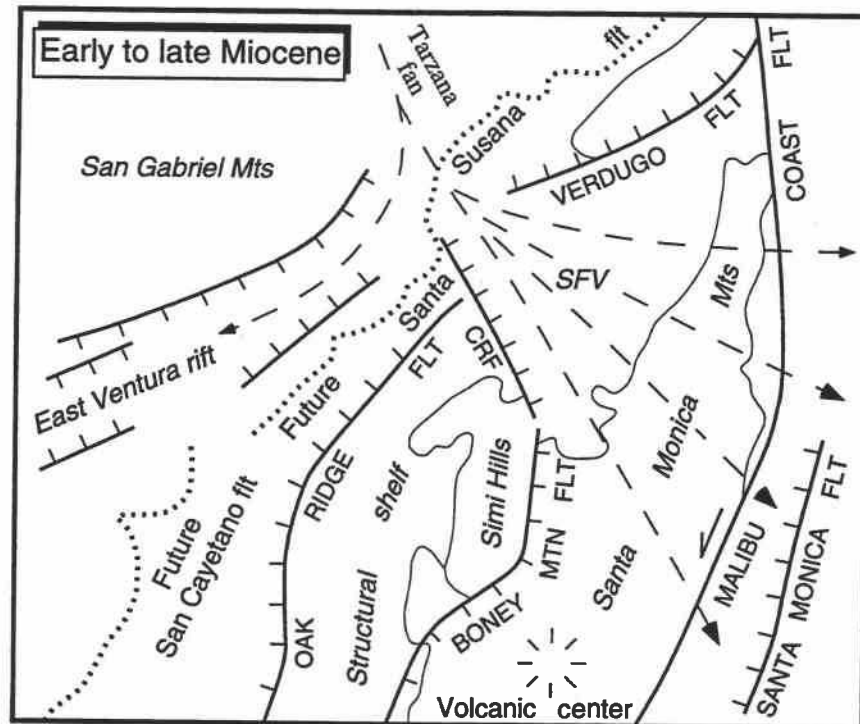


Figure 4.8 The San Fernando Valley and vicinity during the early to late Miocene after removal of 50° - 60° clockwise rotation documented by Kamerling and Luyendyk [1979] and Hornafius et al. [1986]. Modified from Yeats et al. [1994]. Left-slip of 20-40 km on the Malibu Coast fault [Tsutsumi et al., 1996] is removed. The course of Tarzana submarine fan from Sullwold [1960] and Yeats et al. [1994]. CRF, Chatsworth Reservoir fault; SFV, San Fernando Valley.

[Yeats et al., 1994] and may have controlled the depositional pattern of the west edge of the Tarzana fan. We can not determine the displacement on this fault during the middle to late Miocene because the Modelo is present only on the downthrown side of the fault (Figure 4.4a).

Reverse faulting began with the Fernando Formation, predominantly by fault-propagation folds at the Pico and Newhall-Potrero anticlines and by the south-dipping Frew fault system (Figure 4.5) [Yeats, 1987a; Yeats et al., 1994; Huftile and Yeats, 1996]. The Frew fault system was an ancestor of the active south-dipping Oak Ridge reverse fault beneath the Santa Susana Mountains [Yeats and Huftile, 1995]. The Frew fault is truncated by the Torrey-Roosa fault, and both faults are overlain unconformably by the Saugus Formation [Yeats, 1987a].

Quaternary faults include the north-dipping Santa Susana, Mission Hills, Verdugo, San Fernando, and Northridge Hills reverse faults and the south-dipping 1994 Northridge reverse fault. All north-dipping faults have propagated to the surface or to within a few kilometers of the surface, and these have topographic expressions. Although the Northridge fault is overridden by these north-dipping faults [Mori et al., 1995], its forelimb is expressed by moderate to steep north dip of the Saugus Formation from the east Ventura basin to the Merrick syncline (Figure 4.7). The initiation of these Quaternary faults is constrained only as sometime during the deposition of the Saugus Formation, 2.3-0.6 Ma. Huftile and Yeats [1996] proposed that the north-dipping reverse faults may have initiated after the initiation of the south-dipping Northridge fault. The north-dipping faults dip parallel to or with a low angle with respect to the moderately to steeply north-dipping strata in the hanging wall (Figures 4.4f-h). Movement on the Northridge thrust may have rotated strata to a north dip, parallel to a high shear stress orientation [Huftile and Yeats, 1996]. This may have facilitated the north-dipping reverse faults to propagate along bedding planes to the surface, as did the San Fernando fault during the 1971 earthquake. The presence of locally derived clasts from the Santa Susana Mountains in the Saugus Formation suggests that the initiation of uplift of the Santa Susana Mountains was about 0.6-0.7 Ma [Levi and Yeats, 1993]. These faulting episodes in the latest Pliocene to Quaternary in the east Ventura basin and San Fernando Valley coincide with strong compressional crustal deformation in the northern Los Angeles basin documented by Wright [1991].

Conclusion

Based on subsurface mapping from industry oil-well and seismic data, this paper discusses structural geology of the San Fernando Valley, California, the area struck by the

devastating 1971 San Fernando and 1994 Northridge earthquakes. The conclusions are summarized as follows.

1. The thick accumulation of the Plio-Pleistocene Saugus Formation in the Sylmar basin and Merrick syncline on the hanging wall side of the north-dipping reverse faults is a near-surface expression of the forelimb of the fault-propagation fold related to the blind south-dipping Northridge fault. However, this fault-propagation fold does not have an obvious backlimb, although the gentle south slope of the San Fernando Valley to the Los Angeles River just north of the Santa Monica Mountains may be in part the expression of the backlimb.
2. The north-dipping Mission Hills, Verdugo, and Northridge Hills reverse faults are potentially active because the fault-propagation folds above them are expressed in tectonic geomorphology. Minimum dip-slip rates for these faults are estimated as 0.3-1.1 mm/yr. Because of the location, they pose significant seismic hazard to this heavily populated suburb of Los Angeles.
3. The Mission Hills and Northridge Hills faults extend downdip to the aftershock zone of the 1971 earthquake and may be branches of the seismogenic fault. The 1971 surface breaks occurred north of these faults and mostly along bedding planes. There is little topographic expressions along the Mission Wells and Sylmar segments, and the 1971 earthquake may not be a characteristic event on the 1971 fault plane.
4. The northern San Fernando Valley and east Ventura basin originated as a rift basin in the early to middle Miocene. The Simi Hills were uplifted and separated from the valley during this time interval. The Santa Susana and Verdugo reverse faults are reactivated Miocene normal faults.
5. Reverse faulting started with the Pliocene Fernando Formation along the Frew and Torrey-Roosa fault systems. These structures are overlain by the Saugus Formation. Quaternary structures includes the Northridge, Mission Hills, Verdugo, and Northridge Hills faults that initiated sometime during the deposition of the Saugus Formation.

Acknowledgments

This research was supported by NSF-EAR grant 94-16121 to Robert S. Yeats, part of a special appropriation to study the 1994 Northridge earthquake. Subsurface data for this study were provided by the petroleum industry. Seismic lines were acquired by Southern California Earthquake Center with support by NSF-EAR grant 94-16773 to David Okaya. We are grateful to Terry Adcock, David Okaya, Gary Huftile, and Tom Wright for acquiring oil-well and seismic data. Analysis of oil-well logs for seismic time-depth conversions was done by David Okaya.

Appendix

Wells in Figures 4.4 and 4.7

- Figure 4.4a (Section A-A')
1. Shell Davey Core Hole
 2. Shell Schonfeld
- Figure 4.4b (Section B-B')
3. Atlantic Richfield Mulholland 1
 4. Atlantic Richfield Northridge Core Hole, original hole
 5. Texaco 53-23
- Figure 4.4c (Section C-C')
6. Porter Sesnon Greenman Community 52-15
 7. Porter Sesnon Orchard 38-10
 8. Porter Sesnon Quinby 65-10
 9. Union Horse Meadows 3-74
- Figure 4.4d (Section D-D')
10. Chevron Mission 6-1, 6-2A
 11. Chevron Mission 5-1, 5-2, 5-3
 12. Chevron Mission 4-1
- Figure 4.4e (Section E-E')
13. Getty Foothill Orchards 1
 14. Union Edwards 1
 15. UMC Pico Unit 1
 16. UMC O'Melveny Park 2
 17. UMC O'Melveny Park 5
 18. UMC O'Melveny Park 1
 19. Mobil Macson Mission 1
- Figure 4.4f (Section F-F')
20. Chevron Frieda J. Clark Core Hole 1
 21. Chevron Woo 1
 22. Chevron Coffman 1
 23. Chevron Panorama 1
 24. Sunray T.I. & T. 1
 25. Atlantic Richfield T.I. & T. 1
 26. Ajax McCloskey Hansen 1, original hole, redrill
- Figure 4.4g (Section G-G')
27. Chevron Leadwell 1
 28. Chevron Burnet Core Hole 1
 29. Chevron Pacoima EH 1
 30. Chevron Rinaldi Core Hole 1, original hole, redrills 1 and 2
 31. Chevron Carey 1, original hole
 32. Sunray Stetson Sombrero 1
- Figure 4.4h (Section H-H')
33. Chevron Leadwell 1
 34. Chevron Pacoima 2-A
 35. Chevron Pacoima Core Hole 1, original hole, redrill
 36. Chevron Century Properties 1, original hole, redrills 1 and 3
 37. Intex Toon 1
 38. Doheny Reeves 1
- Figure 4.7
39. Chevron Frieda J. Clark Core Hole 1
 40. Chevron Woo 1
 41. Chevron Coffman 1
 42. Chevron Panorama 1
 43. Sunray Stetson Sombrero 1

Chapter 5: Conclusions

This thesis analyzed active geologic structures in densely populated areas in Japan and southern California. Based on geological, geophysical, and paleoseismological observations, we have identified active faults and estimated their slip rates and recurrence intervals of surface-rupturing earthquakes.

Chapter 2 discussed segmentation and paleoseismology of the Median Tectonic Line, Japan. We identified 12 geometric segments along the Median Tectonic Line separated by discontinuities such as en echelon steps, bends, changes in strike, and gaps in the surface trace. The recurrence interval and surficial offset for surface-rupturing earthquakes at four individual sites on the Median Tectonic Line in Shikoku Island are 1000-3000 years and 5-8 m, respectively. Part of the fault zone ruptured most recently during or after the 16th century A.D.; this rupture may be correlated to the 1596 Keicho-Kinki earthquake.

Chapter 3 discussed active and late Cenozoic tectonics of the northern Los Angeles fault system, California. We mapped the subsurface geology of the northern Los Angeles basin from the City of Santa Monica eastward to downtown Los Angeles, based on an extensive set of oil-well data. The northern Los Angeles fault system developed through an early to late Miocene extensional regime and a Plio-Pleistocene contractional regime. The uplift of the oxygen isotope substage 5e marine terrace at Pacific Palisades and an estimated dip greater than 45° suggest a dip-slip rate as large as 1.5 mm/yr for the Santa Monica Mountains blind thrust fault, a rate considerably smaller than a previous estimate.

Chapter 4 discussed the geologic setting of the 1971 San Fernando and 1994 Northridge earthquakes, two of the most devastating earthquakes in southern California history. We mapped the subsurface geology of the northern San Fernando Valley that lies at the updip projection of the two earthquake faults. The San Fernando Valley is underlain by a series of north-dipping blind thrust faults. The thick accumulation of the Plio-Pleistocene Saugus Formation in the Sylmar basin and Merrick syncline is a surface expression of the south-dipping 1994 Northridge thrust that is overlain by the north-dipping 1971 San Fernando fault at a depth of ~5 km.

Bibliography

- Aki, K., Characterization of barriers on an earthquake fault, *J. Geophys. Res.*, **84**, 6140-6148, 1979.
- Allen, C. R., Z. Luo, H. Qian, X. Wen, H. Zhou, and W. Huang, Field study of a highly active fault zone: The Xianshuihe fault of southwestern China, *Geol. Soc. Am. Bull.*, **103**, 1178-1199, 1991.
- Atwater, T., Implications of plate tectonics for the Cenozoic tectonic evolution of western North America, *Geol. Soc. Am. Bull.*, **81**, 3513-3536, 1970.
- Barbat, W. F., The Los Angeles basin area, California, in *Habitat of oil*, edited by L. G. Weeks, pp. 62-77, AAPG, Tulsa, Oklahoma, 1958.
- Bard, E., B. Hamelin, R. G. Fairbanks, and A. Zindler, Calibration of the ^{14}C timescale over the past 30,000 years using mass spectrometric U-Th ages from Barbados corals, *Nature*, **345**, 405-410, 1990.
- Barka, A. A., and K. Kadinsky-Cade, Strike-slip fault geometry in Turkey and its influence on earthquake activity, *Tectonics*, **7**, 663-684, 1988.
- Barnhart, J. T., and J. E. Slosson, The Northridge Hills and associated faults—A zone of high seismic probability?, in *Geology, Seismicity, and Environmental Impact*, edited by D. E. Moran, J. E. Slosson, R. O. Stone, and C. A. Yelverton, pp. 253-256, Spec. Pub., Assoc. Eng. Geol., Univ. Publishers, Los Angeles, 1973.
- Barrows, A. G., *A review of the geology and earthquake history of the Newport-Inglewood structural zone, southern California*, *Calif. Div. Mines Geol. Spec. Rep.*, **114**, 115 pp., 1974.
- Barrows, A. G., Surface effects and related geology of the San Fernando earthquake in the foothill region between Little Tujunga and Wilson Canyons, in *San Fernando, California, Earthquake of 9 February 1971*, edited by G. B. Oakeshott, *Calif. Div. Mines Geol. Bull.*, **196**, 97-117, 1975.
- Blake, G. H., Review of the Neogene biostratigraphy and stratigraphy of the Los Angeles basin and implications for basin evolution, in *Active Margin Basins*, edited by K. T. Biddle, *AAPG Mem.*, **52**, 135-184, 1991.
- Bonilla, M. G., R. K. Mark, and J. J. Lienkaemper, Statistical relations among earthquake magnitude, surface rupture length, and surface fault displacement, *Bull. Seismol. Soc. Am.*, **74**, 2379-2411, 1984.
- Bradley, W. C., Submarine abrasion and wave-cut platforms, *Geol. Soc. Am. Bull.*, **69**, 967-974, 1958.
- Bryant, W. A., The Raymond Hill fault - An urban geological investigation, *Calif. Geol.*, **31**, 127-142, 1978.
- Campbell, R. H., and R. F. Yerkes, Cenozoic evolution of the Los Angeles basin area—relation to plate tectonics—, in *Aspects of the Geologic History of the California Continental Borderland*, edited by D. G. Howell, *Pacific Section, AAPG, Miscellaneous Publication*, **24**, 541-558, 1976.

- Chida, N., Active faults in central Kyushu, southwest Japan—Quaternary faulting along the Median Tectonic Line in Kyushu (in Japanese with English abstract), in *Neotectonics of the Median Tectonic Line: Its Significance and Problems*, edited by A. Okada, Y. Sugiyama, K. Mizuno, H. Yamazaki, and E. Tsukuda, *Mem. Geol. Soc. Jpn.*, 40, 39-51, 1992.
- Colburn, I. P., Stratigraphic relations of the southern California Cretaceous strata, in *Cretaceous stratigraphy of the Santa Monica Mountains and Simi Hills*, edited by I. P. Colburn, and A. E. Fritsche, *Pacific Section, Society of Economic Paleontologists and Mineralogists, Field Trip Guidebook*, 45-73, 1973.
- Colburn, I. P., L. E. R. Saul, and A. A. Almgren, The Chatsworth Formation: A new formation name for the Upper Cretaceous strata of the Simi Hills, California, in *Simi Hills Cretaceous Turbidites, Southern California*, edited by M. H. Link, R. L. Squires, and I. P. Colburn, *Pacific Section, Society of Economic Paleontologists and Mineralogists, Field Trip Volume and Guide Book*, 9-16, 1981.
- Corbató, C. E., Bouguer gravity anomalies of the San Fernando Valley, California, *Univ. Calif. Pub. Geol. Sci.*, 46, 1-32, 1963.
- Crone, A. J., and K. M. Haller, Segmentation and the coseismic behavior of Basin and Range normal faults: Examples from east-central Idaho and southwestern Montana, U.S.A., *J. Struct. Geol.*, 13, 151-164, 1991.
- Crook, R., Jr., C. R. Allen, B. Kamb, C. M. Payne, and R. J. Proctor, Quaternary geology and seismic hazard of the Sierra Madre and associated faults, western San Gabriel Mountains, in *Recent Reverse Faulting in the Transverse Ranges, California*, *U.S. Geol. Surv. Prof. Pap.*, 1339, 27-63, 1987.
- Crook, R., Jr., and R. J. Proctor, The Santa Monica and Hollywood faults and the southern boundary of the Transverse Ranges province, in *Engineering geology practice in southern California*, edited by B. W. Pipkin, and R. J. Proctor, pp. 233-246, *Southern California Section, Association of Engineering Geologists Special Publication*, 4, Star Publishing Company, Belmont, California, 1992.
- Crouch, J. K., and J. Suppe, Late Cenozoic tectonic evolution of the Los Angeles basin and inner California borderland: A model for core complex-like crustal extension, *Geol. Soc. Am. Bull.*, 105, 1415-1434, 1993.
- Crowell, J. C., Implications of crustal stretching and shortening of coastal Ventura basin, California, in *Aspects of the Geologic History of the California Continental Borderland*, edited by D. G. Howell, *Pacific Section, AAPG, Miscellaneous Publication*, 24, 365-382, 1976.
- Crowell, J. C., Late Cenozoic basins of onshore southern California: Complexity is the hallmark of their tectonic history, in *Cenozoic Basin Development of Coastal California, Rubey Volume VI*, edited by R. V. Ingersoll, and W. G. Ernst, pp. 207-241, Prentice Hall, Englewood Cliffs, New Jersey, 1987.
- Davis, T. L., and J. S. Namson, A balanced cross-section of the 1994 Northridge earthquake, southern California, *Nature*, 372, 167-169, 1994.

- dePolo, C. M., and D. B. Slemmons, Estimation of earthquake size for seismic hazards, in *Neotectonics in Earthquake Evaluation*, edited by E. L. Krinitzky and D. B. Slemmons, *Rev. Eng. Geol.*, 8, 1-28, 1990.
- dePolo, C. M., D. G. Clark, D. B. Slemmons, and A. R. Ramelli, Historical surface faulting in the Basin and Range province, western North America: Implications for fault segmentation, *J. Struct. Geol.*, 13, 123-136, 1991.
- Dibblee, T. W., Jr., Geology of the Santa Monica Mountains and Simi Hills, southern California, in *Geology and mineral wealth of the California Transverse Ranges*, edited by D. L. Fife, and J. A. Minch, pp. 94-130, *South Coast Geological Society*, Santa Ana, California, 1982.
- Dibblee, T. W., Jr., Geologic map of the San Fernando and Van Nuys (north 1/2) quadrangles, Los Angeles County, California, *Dibblee Geological Foundation Map*, DF-33, scale 1:24, 000, Santa Barbara, California, 1991a.
- Dibblee, T. W., Jr., Geologic map of the Sunland and Burbank (north 1/2) quadrangles, Los Angeles County, California, *Dibblee Geological Foundation Map*, DF-32, scale 1:24, 000, Santa Barbara, California, 1991b.
- Dibblee, T. W., Jr., Geologic map of the Oat Mountain and Canoga Park (north 1/2) quadrangles, Los Angeles County, California, *Dibblee Geological Foundation Map*, DF-36, scale 1:24, 000, Santa Barbara, California, 1992.
- Dolan, J. F., and K. Sieh, Tectonic geomorphology of the northern Los Angeles basin: Seismic hazards and kinematics of young fault movement, in *Engineering Geology Field Trips: Orange County, Santa Monica Mountains, and Malibu*, *Association of Engineering Geologists, 35th Annual Meeting, Field Trip Guidebook*, B20-B26, 1992.
- Dolan, J. F., K. Sieh, and T. K. Rockwell, Paleoseismology and geomorphology of the northern Los Angeles basin: Evidence for Holocene activity on the Santa Monica fault and identification of new strike-slip faults through downtown Los Angeles (abstract), *Eos Trans. AGU*, 73, 589, 1992.
- Dolan, J. F., K. Sieh, P. Guphill, G. Miller, T. Rockwell, and T. Smirnov, Structural geology, fault kinematics, and preliminary paleoseismologic results from the Hollywood fault: New data from continuously cored borings and geotechnical trenches, Hollywood, California (abstract), *Eos Trans. AGU*, 74, 427, 1993.
- Dolan, J. F., K. Sieh, T. K. Rockwell, R. S. Yeats, J. Shaw, J. Suppe, G. J. Huftile, E. M. Gath, Prospects for larger or more frequent earthquakes in the Los Angeles metropolitan region, *Science*, 267, 199-205, 1995.
- Driver, H. L., Inglewood oil field, in *Geologic formations and economic development of the oil and gas fields of California*, *Calif. Div. Mines Geol. Bull.*, 118, 306-309, 1943.
- Drumm, P. L., Holocene displacement of the central splay of the Malibu Coast fault zone, Latigo Canyon, Malibu, in *Engineering geology practice in southern California*, edited by B. W. Pipkin, and R. J. Proctor, pp. 247-254, *Southern California Section, Association of Engineering Geologists Special Publication*, 4, Star Publishing Company, Belmont, California, 1992.

- Engebretson, D. C., A. Cox, and R. G. Gordon, Relative motion between oceanic and continental plates in the Pacific basin, *Geol. Soc. Am. Spec. Pap.*, 206, 1-59, 1985.
- Feigl, K. L., et al., Space geodetic measurement of crustal deformation in central and southern California, 1984-1992, *J. Geophys. Res.*, 98, 21677-21712, 1993.
- Fitch, T. J., Plate convergence, transcurrent faults, and internal deformation adjacent to southeast Asia and the western Pacific, *J. Geophys. Res.*, 77, 4432-4460, 1972.
- Freeman, T. S., E. G. Heath, P. D. Guphill, and J. T. Waggoner, Seismic hazard assessment, Newport-Inglewood fault zone, in *Engineering geology practice in southern California*, edited by B. W. Pipkin, and R. J. Proctor, pp. 211-231, *Southern California Section, Association of Engineering Geologists Special Publication, 4*, Star Publishing Company, Belmont, California, 1992.
- Geological Survey of Japan, Excavation survey of the Gomura-Yamada fault system, Tango Peninsula, Kyoto (in Japanese), *Rep. Coord. Comm. Earthquake Predict.*, 36, 370-381, 1986.
- Geological Survey of Japan, Shallow seismic reflection survey and acoustic exploration of the Median Tectonic Line in the west of Wakayama city (in Japanese), *Rep. Coord. Comm. Earthquake Predict.*, 53, 663-668, 1995.
- Hanks, T. C., The faulting mechanism of the San Fernando earthquake, *J. Geophys. Res.*, 79, 1215-1229, 1974.
- Harbert, W., and A. Cox, Late Neogene motion of the Pacific plate, *J. Geophys. Res.*, 94, 3052-3064, 1989.
- Harding, T. P., Newport-Inglewood trend, California-An example of wrenching style of deformation, *AAPG Bull.*, 57, 97-116, 1973.
- Hashimoto, M., and K. Kanmera, Pre-Neogene sedimentary and metamorphic rocks, in *Geology of Japan, Dev. Earth Planet. Sci.*, vol. 8, edited by M. Hashimoto, pp. 13-55, Terra Sci., Tokyo, 1991.
- Hauksson, E., Seismotectonics of the Newport-Inglewood fault zone in the Los Angeles basin, southern California, *Bull. Seismol. Soc. Am.*, 77, 539-561, 1987.
- Hauksson, E., Earthquakes, faulting, and stress in the Los Angeles basin, *J. Geophys. Res.*, 95, 15365-15394, 1990.
- Hauksson, E., Seismicity, faults, and earthquake potential in Los Angeles, southern California, in *Engineering geology practice in southern California*, edited by B. W. Pipkin, and R. J. Proctor, pp. 167-179, *Southern California Section, Association of Engineering Geologists Special Publication, 4*, Star Publishing Company, Belmont, California, 1992.
- Hauksson, E., and G. V. Saldivar, The 1930 Santa Monica and the 1979 Malibu, California, earthquakes, *Bull. Seismol. Soc. Am.*, 76, 1542-1559, 1986.
- Hauksson, E., and R. S. Stein, The 1987 Whittier Narrows, California, earthquake: A metropolitan shock, *J. Geophys. Res.*, 94, 9545-9547, 1989.

- Hauksson, E., and S. Gross, Source parameters of the 1933 Long Beach earthquake, *Bull. Seismol. Soc. Am.*, 81, 81-98, 1991.
- Hauksson, E., L. M. Jones, and K. Hutton, The 1994 Northridge earthquake sequence in California: Seismological and tectonic aspects, *J. Geophys. Res.*, 100, 12335-12355, 1995.
- Hecker, S., D. J. Ponti, C. D. Garvin, T. J. Powers, T. E. Fumal, J. C. Hamilton, R. V. Sharp, M. J. Rymer, C. S. Prentice, and F. R. Cinti, Ground deformation in Granada Hills and Mission Hills resulting from the January 17, 1994, Northridge, California, earthquake, *U.S. Geol. Surv. Open File Rep.*, 95-62, 11 pp., 1995.
- Hill, M. L., Newport-Inglewood zone and Mesozoic subduction, California, *Geol. Soc. Am. Bull.*, 82, 2957-2962, 1971.
- Hill, R. L., Potrero Canyon fault and University High School escarpment, in *Field guide to selected engineering geologic features, Santa Monica Mountains*, J. R. Keaton, Field trip chairman, *Southern California Section, Association of Engineering Geologists, Annual Field Trip Guide*, 83-103, 1979.
- Hill, R. L., E. C. Sprotte, J. H. Bennett, C. R. Real, and R. C. Slade, Location and activity of the Santa Monica fault, Beverly Hills-Hollywood area, California, in *Earthquake hazards associate with faults in the greater Los Angeles metropolitan area, Los Angeles County, California, including faults in the Santa Monica-Raymond, Verdugo-Eagle Rock, and Benedict Canyon fault zones*, *Calif. Div. Mines Geol. Open-File Rep.*, 79-16, B1-B42, 1979.
- Hoots, H. W., Geology of the eastern part of the Santa Monica Mountains, Los Angeles County, California, *U.S. Geol. Surv. Prof. Pap.*, 165, 83-134, 1931.
- Hornafius, S. J., B. P. Luyendyk, R. R. Terres, and M. J. Kamerling, Timing and extent of Neogene tectonic rotation in the western Transverse Ranges, California, *Geol. Soc. Am. Bull.*, 97, 1476-1487, 1986.
- Hudnut, K. W., Z. Shen, M. Murray, S. McClusky, R. King, T. Herring, B. Hager, Y. Feng, P. Fang, A. Donnellan, and Y. Bock, Co-seismic displacements of the 1994 Northridge, California, Earthquake, *Bull. Seismol. Soc. Am.*, in press, 1996.
- Huftile, G. J., and R. S. Yeats, Deformation rates across the Placerita (Northridge $M_w=6.7$ aftershock zone) and Hopper Canyon segments of the western Transverse Ranges deformation belt, *Bull. Seismol. Soc. Am.*, in press, 1996.
- Hummon, C., Subsurface Quaternary and Pliocene structures of the northern Los Angeles basin, California, M.S. thesis, Oregon State Univ., Corvallis, 1994.
- Hummon, C., C. L. Schneider, R. S. Yeats, J. F. Dolan, K. E. Sieh, and G. J. Huftile, Wilshire fault: Earthquakes in Hollywood?, *Geology*, 22, 291-294, 1994.
- Hydrographic Department Maritime Safety Agency, Submarine topography and geological structure of the Naruto Strait (in Japanese), *Rep. Coord. Comm. Earthquake Predict.*, 21, 137-139, 1979.

- Ikeda, Y., Thrust-front migration and its mechanism—Evolution of intraplate thrust fault systems—, *Bull. Dept. Geogr., Univ. Tokyo*, 15, 125-159, 1983.
- Ishibashi, K., Possible rupturing of the Median Tectonic Line in Shikoku, Japan, during the 1596 Keicho Kinki earthquake and its effect on the 1605 Nankai-trough tsunami earthquake (in Japanese) (abstract), *Programme Abstr. Seismol. Soc. Jpn.*, No.1, 62, 1989.
- Ishikawa, Y., Tectonics in eastern Asia and the seismicity around the Median Tectonic Line (in Japanese with English abstract), in *Neotectonics of the Median Tectonic Line: Its Significance and Problems*, edited by A. Okada, Y. Sugiyama, K. Mizuno, H. Yamazaki, and E. Tsukuda, *Mem. Geol. Soc. Jpn.*, 40, 205-218, 1992.
- Jennings, C. W., Fault activity map of California and adjacent areas, *Calif. Geol. Data Map Ser.*, 6, scale 1:750,000, 2 sheets, explanatory text, 92 pp., Calif. Div. Mines Geol., Sacramento, 1994.
- Jones, L. M., K. E. Sieh, E. Hauksson, and K. L. Hutton, The 3 December 1988 Pasadena, California earthquake: Evidence for strike-slip motion on the Raymond fault, *Bull. Seismol. Soc. Am.*, 80, 474-482, 1990.
- Kamb, B., L. T. Silver, M. J. Abrams, B. A. Carter, T. H. Jordan, and J. B. Minster, Pattern of faulting and nature of fault movement in the San Fernando earthquake, in *The San Fernando, California, Earthquake of February 9, 1971*, U.S. Geol. Surv. Prof. Pap., 733, 41-54, 1971.
- Kamerling, M. J., and B. P. Luyendyk, Tectonic rotations of the Santa Monica Mountains region, western Transverse Ranges, California, suggested by paleomagnetic vectors, *Geol. Soc. Am. Bull.*, 90, 331-337, 1979.
- Kanamori, H., Tectonic implications of the 1944 Tonankai and the 1946 Nankaido earthquakes, *Phys. Earth Planet. Inter.*, 5, 129-139, 1972.
- Kanamori, H., The Kobe (Hyogo-ken Nanbu), Japan, earthquake of January 16, 1995, *Seismol. Res. Lett.*, 66, No. 2, 6-10, 1995.
- Kanamori, H., and C. R. Allen, Earthquake repeat time and average stress drop, in *Earthquake Source Mechanics*, *Geophys. Monogr. Ser.*, vol. 37, edited by S. Das, J. Boatwright, and C. H. Scholz, pp. 227-235, AGU, Washington, D. C., 1986.
- Kaneko, S., Transcurrent displacement along the Median Line, south-western Japan, *N. Z. J. Geol. Geophys.*, 9, 45-59, 1966.
- Kew, W. S. W., Geology and oil resources of a part of Los Angeles and Ventura Counties, California, *U.S. Geol. Surv. Bull.*, 753, 1-202, 1924.
- King, G. C. P., Speculations on the geometry of the initiation and termination processes of earthquake rupture and its relation to morphology and geological structure, *Pure Appl. Geophys.*, 124, 567-585, 1986.
- Kleinpell, R. M., *Miocene stratigraphy of California*, 450 pp., AAPG, Tulsa, Oklahoma, 1938.

- Kleinpell, R. M., *The Miocene stratigraphy of California revisited, Studies in Geology, 11*, 349 pp., AAPG, Tulsa, Oklahoma, 1980.
- Knuepfer, P. L. K., Implications of the characteristics of end-points of historical surface fault ruptures for the nature of fault segmentation, in *Fault Segmentation and Controls of Rupture Initiation and Termination*, edited by D. P. Schwartz and R. H. Sibson, *U.S. Geol. Surv. Open File Rep.*, 89-315, 193-228, 1989.
- Lamar, D. L., Structural evolution of the northern margin of the Los Angeles basin, Ph.D. dissert., Univ. of California, Los Angeles, 1961.
- Lant, K. J., Structure of the Aliso Canyon area, east Ventura basin, California, M.S. thesis, Ohio Univ., Athens, 1977.
- Larsen, E. S., Jr., D. Gottfried, H. W. Jaffe, and C. L. Waring, Lead-alpha ages of the Mesozoic batholiths of western North America, *U.S. Geol. Surv. Bull.*, 1070-B, 35-62, 1958.
- Lawson, A. C., G. K. Gilbert, H. F. Reid, J. C. Branner, A. O. Leuschner, G. Davidson, C. Burckhalter, and W. W. Campbell, *Atlas of maps and seismograms accompanying the report of the State Earthquake Investigation Commission upon the California earthquake of April 18, 1906*, Carnegie Institution of Washington, 1908.
- Levi, S., and R. S. Yeats, Paleomagnetic constraints on the initiation of uplift on the Santa Susana fault, western Transverse Ranges, California, *Tectonics*, 12, 688-702, 1993.
- Link, M. H., R. L. Squires, and I. P. Colburn, Slope and deep-sea fan facies and paleogeography of Upper Cretaceous Chatsworth Formation, Simi Hills, California, *AAPG Bull.*, 68, 850-873, 1984.
- Lonsdale, P., Structural patterns of the Pacific floor offshore of Peninsular California, in *Gulf and Peninsular Province of the Californias*, edited by J. P. Dauphin, and B. T. Simoneit, *AAPG Mem.*, 47, 87-125, 1991.
- Luyendyk, B. P., A model for Neogene crustal rotations, transtension, and transpression in southern California, *Geol. Soc. Am. Bull.*, 103, 1528-1536, 1991.
- Machette, M. N., S. F. Personius, A. R. Nelson, D. P. Schwartz, and W. R. Lund, The Wasatch fault zone, Utah—Segmentation and history of Holocene earthquakes, *J. Struct. Geol.*, 13, 137-149, 1991.
- Machida, H., and F. Arai, *Atlas of Tephra in and Around Japan* (in Japanese), 276 pp., Univ. of Tokyo Press, Tokyo, 1992.
- Masek, J. G., B. L. Isacks, E. J. Fielding, and J. Browaeys, Rift flank uplift in Tibet: Evidence for a viscous lower crust, *Tectonics*, 13, 659-667, 1994.
- Matsuda, T., Surface faults associated with Nobi (Mino-Owari) earthquake of 1891, Japan, *Spec. Bull. Earthquake Res. Inst. Univ. Tokyo*, 13, 85-126, 1974.
- Matsuda, T., Estimation of future destructive earthquakes from active faults on land in Japan, *J. Phys. Earth*, suppl., 251-260, 1977.

- McGill, J. T., Geologic maps of the Pacific Palisades area, Los Angeles, California, *U.S. Geol. Surv. Miscellaneous Investigations Ser. Map, I-1828*, scale 1:4 800, 2 sheets, 1989.
- Mizuno, K., A. Okada, A. Sangawa, and F. Shimizu, Strip map of the Median Tectonic Line active fault system in Shikoku (in Japanese with English abstract), *Tectonic Map Ser.*, 8, scale 1:25,000, explanatory text, 63 pp., Geol. Surv. of Jpn., Tsukuba, 1993.
- Mizuno, K., A. Sangawa, and E. Tsukuda, Strip map of the Median Tectonic Line active fault system in Kinki, *Tectonic Map Ser.*, 9, scale 1:25,000, Geol. Surv. of Jpn., Tsukuba, 1994.
- Mori, J., D. J. Wald, and R. L. Wesson, Overlapping fault planes of the 1971 San Fernando and 1994 Northridge, California earthquakes, *Geophys. Res. Lett.*, 22, 1033-1036, 1995.
- Nakamura, K., Possible nascent trench along the eastern Japan Sea as the convergent boundary between Eurasian and North American plates (in Japanese with English abstract), *Bull. Earthquake Res. Inst. Univ. Tokyo*, 58, 711-722, 1983.
- Natland, M. L., Pleistocene and Pliocene stratigraphy of southern California, Ph.D. dissert., Univ. of California, Los Angeles, 1952.
- Oakeshott, G. B., *Geology and Mineral Deposits of San Fernando Quadrangle, Los Angeles County, California, Calif. Div. Mines Bull.*, 172, 147 pp., 1958.
- Ogawa, M., M. Okamura, K. Shimazaki, T. Nakata, N. Chida, T. Nakamura, T. Miyatake, H. Maemoku, and H. Tsutsumi, Holocene activity on a submarine active fault system of the Median Tectonic Line beneath the northeastern part of Iyonada, the Inland Sea, southwest Japan (in Japanese with English abstract), in *Neotectonics of the Median Tectonic Line: Its Significance and Problems*, edited by A. Okada, Y. Sugiyama, K. Mizuno, H. Yamazaki, and E. Tsukuda, *Mem. Geol. Soc. Jpn.*, 40, 75-97, 1992.
- Okada, A., Strike-slip faulting of late Quaternary along the Median Dislocation Line in the surroundings of Awa-Ikeda, northeastern Shikoku (in Japanese with English abstract), *Quat. Res.*, 7, 15-26, 1968.
- Okada, A., Fault topography and rate of faulting along the Median Tectonic Line in the drainage basin of the River Yoshino, northeastern Shikoku, Japan (in Japanese with English abstract), *Geogr. Rev. Jpn.*, 43, 1-21, 1970.
- Okada, A., Quaternary faulting of the Median Tectonic Line fault system in the northwestern part of Shikoku (in Japanese), *Bull. Fac. Liter. Aichi Prefect. Univ.*, 23, 68-94, 1972.
- Okada, A., On the Quaternary faulting along the Median Tectonic Line (in Japanese with English abstract), in *Median Tectonic Line*, edited by R. Sugiyama, pp. 49-86, Tokai Univ. Press, Tokyo, 1973a.
- Okada, A., Quaternary faulting along the Median Tectonic Line in the central part of Shikoku (in Japanese with English abstract), *Geogr. Rev. Jpn.*, 46, 295-322, 1973b.

- Okada, A., Quaternary faulting along the Median Tectonic Line of southwest Japan, in *Median Tectonic Line of southwest Japan*, edited by K. Ichikawa, *Mem. Geol. Soc. Jpn.*, 18, 79-108, 1980.
- Okada, A., and A. Sangawa, Fault morphology and Quaternary faulting along the Median Tectonic Line in the southern part of the Izumi Range (in Japanese with English abstract), *Geogr. Rev. Jpn.*, 51, 385-405, 1978.
- Okada, A., and H. Tsutsumi, Data on fault exposures of the Median Tectonic Line and geomorphic surface chronology in the central to eastern part of Shikoku, southwest Japan (in Japanese), *Active Fault Res.*, 8, 31-47, 1990.
- Okada, A., and T. Matsuda, Late Quaternary activity of the Neodani (Neo-Valley) fault at Midori and Naka, Neo Village, central Japan (in Japanese with English abstract), *J. Geogr.*, 101, 19-37, 1992.
- Petersen, M. D., and S. G. Wesnousky, Fault slip rates and earthquake histories for active faults in southern California, *Bull. Seismol. Soc. Am.*, 84, 1608-1649, 1994.
- Ponti, D. J., J. A. Barron, A. M. Sarna-Wojcicki, M. L. Cotton, C. Hummon, and C. L. Schneider, Benthic foram biostratigraphy and the age of the Pico Formation in the northern Los Angeles basin: Potential problems for evaluating activity of blind thrust faults (abstract), *Eos Trans. AGU*, 74, 434, 1993.
- Redin, T., Oil and gas production from submarine fans of the Los Angeles basin, in *Active Margin Basins*, edited by K. T. Biddle, *AAPG Mem.*, 52, 239-259, 1991.
- Reid, H. F., Sudden earth-movements in Sumatra in 1892, *Bull. Seismol. Soc. Am.*, 3, 72-79, 1913.
- Research Group for Active Faults of Japan, The, *Active Faults in Japan: Sheet Maps and Inventories* (in Japanese with English abstract), rev. ed., 437 pp., Univ. of Tokyo Press, Tokyo, 1991.
- Research Group for Active Faults of Japan, The, *Maps of Active Faults in Japan with an Explanatory Text*, 73 pp., Univ. of Tokyo Press, Tokyo, 1992.
- Rockwell, T. K., E. M. Gath, and T. Gonzalez, Sense and rate of slip on the Whittier fault zone, eastern Los Angeles basin, California, *Association of Engineering Geologists, 35th Annual Meeting Proceedings*, pp. 679, Los Angeles, California, 1992.
- Sage, O. G., Jr., Geology of the eastern portion of the "Chico" Formation, Simi Hills, California, M.A. thesis, Univ. Calif., Santa Barbara, 1971.
- Sage, O. G., Jr., Paleocene geography of southern California, Ph.D. dissert., Univ. of California, Santa Barbara, 1973.
- Sangawa, A., Geomorphic development of the Izumi and Sanuki Ranges and relating crustal movement, *Sci. Rep. Tohoku Univ.*, 7th Ser., 28, 313-338, 1978.
- Sangawa, A., The history of fault movement since late Pliocene in the central part of southwest Japan, *Bull. R. Soc. N. Z.*, 24, 75-85, 1986.

- Sangawa, A., Evidence of paleoearthquakes found out in some archaeological sites (in Japanese with English abstract), *J. Geogr.*, 99, 471-482, 1990.
- Saul, R. B., Geology of the southeast slope of the Santa Susana Mountains and geologic effects of the San Fernando earthquake, in *San Fernando, California, Earthquake of 9 February 1971*, edited by G. B. Oakeshott, *Calif. Div. Mines Geol. Bull.*, 196, 53-70, 1975.
- Schneider, C. L., Pre-Pliocene structural geology and structural evolution of the northern Los Angeles basin, southern California, M.S. thesis, Oregon State Univ., Corvallis, 1994.
- Schneider, C. L., C. Hummon, R. S. Yeats, and G. J. Huftile, Structural evolution of the northern Los Angeles basin, California, based on growth strata, *Tectonics*, 15, in press, 1996.
- Schnurr, P. E., and C. E. Koch, Pacific Section AAPG field summaries—Pacoima field—, *Pacific Petroleum Geologists Newsletter*, Winter 1979-80, 34-4, 4-5, 1979.
- Schoellhamer, J. E., and A. O. Woodford, The floor of the Los Angeles basin, Los Angeles, Orange, and San Bernardino Counties, California, *U.S. Geol. Surv. Oil Gas Investigations Map, OM 117*, 2 sheets, 1951.
- Schwartz, D. P., and K. J. Coppersmith, Fault behavior and characteristic earthquakes: Examples from the Wasatch and San Andreas fault zones, *J. Geophys. Res.*, 89, 5681-5698, 1984.
- Schwartz, D. P., and K. J. Coppersmith, Seismic hazards: New trends in analysis using geologic data, in *Active Tectonics*, pp. 215-230, Nat. Acad. Press, Washington, D. C., 1986.
- Scientists of the U.S. Geological Survey and the Southern California Earthquake Center, The magnitude 6.7 Northridge, California, earthquake of 17 January 1994, *Science*, 266, 389-397, 1994.
- Sedlock, R. L., and D. H. Hamilton, Late Cenozoic tectonic evolution of southwestern California, *J. Geophys. Res.*, 96, 2325-2351, 1991.
- Seedorf, D. C., Upper Cretaceous through Eocene subsurface stratigraphy, Simi Valley and adjacent regions, California, in *Cenozoic Geology of the Simi Valley Area, Southern California*, edited by R. L. Squires, and M. V. Filewicz, *Pacific Section, Society of Economic Paleontologists and Mineralogists, Field Trip Volume and Guide Book*, 109-128, 1983.
- Seno, T., S. Stein, and A. E. Gripp, A model for the motion of the Philippine Sea plate consistent with NUVEL-1 and geological data, *J. Geophys. Res.*, 98, 17941-17948, 1993.
- Sharp, R. V., Displacement on tectonic ruptures, in *San Fernando, California, Earthquake of 9 February 1971*, edited by G. B. Oakeshott, *Calif. Div. Mines Geol. Bull.*, 196, 187-194, 1975.
- Shaw, J. H., Active blind-thrust faulting and strike-slip fault-bend folding in California, Ph.D. dissert., Princeton Univ., New Jersey, 1993.

- Shields, K. E., Structure of the northwestern margin of the San Fernando Valley, Los Angeles County, California, M.S. thesis, Ohio Univ., Athens, 1977.
- Shimazaki, K., T. Nakata, N. Chida, T. Miyatake, M. Okamura, H. Shiragami, H. Maemoku, H. Matsuki, M. Tsujii, S. Kiyokawa, and K. Hirata, A preliminary report on the drilling project of submarine active faults beneath Beppu Bay, southwest Japan, for longterm earthquake prediction (in Japanese), *Active Fault Res.*, 2, 83-88, 1986.
- Sibson, R. H., Stopping of earthquake ruptures at dilational fault jogs, *Nature*, 316, 248-251, 1985.
- Sibson, R. H., Rupture interaction with fault jogs, in *Earthquake Source Mechanics, Geophys. Monogr. Ser.*, vol. 37, edited by S. Das, J. Boatwright, and C. H. Scholz, pp. 157-167, AGU, Washington, D. C., 1986.
- Sibson, R. H., Effects of fault heterogeneity on rupture propagation, in *Directions in Paleoseismology*, edited by A. J. Crone and E. M. Omdahl, *U.S. Geol. Surv. Open File Rep.*, 87-673, 362-373, 1987.
- Sieh, K. E., and R. H. Jahns, Holocene activity of the San Andreas fault at Wallace Creek, California, *Geol. Soc. Am. Bull.*, 95, 883-896, 1984.
- Sieh, K., et al., Near-field investigations of the Landers earthquake sequence, April to July 1992, *Science*, 260, 171-176, 1993.
- Sorensen, S., Petrologic evidence for Jurassic, island-arc-like basement rocks in the southwestern Transverse Ranges and California Continental Borderland, *Geol. Soc. Am. Bull.*, 96, 997-1006, 1985.
- Stephenson, W. J., T. K. Rockwell, J. K. Odum, K. M. Shedlock, and D. A. Okaya, Seismic reflection and geomorphic characterization of the onshore Palos Verdes fault zone, Los Angeles, California, *Bull. Seismol. Soc. Am.*, 85, 943-950, 1995.
- Stuiver, M., and P. J. Reimer, Extended ^{14}C data base and revised CALIB 3.0 ^{14}C age calibration program, *Radiocarbon*, 35, 215-230, 1993.
- Sugiyama, Y., Neotectonics of southwest Japan due to the right-oblique subduction of the Philippine Sea plate, *Geofis. Int.*, 33, 53-76, 1994.
- Sullwold, H. H., Jr., Tarzana fan, deep submarine fan of late Miocene age, Los Angeles County, California, *AAPG Bull.*, 44, 433-457, 1960.
- Suppe, J., and D. A. Medwedeff, Geometry and kinematics of fault-propagation folding, *Eclogae Geologicae Helveticae*, 83, 409-454, 1990.
- Suppe, J., G. T. Chou, and S. C. Hook, Rates of folding and faulting determined from growth strata, in *Thrust Tectonics*, edited by K. R. McKlay, pp. 105-121, Chapman and Hall, London, 1992.
- Tanna Fault Trenching Research Group, The, Trenching study for Tanna fault, Izu, at Myoga, Shizuoka Prefecture, Japan (in Japanese with English abstract), *Bull. Earthquake Res. Inst. Univ. Tokyo*, 58, 797-830, 1983.

- Tennyson, M. E., Pre-transform early Miocene extension in western California, *Geology*, *17*, 792-796, 1989.
- Tsukuda, E., Migration of historical earthquakes, central Japan, in *Directions in Paleoseismology*, edited by A. J. Crone and E. M. Omdahl, *U.S. Geol. Surv. Open File Rep.*, 87-673, 271-284, 1987.
- Tsukuda, E., Geometrical barriers on faults and their rupturing processes (in Japanese with English abstract), *J. Geogr.*, *100*, 417-428, 1991.
- Tsukuda, E., Active tectonics of southwest Japan arc controlled by the westward translation of the forearc sliver (in Japanese with English abstract), in *Neotectonics of the Median Tectonic Line: Its Significance and Problems*, edited by A. Okada, Y. Sugiyama, K. Mizuno, H. Yamazaki, and E. Tsukuda, *Mem. Geol. Soc. Jpn.*, *40*, 235-250, 1992.
- Tsutsumi, H., A. Okada, T. Nakata, M. Ando, and T. Tsukuda, Timing and displacement of Holocene faulting on the Median Tectonic Line in central Shikoku, southwest Japan, *J. Struct. Geol.*, *13*, 227-233, 1991.
- Tsutsumi, H., R. S. Yeats, C. Hummon, C. L. Schneider, and G. J. Huftile, Active and late Cenozoic tectonics of the northern Los Angeles fault system, California, *Geol. Soc. Am. Bull.*, in review, 1996.
- Uemura, Y., Fault topography and Quaternary faulting along the Gomura and Yamada fault systems in the Tango area, central Japan (in Japanese), *Active Fault Res.*, *1*, 81-92, 1985.
- Usami, T., *Materials for Comprehensive List of Destructive Earthquakes in Japan* (in Japanese), 434 pp., Univ. of Tokyo Press, Tokyo, 1987.
- U.S. Geological Survey Staff, Surface faulting, in *The San Fernando, California, Earthquake of February 9, 1971*, *U.S. Geol. Surv. Prof. Pap.*, *733*, 55-76, 1971.
- Wald, D. J., and T. H. Heaton, Spatial and temporal distribution of slip for the 1992 Landers, California, earthquake, *Bull. Seismol. Soc. Am.*, *84*, 668-691, 1994.
- Wald, D. J., T. H. Heaton, and K. W. Hudnut, A dislocation model of the 1994 Northridge, Calif., earthquake determined from strong-motion, GPS and leveling-line data, *Bull. Seismol. Soc. Am.*, in press, 1996.
- Weber, H. F., Jr., Surface effects and related geology of the San Fernando earthquake in the Sylmar area, in *San Fernando, California, Earthquake of 9 February 1971*, edited by G. B. Oakeshott, *Calif. Div. Mines Geol. Bull.*, *196*, 71-96, 1975.
- Weber, H. F., Jr., Geological features related to character and recency of movement along faults, north-central Los Angeles area, Los Angeles County, California, in *Earthquake Hazards Associated With the Verdugo-Eagle Rock and Benedict Canyon Fault Zones, Los Angeles County, California*, *Calif. Div. Mines Geol. Open-File Rep.*, *80-10*, B1-B116, 1980.

- Weigand, P. W., and K. L. Savage, Review of the petrology and geochemistry of the Miocene Conejo Volcanics of the Santa Monica Mountains, California, in *Depositional and Volcanic Environments of Middle Tertiary Rocks in the Santa Monica Mountains, Southern California*, edited by P. W. Weigand, A. E. Fritsche, and G. E. Davis, pp. 93-112, Pacific Section, Society of Sedimentary Geology, Bakersfield, California, 1993.
- Wells, D. L., and K. J. Coppersmith, Updated empirical relationships among magnitude, rupture length, rupture area, and surface displacement, *Bull. Seismol. Soc. Am.*, **84**, 974-1002, 1994.
- Wentworth, C. M., and R. F. Yerkes, Geologic setting and activity of faults in the San Fernando area, California, in *The San Fernando, California, Earthquake of February 9, 1971*, U.S. Geol. Surv. Prof. Pap., 733, 6-16, 1971.
- Wesnousky, S. G., Seismological and structural evolution of strike-slip faults, *Nature*, **335**, 340-343, 1988.
- Whitcomb, J. H., C. R. Allen, J. D. Garmany, and J. A. Hileman, San Fernando earthquake series, 1971: Focal mechanisms and tectonics, *Rev. Geophys. Space Phys.*, **11**, 693-730, 1973.
- Wissler, S. G., Stratigraphic formations of the producing zones of the Los Angeles basin oil fields, in *Geologic formations and economic development of the oil and gas fields of California*, Calif. Div. Mines Geol. Bull., **118**, 209-234, 1943.
- Wissler, S. G., Correlation chart of producing zones of Los Angeles basin oil fields, in *A guide to the geology and oil fields of the Los Angeles and Ventura regions*, edited by J. W. Higgins, pp. 59-61, Pacific Section, AAPG, 1958.
- Woodford, A. O., Bedrock patterns and strike-slip faulting in southwestern California, *Am. J. Sci.*, **258-A**, 400-417, 1960.
- Wozab, D. H., Chemical characteristics of ground water in San Fernando Valley, California, M.S. thesis, Univ. Southern Calif., Los Angeles, 1952.
- Wright, T., The Inglewood oil field, in *Petroleum geology of coastal southern California*, edited by T. Wright, and R. Heck, *Pacific Section, AAPG, Guidebook*, **60**, 41-49, 1987.
- Wright, T. L., Structural geology and tectonic evolution of the Los Angeles basin, California, in *Active Margin Basins*, edited by K. T. Biddle, *AAPG Mem.*, **52**, 35-134, 1991.
- Yamazaki, H., E. Tsukuda, K. Okumura, Y. Kinugasa, A. Okada, T. Nakata, H. Tsutsumi, and S. Hasegawa, Trench excavation of the Okamura fault in the Median Tectonic Line fault system at Saijo, southwest Japan (in Japanese with English abstract), in *Neotectonics of the Median Tectonic Line: Its Significance and Problems*, edited by A. Okada, Y. Sugiyama, K. Mizuno, H. Yamazaki, and E. Tsukuda, *Mem. Geol. Soc. Jpn.*, **40**, 129-142, 1992.

- Yeats, R. S., Rifting and rafting in the southern California borderland, in *Proceedings of conference on geologic problems of San Andreas fault system*, edited by W. R. Dickinson, and A. Grantz, *Stanford University Publications, Geological Sciences, XI*, 307-322, 1968.
- Yeats, R. S., Newport-Inglewood fault zone, Los Angeles basin, California, *AAPG Bull.*, 57, 117-135, 1973.
- Yeats, R. S., Extension versus strike-slip origin of the southern California borderland, in *Aspects of the Geologic History of the California Continental Borderland*, edited by D. G. Howell, *Pacific Section, AAPG, Miscellaneous Publication, 24*, 455-485, 1976.
- Yeats, R. S., Active faults related to folding, in *Active Tectonics*, pp. 63-79, Nat. Acad. Press, Washington, D. C., 1986.
- Yeats, R. S., Late Cenozoic structure of the Santa Susana fault zone, in *Recent Reverse Faulting in the Transverse Ranges, California*, *U.S. Geol. Surv. Prof. Pap.*, 1339, 137-160, 1987a.
- Yeats, R. S., Changing tectonic styles in Cenozoic basins of southern California, in *Cenozoic Basin Development of Coastal California, Rubey Volume VI*, edited by R. V. Ingersoll, and W. G. Ernst, pp. 284-298, Prentice Hall, Englewood Cliffs, New Jersey, 1987b.
- Yeats, R. S., G. J. Huftile, and L. T. Stitt, Late Cenozoic tectonics of the east Ventura basin, Transverse Ranges, California, *AAPG Bull.*, 78, 1040-1074, 1994.
- Yeats, R. S., and G. J. Huftile, The Oak Ridge fault system and the 1994 Northridge earthquake, *Nature*, 373, 418-420, 1995.
- Yerkes, R. F., *Geology and oil resources of the western Puente Hills area, southern California*, *U.S. Geol. Surv. Prof. Pap.*, 420-C, 63 pp., 1972.
- Yerkes, R. F., T. H. McCulloh, J. E. Schoellhamer, and J. G. Vedder, *Geology of the Los Angeles basin, California-An introduction*, *U.S. Geol. Surv. Prof. Pap.*, 420-A, 57 pp., 1965.
- Yerkes, R. F., and R. H. Campbell, *Stratigraphic nomenclature of the central Santa Monica Mountains, Los Angeles County, California*, *U.S. Geol. Surv. Bull.*, 1457-E, 31 pp., 1979.
- Zhang, P., D. B. Slemmons, and F. Mao, Geometric pattern, rupture termination and fault segmentation of the Dixie Valley-Pleasant Valley active normal fault system, Nevada, U.S.A., *J. Struct. Geol.*, 13, 165-176, 1991.